Contribution of demyelination and remyelination in Xenopus laevis

Sowmya Sekizar

THÈSE DE DOCTORAT DE L'UNIVERSITÉ PIERRE ET MARIE CURIE

Spécialité: Neurosciences

École Doctorale 3C – Cerveau, Cognition, Comportement

Présentée par:

Mme. Sowmya SEKIZAR

pour obtenir le grade de

DOCTEUR DE L'UNIVERSITÉ PIERRE ET MARIE CURIE

Sujet de la thèse:

CONTRIBUTION A L'ETUDE DE LA DEMYELINISATION ET LA REMYELINISATION CHEZ XENOPUS

Soutenuce le 4 novembre 2014

Devant le jury composé de:

Mme.	**Le Professeur**	**Ann LOHOF**	**Président**
M.	**Le Docteur**	**Bernard ZALC**	**Directeur de thèse**
Mlle.	**Le Docteur**	**Marion WASSEF**	**Rapporteur**
Mme.	**Le Docteur**	**Geneviève ROUGON**	**Rapporteur**
Mme.	**Le Professeur**	**Barbara DEMENEIX**	**Examinateur**
M.	**Le Docteur**	**Brahim NAIT OUMESMAR**	**Examinateur**

Acknowledgements

It has been four years since I have started my Thesis; I have learnt a lot and also made good friends. Coming from India it has been a pleasure to be a part of the culture on France, Paris to be precise.

I would like to thank the following people who have been part of these four years.

Boris, thank you for all the support and opportunity that you have given me. I should mention the immense patience you have had with all the paper work I had to endure as an international student. I am fortunate to have a boss who looks for the growth of the student in the process of doing the PhD. I have also begin to like the oligodendrocytes as much as you now!.

Jean-Léon Thomas, thank you for giving me the opportunity to work in your lab the lab. I enjoyed the discussions we had when you come down from the states.

The Jury: Thank you for taking your time and accept the invitation

Michel Mallat and Catherine Colin, Thank you for the help in the last few months for the paper,

Catherine Lubetski and Anne Demazieres thank you for all the help and letting me be almost a member of your group. Anne, you have been a angel to me, thank you very much.

Barbara Demenenix, thank you for opening up your lab for me, I have spent more time at MNHN than ICM. You have a wonderful team I cannot thank enough the support and time that your lab members have given me.

Seb, JB and Gerard; Thank you very much for all the help. I do not know how I could have managed my work at the museum without you guys. Special thanks to Gerard for the French lessons.

David Du Pasquier ,Andrew and Nicole, thank you very much. It was a great comfort to know that I could call for help any time for super food for the tadpoles and some Indian takeaway.

Kurt Haas, Thank you being the perfect host, I enjoyed my time in you lab. You have a great team.

Karim, thank you for all the help. I enjoyed the time when we used to travel all the way to Every or Orsay for experiements. We have had some good laughs… Thank you.
Carlos and his team, thank you for your help

Ayeshgul, Anne laure Delphine Laëtitia, **Marion and Hatem** for the fun time we had while doing mundane things… You guys keep the spirits up!!

My Vancouver buddies who helped soo much, made me feel completely at home, Kathryn, Serge, Jana, Kelly DK and Kasper… Thank you…

I would also like to thank **Rosette and Hugo** you are like family, thank you for being there for me through thick and thin.

Ma'am, I thank you for the support, help and inspiration that you have given me from the time I have come to France. Your care and concern has been very warm. Thank you.

Amma , Appa, Anniamma and vandu thank you for being such a positive support and being there for me.

Hari, I am, who I am, because of the support from you. Thank you.

I wish to dedicate my work to my dearest **Hari**, this is also your effort and to my dearest **Appa and Amma.**

ABSTRACT

We have generated a *Xenopus laevis* transgenic line, *pMBP-eGFP-NTR*, allowing conditional ablation of myelin-forming oligodendrocytes. In this transgenic line the transgene is driven by the proximal portion of myelin basic protein (MBP) regulatory sequence, specific to mature oligodendrocytes. The transgene protein is formed by GFP reporter fused to the *E. coli* nitroreductase (NTR) selection enzyme. This enzyme converts the innocuous pro-drug metronidazole (MTZ) to a cytotoxin. My PhD project is to study the effect of demyelination and remyelination in *Xenopus Laevis* in this transgenic line. We wish to answer two questions using this transgenic. First, the origin of remyelinating cells that replace the ablated oligodendrocytes. We have shown that, $Sox10^{+}$ OPCs, which are already present in the optic nerve prior to the experimentally induced demyelination, are responsible for remyelination. The second question is to examine the effect of demyelination of retinal ganglion cell (RGC) axonal arbor morphology. We developed an experimental set up to image the RGC arbor morphology in an awake stage 55 tadpole in real time. We show that the arbor is more sensitive than the control to imaging but there is no change in motility of the arbor.

INTRODUCTION

1.1 HISTORICAL PERSPECTIVE

The rapid conduction of action potential is a requirement for the nervous system of animals in need of quick reflexes to over come risky environment. The Nervous system has developed two adaptations to increase the speed of conduction; the first adaptation is to increase the diameter of the axon and the second adaptation is wrap the axon with multiple layers of insulating material – Myelin, the lipid enriched extension of the plasma membrane of specialized glial cells.
Oligodendrocytes in the central nervous system (CNS) and Schwann cells in the peripheral nervous system (PNS) are the two types of myelin-forming glial cells.

The earliest observation of myelin was by Leeuwenhoek in 1717, he refers to myelin as fatty covering “new tunic” that cover “nervules” that exit the spinal cord. Based on the current knowledge we can speculate that the fatty parts and tunic represent myelin that wrap around nerve fibers.

The first person to ascribe a function to myelin was Galvani in 1791. He considered the nerve to include the conduction and insulating elements, the outer most oily layer he states prevents the dispersion of electricity and permits its accumulation.
The discovery of myelinated fiber is attributed to Ehrenberg. In 1833, he described nerve fibers consisting of four parallel lines, inner two lines indicating the interior cavity and the outer two lines that form the boundary (myelin wrap). He also describes varicosities that tend to be formed in freshly dissected myelinated fibers.

At this point myelin was thought to be produced by nerve fiber and was likened to marrow of bones. Based on this misconception the term Myelin was coined by Rudolf Virchow in 1858. Greek for marrow is *Myelos*. Virchow considered myelin to be present between the surface of nerve fiber and the external membrane.
In 1838, Robert Remak reported that two types of axons coexist in peripheral nerves: larger ones are covered with a thick greasy type of sheath associated at their surface to a nucleus, the others much thinner fibers were not covered by such a sheath. Theodor Schwann confirmed this discovery one year latter and it is the French histologist Louis Ranvier who proposed in 1871 these cells should be named Schwann cells, probably because the name of Remak was

already associated to the tracks of nude fibers he had described in the sympathetic nerve. It was still not clear where the fatty acid or white tunic originated, since for a long time it was proposed that the myelin was secreted by the axon, and that the Schwann cells were providing only the external membrane protecting the myelin.

In the CNS, however, the situation was even more complicated since there are no nuclei associated to the myelin. In 1921 Pio del Rio Hortega visualized the cells that myelinate the CNS by silver carbonate impregnation and coined the term- Oligodendrocyte (*Oligo* –few, *Dendro*- tree). He could not however ascertain the function of these cells. With the technological breakthrough of electron microscope Richard and Mary Bunge in 1962 proved that myelin was an extension of the plasma membrane of oligodendrocytes. Myelin was no longer considered a secretion but a dynamic cellular membrane extension.

1.2 FUNCTION OF THE MYELIN SHEATH

1.2.1 SPEED OF CONDUCTION OF NERVE INFLUX

Myelination is a unique way of increasing the conduction velocity along axon. It is a recent adaptation in vertebrates. There are two mechanisms to increase the speed of conduction of action potential, the first is to increase the diameter of the axon and the second is to insulate the axon by myelination. Increasing the diameter of axons so as to decrease the resistance to impulse propagation, as seen in squids, mediate rapid reflex, albeit they occupy space. The second mechanism is insulating the axon fiber with lipid rich insulating myelin membrane. In myelinated fibers sodium ions enter at the node of Ranvier through the voltage gated sodium channels, this flux of sodium ions depolarize the adjacent membrane of the axon. Myelin that covers the axon at internodes prevents loss of ions and hence decreasing the energy spent to depolarize the membrane. The impulse propagates to the subsequent node with negligible loss of energy (Hartline and Colman, 2007) by saltatory conduction (from the latin saltare : to jump). As the conduction velocity is increased the fiber diameter need not increase in size.

Demyelination leads to a reduction of conduction velocity and in severely affected fibers there could be a complete block of impulse propagation. (McDonald, 1974; Smith and Hall,

1980;Waxman, 1981). In the PNS it is assumed that conduction block occurs when 3 to 5 internodes are demyelinated. Demyelinated axon has low densities of sodium channels, too low to support high-frequency impulse conduction (Waxman, 1982).

The most frequent demyelinating disease is Multiple sclerosis, which associates three components: inflammation, demyelination and finally axonal degeneration. Importantly, patients with MS experience remissions, in which they recover previously lost functions such as vision or the ability to walk. These remissions occur most likely when only the inflammation is involved: decrease of inflammation resulting in recovery of the symptoms. However, if the inflammation leads to demyelination, remission can still be observed in the absence of substantial remyelination. Recovery of clinical functions in these instances appears to depend on molecular reorganization of chronically demyelinated axons, which acquire a higher-than-normal density of sodium channels in demyelinated (and previously sodium-channel-poor) regions (Craner et al., 2004). This molecular remodelling permits the demyelinated axon membrane to support continuous impulse conduction. Where as in fibers that are normally non-myelinated conduction velocity is low (Bostock and Sears 1972; Smith and Waxman, 2005). Of course recovery is seriously improved when remyelination is occurring, in as much as sustained demyelination weakened the axons and render them more vulnerable to transsection, leading to permanent handicap as observed in latter stages of the illness (see below).

1.2.2 METABOLIC SUPPORT TO THE AXON

Oligodendrocytes have an additional function of providing metabolic support to the axon. Neurons are constantly in need of energy to maintain the sodium gradient across the axonal membrane and transport ion channels, synaptic vesicle proteins along the axon from the soma. Energy in the form of ATP is generated by transport of lactose across the axonal membrane. In myelinated fibers myelin forms a barrier for transport of lactose, the nodes being the only regions available for access of fuel source of energy. Oligodendrocytes and Astrocytes in contact with the axon are speculated to be the source for metabolic energy to the axon (Nave, 2010). Astrocytes and oligodendrocytes are gap junction coupled (Tress et al., 2012); this allows access of oligodendrocytes to blood brain barrier and blood vessels. The function of oligodendrocytes-astrocytes gap junction is not clear, but it could transport metabolites.

Together these glial cells maintain ionic homeostasis and also serve as energy repositories for axons. In connexin 32 and 47 null mice, connexin 30 and 47 are oligodendrocyte proteins that form the gap junction along with connexin 32 and 43 in astrocytes, there is severe demyelination and axonal damage with premature death of the mice.

It has been shown that oligodendrocytes transport metabolites through the monocarboxylate transporter 1 (MCT1) and this is critical for the health of the axon (Lee et al., 2012; Funfschilling et al., 2012). In glycolytic cells there is large production of lactate from pyruvate and the lactate is transported along the concentration gradient through MCTs. It has been shown both in vitro and in vivo, blocking or knocking down MCT1 cause neuronal loss. In spinal cord organotypic cultures motor neurons were functional and healthy with glucose in the medium. In medium deprived of glucose neuronal loss could be averted by adding lactate to the medium. To test if MCT1 is required for this process, pharmacological inhibitor of MCT1 (the monocarboxylate transporter found in oligodendrocytes) was added to the medium, the death of neurons was immediate. Providing exogenous lactate prevented the death of neurons. The blocking of MCT1 was not toxic to oligodendrocytes. The experiment provides evidence that oligodendrocytes have a role in providing metabolites to the axon.

1.2.2 PROTECTION OF AXON

Myelin forms a protective covering around axon, provides metabolic support and increases the speed of conduction of axons without increase in diameter of axon.

In demyelinating disease the lack of myelin makes the axon susceptible to damage. In case of immune based multiple sclerosis there is an increase in nitric oxide synthase enzyme at the site of demyelination (Bö et al., 1994). Nitric oxide affects mitochondrial metabolism and ATP synthesis; ATP is essential to maintain the sodium – potassium homeostasis in the axon. If sodium ions accumulate and are not pumped out, the calcium-sodium exchanger work in the opposite manner and allows calcium to enter the axon and activate a series of enzymes that cause axonal damage.

In animal model of oligodendropathy, mature oligodendrocytes are ablated by cell-specific expression of diphtheria toxin. Myelinated axons survived long after the death of the oligodendrocyte soma (Traka et al., 2010). This suggests that the glycolytic enzymes and transporters are functional for several days until the macrophages remove the myelin (Saab et al., 2013).

1.3 STRUCTURE AND FUNCTION OF OLIGODENDROCYTES

Astrocytes, microglia and oligodendrocytes are glial cells, and constitute the majority of the cell population in the central nervous system (CNS) of vertebrates. Oligodendrocytes are the myelinating cells of the CNS. They are ubiquitously distributed throughout the adult CNS, mainly in white matter, but also in the gray matter (Miller, 2002). On the basis of morphological criteria (size of the cell body, number of myelinated axons, diameter of myelinated axons), del Rio-Hortega (1928) Penfield (1932) described four subgroups of oligodendrocytes. It has also been observed that subsets of oligodendrocytes are not equally resistant to toxic agents such as cuprizone (Komoly et al., 1987). Other subpopulations have been described based on biochemical criteria, like expression of members of the collapsin response mediator protein (CRMP) family (Ricard et al., 2001). Recently, two distinct types of morphologically identical oligodendrocyte precursor cells (OPCs) have been identified depending on their synaptic input and their ability to generate action potentials (Káradóttir et al., 2008). However, this morphological, biochemical and physiological heterogeneity of the oligodendrocyte population has not yet been correlated with a specific embryonic origin nor with functionally different subtypes of oligodendrocytes.

1.3.1 MYELIN SHEATH

Oligodendrocytes have a specialized membrane extension which enwraps axons, known as myelin (Bunge et al., 1962). Each oligodendrocyte can myelinate a segment on several axons (**Figure 1**), unlike the Schwann cells in the peripheral nervous system (PNS), which just myelinate a segment on a single axon. The myelin sheath has been a crucial acquisition of vertebrates (Zalc and Colman, 2000), its major function being to increase the velocity of propagation of nerve impulses acting as an electrical insulator. Oligodendroglial processes wrap tightly in a spiral fashion around segments of axons to form internodes, delimited at each extremity by nodes of Ranvier (**Figure 1**). Thus, nodes of Ranvier interrupt myelin at regular intervals, permitting the access of the axonal membrane to the extracellular milieu and a faster propagation of the nerve impulse from node to node, known as saltatory conduction (Huxley and Sämpfli, 1949). The node of Ranvier is flanked by paranodal regions, interposed between the node and the juxtaparanode, and where the myelin loops are anchored to the axon (**Figure 1**).

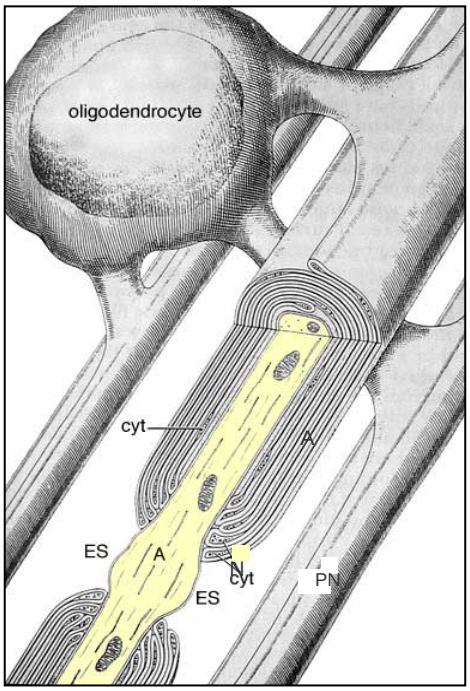

Figure 1. Myelinating oligodendrocyte. The myelin sheath is formed by wrappings of oligodendrocyte plasma membrane (cyt) around axons (A), forming the internodes. These internodes are interrupted by nodes (N), where myelin is absent and the axon is exposed to extracellular space (ES). PN, paranodes. Adapted from *Veterinary Neurohistology Atlas*, T.F. Fletcher, adapted from the original schematic drawing by Bunge & Bunge (1961).

Myelin has unique ultrastructural and biochemical characteristics (reviewed in Zalc and Lubetzki, 2008). With the electron microscope, it appears as a double membrane leaflet formed by a succesion of clear and dense lines, with a periodicity of 15 nm in the CNS (**Figure 2**). The clear lines are formed by the lipid bilayers of the oligodendroglial membrane, while the dense lines correspond to the electron dense proteins of the membranes. Myelin thickness depends on axon caliber (Friede and Bischhausen, 1982).

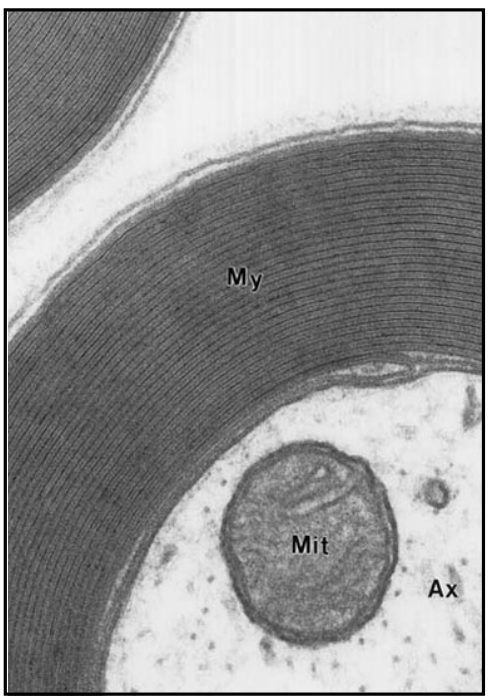

Figure 2. **Ultrastructure of the myelin sheath.** Electron microscopy picture of a myelinated axon (Ax). The myelin sheath (My) appears as a double membrane leaflet formed by a succesion of clear and dense lines. From *Fundamental Neuroscience*, Second Edition, Squire , 2002.

Myelin has peculiar and specific biochemical characteristics, presenting a low water content (40%) and a lipid enrichment, with a lipid:protein ratio of 70:30, i.e., the inverse ratio than any other cytoplasmic membrane, including the myelin forming cell. The three major groups of myelin lipids are cholesterol, phospholipids and glycolipids. Glycolipids are the most abundant, in particular galactolipids like galactosylceramide (GalC), which represents 20-25% of the total myelin lipids and is used as a selective marker of myelin and oligodendrocytes (Dupouey et al., 1979a; Raff et al., 1979; Zalc et al., 1981). The major CNS myelin proteins are the proteolipid protein (PLP), myelin basic protein (MBP), 2',3'-cyclic nucleotide 3'-phosphodiesterase (CNP), myelin associated glycoprotein (MAG) and myelin oligodendrocyte glycoprotein (MOG) (reviewed in Baumann and Pham-Dinh, 2001). In mammals PLP represents 50% of myelin proteins and its transcripts have been shown to define a subpopulation of oligodendrocyte precursor cells (OPCs) that do not depend on PDGFRα signaling for their proliferation and survival (Spassky et al., 2001). MBP is the second most abundant protein of myelin (30% of total myelin proteins) and plays an important role in the compaction of the myelin sheath (Dupouey et al., 1979b).

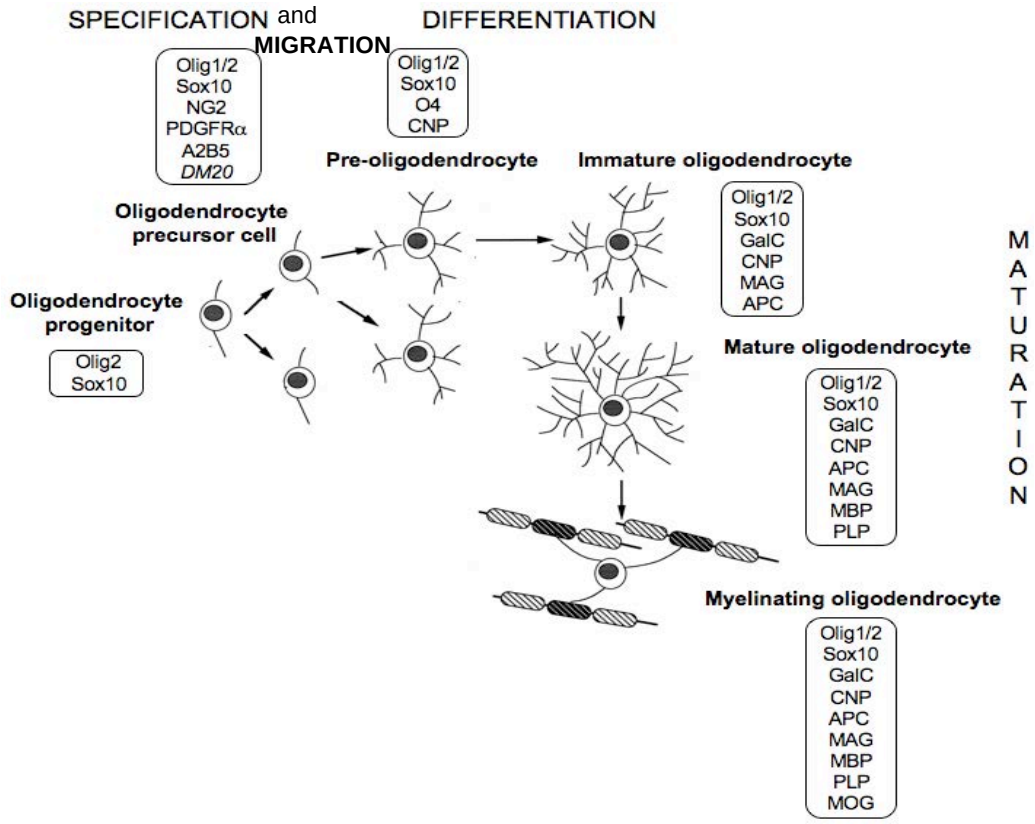

Fig 3: Schematic representation of the morphological and antigenic progression from precursor cells to myelinating mature oligodendrocytes

1.3.2 DIFFERENTIATION AND MATURATION OF OLIGODENDROCYTES

Oligodendrocytes express sequentially a number of cell lineage specific markers from the progenitor stage to the mature myelinating stage. Expressions of some of the markers are retained while the others are lost. The well-defined profile of stage-specific cell surface markers has allowed the progressive differentiation and maturation of oligodendrocyte lineage cells to be followed, providing insights into particular functions carried out by these cells. Prior to myelin formation, oligodendroglial cells undergo a series of phenotypic stages of development characterized by unique antigenic and morphological phenotypes (Figure 3), as well as a change in their mitotic and migratory status (reviewed in Miller, 2002; Zalc and Lubetzki, 2008). Both in culture and in vivo, the oligodendrocyte lineage has been subcategorized into 6 stages: oligodendrocyte progenitor (OLP), oligodendrocyte precursor cell (OPC), pre-oligodendrocyte, immature oligodendrocyte, mature oligodendrocyte and myelinating oligodendrocyte (Figure 3).

Olig2 and Sox10 are the earliest known transcription factors to be specifically turned on in the oligodendrocyte lineage, and they are expressed throughout oligodendrocyte development (Figure 3). During the first stage of oligodendrogenesis, OPCs are highly mitotic and migratory, featuring a bipolar morphology. They express Sox10 and Olig1/2 transcription factors, as well as cell surface markers that include NG2, the platelet derived growth factor receptor alpha (PDGFRα) and a complex ganglioside recognized by the monoclonal antibody A2B5 (Abney et al., 1983; Raff et al., 1979) (Figure 3). When OPCs finish migrating they divide and, at the same time, start to acquire a multipolar morphology, typical of the pre-oligodendrocyte stage. Pre-oligodendrocytes are still mitotic and they express sulfated surface epitopes recognized by the O4 monoclonal antibody (Bansal and Pfeiffer, 1989) (Figure 3). Progression of these cells to the immature oligodendrocyte stage occurs when they become post-mitotic and highly branched. Immature oligodendrocytes express GalC, CNP, MAG and also the tumor suppressor protein APC (adenomatous polyposis coli), recognized by the CC1 monoclonal antibody (Figure 3).

After having exited the cell cycle, the maturation period begins. In rodents, this phase lasts approximately 3-5 days and is characterized by the expression of most of the major myelin proteins, including MBP, PLP, MAG and, at the latest stage, MOG. The mature oligodendrocyte presents an extremely rich array of processes (Figure 3) and it starts to establish contacts with nearby axons. Eventually, a dramatic simplification in the morphology

occurs in the myelinating oligodendrocyte. Only processes having reached an axon will be maintained, all others being pruned (Figure 3).

1.3.3 NODE OF RANVIER

Myelin sheaths are discontinuous, they display periodic interruptions associated with axonal constrictions called node of Ranvier. In 1871, French pathologist and anatomist Louis-Antoine Ranvier discovered these nodes. These domains are crucial for normal saltatory conduction. The node consists of multiprotein complexes of cell adhesion molecules, ion channels and scaffolding molecules. The molecular organization of the node depends upon specialized cytoskeletal and scaffolding proteins such as spectrins, ankyrins and 4.1 proteins. The cytoskeletal proteins are important for the formation, localization and maintenance of the membrane proteins present in the node and axon initial segment (AIS). The node has a high density of voltage gated sodium and Potassium channel. Functional sodium channel at the AIS are responsible for action potential generation and opening of the sodium channel at the node are responsible for saltatory conduction of action potential. Soluble factors secreted by oligodendrocytes have been shown to promote sodium channel clustering in CNS axon culture in the absence of axoglial contact (Kaplan et al., 1997). Cell adhesion molecules present at the CNS node are contactin and the neuronal 186-kDa isoform of Neurofascin (Nfasc 186), the interaction of these cell adhesion molecules with the ankyrinG and membrane proteins promote their stable and restricted localization (Davis et al.,1996 ;Berghs et al.,2000;Tait et al.,200;Jenkins and Bennett,2002;Yang et al.,2004).

The paranode flanks both sides of the nodes of Ranvier. At these sites, myelin and axons form septate-like junctions, which acts as a diffusion barrier that contributes to the formation and maintenance of nodal sodium channel complex. The cell adhesion proteins at the paranode are, contactin-associated protein (caspr), contactin, and the glial 155-kDa isoform of Neurofascin (Nfasc 155) are present. The cytokeleton at the paranode consists of αII spectrin, βII spectrin, ankyrinB and protein4.1B (James, 2003 ; Sherman and Brophy, 2005; Sherman et al., 2005)

Another polarized domain is the juxtaparanode, it is at the innermost axo-glial junction. This domain is characterized by the presence of high-density potassium channels (Rhodes et al., 1997;Wang et al 1993). The cell adhesion molecules found at the juxtaparanode are caspr2 and Tag1. Caspr 2 interacts with cytoskeleton protein, protein 4.1B (Traka et al., 2002; Poliak et al, 2003)

It has been shown that autoantibodies to Neurofascin may cause axonal injury via complement mediated immune pathway and lead to axonal transection in MS disease (Mathey et al., 2007) The cell adhesion molecules (CAM) at the polarized domains are the sites for axo-glial interaction. The mechanism of assembly of these CAMs is not very well understood in the CNS. Understanding the signaling mechanism between the neuronal and glial CAMs at the polarized domains could shed light on initiation of myelination and also to remyelinate axons after demyelination.

1.4 OLIGODENDROCYTE AND NEURONAL INTERACTION

During the development of the central nervous system the reciprocal communication between neurons and oligodendrocytes is essential for the generation of myelin. Intrinsic program within oligodendrocytes along with external factors such as neuron-derived signaling molecules regulate OPC proliferation, differentiation and survival of oligodendrocytes (Barres and Raff, 1999;Temple and Raff, 1986). Studies in cell culture show that at an early stage in development, axons that fire action potential release ATP, that is degraded to adenosine which activates P1 purinergic receptors on OPC's and stimulate their differentiation and also increase the number of axons it myelinates (Stevens et al.,2002). Astrocytes another important glial cell are also involved in stimulating the oligodendrocytes to myelinate. Axons firing impulses release ATP which activate P2 purinergic receptors on astrocytes, causing the release of LIF (leukemia inhibitory factor) and CNTF(Ciliary neurotrophic factor). These factors stimulate formation of myelin by oligodendrocytes (Ishibashi et al., 2006; Stankoff et al., 2002). These signals help control the proper timing of OPC differentiation to ensure that myelination occurs at the appropriate time and place.

Neuronal activity triggers OPC proliferation has been shown *in vivo* and *in vitro* system by blocking neuronal activity with tetrodotoxin (Demerens et al., 1996). Neuron-oligodendrocyte signalling promotes myelination of electrically active axons to regulate neural plasticity. In dorsal root ganglion cultures it has been shown that glutamate release from synaptic vesicles induce the formation of cholesterol rich domains between neurons and oligodendrocytes. These domains are rich in Fyn kinase and facilitate the generation of proteins in the myelin sheath by the Fyn kinase-dependent signalling (Wake et al., 2011). Optogeneticaly stimulating the premotor cortex in awake mice elicits a mitogenic response of neural progenitor cells and

OPCs and increases myelination within deep layers of the premotor cortex and sub cortical white matter (Gibson et al., 2014). Myelination is a multi-step process requiring precise coordination of several different signals.

Myelination continues for decades in the human brain it is modifiable by experience. Myelination affects information processing my regulating the velocity of impulse conduction. Changes in the thickness of myelin sheath, the spacing between nodes and the density of ion channels at the nodes of Ranvier can be attenuated to change the conduction velocity. Rapid structural changes in the myelin insulation are suspected to account for the rapid changes in conduction velocity (Yamazaki, 2008). A single oligodendrocyte can myelinate a set of axons, changes that are caused in one oligodendrocytes can affect the conduction velocity of the set of axons it myelinates. Myelinating glia influences the aggregation and density of sodium channel at the node and potassium channel at the juxtaparanode. These ion channels regulate the excitability, frequency of impulse firing and refractory period of an impulse. Lower refractory period enables transmission of high frequency spike trains. These aspects of impulse conduction are critical in neural encoding, information processing and synaptic function. Myelin plasticity might provide another cellular mechanism of learning complementing the well-studied mechanisms of synaptic plasticity.

Noninvasive brain imaging advances have shed light into the structural differences in myelinated tracts associated with neurological and psychiatric illness such as depression, bipolar disorder, posttraumatic stress, schizophrenia, ADHD, autism and dyslexia to name a few (Fayed and Mondrego, 2005;Basha, 2007)) It is important to discern the fact if structural changes in white matter is a cause of neurological and psychiatric disorder or a consequence of it. Increase in the mRNA transcripts of myelin genes and no change in neuronal genes suggests that changes in white matter are a cause of many disorders that affect cognition.

Defects in myelination due to aberrant communication between neurons and oligodendrocytes could lead to drastic changes in impulse conduction, neuronal plasticity and cognitive ability. The interaction between neuron and glia therefore will not only provide new exciting insights into the development of the nervous system but also help us to find new treatment strategies for various neurological diseases.

1.5 HUMAN DEMYELINATING DISEASES

1.5.1 LEUKODYSTROPHY

Leukodystrophies are a group of heritable myelin disorders. The disease manifests in early childhood, symptoms such as altered gait, hypotonia and cognitive impairment that progresses to spasticity over time. White matter loss could occur in the CNS, PNS or both. White matter loss could be classified biochemically based on defects in any one of the following: lipids, myelin protein or organic acids. Defects in energy metabolism also cause white matter loss. Disease such as MELAS (mitochondrial encephalopathy, lactic acid acidosis and stroke), Leber hereditary optic atrophy, ubiquinone deficiency, Complex I and III deficiency, cytochrome oxidase deficiency and mitochondrial deletions affect white matter along with other parts of the brain and systemic organs.

1.5.1.1 Leukodystrophy associated with lipid abnormalities

Adrenoleukodystrophy (ADL): This is an X-linked inheritable disease. Demyelination beginning in the parieto-occipital white matter. In children visual loss and hypotonia are the clinical presentation. The disease is caused due to a mutation in the Adrenoleukodystrophy protein (ALDP) gene (Moser et al., 1999). In ADL there is an increase of very long chain unbranched fatty acid (VLCFA), the accumulation of the fatty acid is used as a diagnostic marker for the disease (Moser et al., 1999). VLCFA is activated to VLCFA-CoA before its oxidation. The enzyme responsible for the step is VLCFA-CoA synthetase. In patients with a mutation in the ALD gene ALDP protein does not transport enzyme VLCFA-CoA synthetase to the peroxisome, which leads to the impairment of the function of the enzyme (Yamada et al., 1999).

Globoid cell leukodystrophy (Krabbe's Disease): Is an autosomal recessive inherited glycospingolipid storage disorder. The clinical symptoms include rigidity, tonic spasms, ataxia, spasticity, visual loss and mental retardation. The disease is caused by deficiency of lysosomal enzyme galactosylceramide beta-galactosidase, which is required to degrade the lipid galactosylceramide (Malone, 1970;Suzuki et al., 1970). This disease causes an increase in lipid in microglial cells called globoid cells. Psychosine is a glycolipid broken by galactosylceramide beta-galactosidase enzyme; in Krabbe's disease the lack of this enzyme

causes accumulation of psychosine, which is toxic to oligodendrocytes. There are 60 mutations known to be associated with Krabbe's disease (Suzuki, 1998).

Metachromatic leukodystrophy (MLD): is a lysosomal storage disease involving glycosphingolipid metabolism. The clinical symptoms of the disease include ataxia, loss of speech, cognitive impairment that eventually leads to spasticity. The disease is associated with the accumulation of lipids in oligodendrocytes and macrophages throughout the white matter and also in retinal ganglion cells and selected neurons. Sulfatides accumulation in Schwann cells and oligodendrocytes precedes demyelination. Demyelination could be due to the toxic effect of accumulated sulfatides. Deficiency of Arylsulfatase A, sphingolipid activator protein 'saposin B' and multiple sulphatase are the etiologies of MLD (Lyon et al., 1996; MacFaul et al., 1982).

1.5.1.2 Leukodystrophy associated with myelin protein

Pelizaeus-Merzbacher Disease (PMD): Is a typical example of hypomyelinating leukoencephalopathy. This disorder is X-linked leukoencephalopathy. The clinical symptoms of the disease consist of horizontal, vertical or pendular eye movements, stidor, hypotonia, ataxia and spasticity. The cause of the disease is defective biosynthesis of proteolipid protein (PLP) (Willard et al., 1985; Koeppen et al., 1987). DM20 in an alternatively spliced gene derived from PLP locus. DM20 gene has been implicated in the maintenance of oligodendrocytes and myelin assembly. Mutations that are associated with PLP and DM20 cause different variants of PMD (Gow et al., 1996). These mutations could be either point mutations, some introducing an early STOP codon, PLP gene duplication or PLP gene deletion, which explain different clinical phenotypes. Interestingly enough, there exist in the mouse (and other mammals as well) different type of mutations, occurring either spontaneously (Jimpy, Jimpy rumshaker) or by transgenesis (targeted deletion or duplication). These animal models reproduce quite faithfully in terms of gravity, the clinical phenotypes, described in human (Werener et al., 1998).

1.5.1.3 Myelin basic protein deficiency

A deletion of myelin basic protein (MBP) locus on the 18th chromosome in a 25-year-old female caused clinical symptoms such as ataxia and mild mental retardation. The 18th month infant of the female also was affected, which shows that the disease is inheritable. In 18q chromosomal deletion syndrome children have decreased or diffused white matter in the CNS, which could be due to deletion of the MBP gene (Gay et al., 1997). Naturally occurring mouse models of *MBP* gene have been described (shiverer, shiverer mld), as well as by targeted deletion (Readhead et al., 1990; Matthieu et al., 1981).

1.5.1.4 Leukodystrophy associated with organic acid

Canavan's Disease: Is an autosomal recessive neurological disorder associated with macrocephaly and spongiform degeneration of brain. Canavan's disease is identified as deficiency of aspartylacylase, which causes an increase in N-acetyl aspartic acid (NAA) in the brain and urine. The clinical symptoms include hypotonia, head lag and macrocephaly. Infants with Canavan's disease show symptoms only after 3 months of age. Clinical diagnosis is confirmed after confirmed elevation of NAA in the urine. The gene for human aspartoacylase is localized on the 17th chromosome. The protein has 313 amino acid residues. The identified mutation can be divided into Ashkenazi Jewish and non–Jewish mutation. The mutations that are common in the Ashkenazi Jewish mutation are substitution of glutamic acid for alanine at codon 285 and changing tyrosine at codon 231 to a stop codon. The most common non-Jewish mutation is the substitution of Alanine to Glutamic acid at codon 305 (Matalon et al., 1992). If there is a high risk of a mother to give birth to a child with Canavan's disease then the chorionic villus can be analyzed for mutations. At present there is no treatment for Canavan's disease.

1.5.2 MULTIPLE SCLEROSIS

Multiple Sclerosis (MS) is a sporadic, spontaneous and acquired inflammatory demyelinating disease of the human CNS. MS involves the interaction of the immune system and the CNS. There have been possible references to the disease about 500 years ago, although the first clinical description can be attributed to Augustus d'Este (1794-1848) the earliest recorded person for whom a definite diagnosis of multiple sclerosis can be made. Neuropathological

signs were first described in 1835-1838 by Cruveiller in France and separately in England by Carswell. In 1865-68 Jean Martin Charcot was the first person to establish the correlation between the clinical and pathological relationship of MS. Less understood in MS is the cause of the disease. Environmental factors, such as infection by Epstein-Barr virus have been accused to be causative, and genetic predisposition are touted as possible factors that cause the disease (Ascherio et al., 2012) MS shares genetic characteristics with organ-specific inflammatory disorders such as rheumatic arthritis and inflammatory bowel disorder (Sawcer et al., 2011).

The pathogenesis of MS is heterogeneous; no single predominant mechanism for the disease has emerged. One hypothesis is that there is a disruption in the integrity of BBB in a genetic predisposed person or by environmental factors, or both. This disruption of the BBB leads to the increase of adhesion molecules on the endothelium of the brain and spinal cord, lymphocytes begin to enter the CNS. If lymphocytes that recognize myelin antigen exist they could trigger a cascade of reaction leading to inflammation and demyelination. It is still not known how myelin proteins are presented as possible antigen, and there has not been any conclusive myelin antigen that could be reliably linked to MS; whatever, the lymphocyte aggression is what leads to the autoimmune aspect of this disease (Prineas et al., 2006).

Typically, the disease beings in a person's late 20s to early 30s and is chronic and progresses to be a debilitating disease. The first phase of MS also called the relapse and remitting phase, the characteristic symptoms of this phase are blurred vision, sensory disturbance, and motor impairment. These episodes would occur with an unpredictable frequency for about 5-30 years. MRI signals are observed dispersed in the white matter of the brain and spinal cord. Pathological change such as disruption of the blood brain barrier is observed as illustrated by gadolinium contrasting agent.

Secondary progressive MS follows remitting and relapse phase of MS, at this point there is loss of ability to walk, motor function and cognitive ability is affected. These are the most common phases of MS; there could be variations with respect to age and cause of the disease. At the tissue level MS is characterized by disruption of the blood brain barrier, infiltration of the CNS by lymphocytes, and colonization of lesions by microglia. Cytokines are produced by T-cells, macrophages, astrocytes and microglia. The cytokines include interleukins (IL)-1β,IL-6, interferon (IFN)-γ, IL-23 and IL-17. Reactive oxygen and nitrogen species, prostaglandins, vasoactive factors and chemokine are found at the site of lesion (Frohman et al., 2006). In lesions, demyelinated axons are present in a milieu of inflammatory molecules, if there is no

clearance of myelin debris followed by in adequate remyelination, the axon could be permanently damaged leading to functional impairment. In case of acute lesion there is extensive loss of oligodendrocyte. Consequent progress in the treatment of the inflammatory component of the disease have been accomplished in the past 20 years by introduction of interferon beta, copolymer 1 (copaxone), and more recently by different immunosuppressive antibodies or antibodies aimed at preventing entry of lymphocytes in the CNS (Johson et al., 1995). Unfortunately, these immunomodulatory and/or immunosuppressive treatments results mostly in a diminution in the numbers of relapses over a five year period, which is a great improvement for the quality of life of the patients, but so far no or little positive consequences on the evolution of the handicap, compared to natural history of the disease.

1.6 ANIMAL MODELS OF DEMYELINATION-REMYELINATION

1.6.1 RODENTS

1.6.1.1 Experimental autoimmune encephalomyelitis (EAE)

EAE is a family of disease models. It has contributed towards understanding autoimmune, neuroinflammation, cytokine biology and immunogenetics of demyelinating disease.

EAE mice are produced by active immunization of mice with purified myelin proteins or activated antigen-specific T cells (Tiwari et al., 2007; Genani and Hauser, 2001). The model has high degree of variability based on the mice strain, gender and the peptide that is used to immunize the mice. Mice of the same strain immunized with the same peptide could also have large variations in the pattern of demyelination (in terms of numbers of demyelinating lesions, size and localization of lesions). The C57BL/6 mice genetics is well known and this offers important advantage while using this strain to develop the EAE mice model. Nowadays, the most frequently developed EAE strategy relies on immunization with Myelin Oligodendrocyte Glycoprotein (MOG) peptide (Bittner et al., 2014). C57BL/6 mice are injected subcutaneously with MOG peptide emulsified in Freund's adjuvant supplemented with *Mycobacterium tuberculosis*, followed by two injections of pertussis toxin 2 days apart. In 2 weeks these mice developed inflammation, demyelination, death of OL and axonal damage. In these mice CD4 positive T cells are activated. Compared to other myelin proteins antigens, the MOG-EAE mice have become now as more or less the reference animal model of MS as it associates both the neuroinflammation and demyelination aspect. There are some limitations to this model:

the C57BL/6 model of EAE is monophasic and without relapse, which is an important characteristic of MS; the lesions are random and it is difficult to make comparison between samples; In most EAE models the immune response is initiated via $CD4^+$ T cells, while in MS $CD8^+$T cells are predominant; in EAE models relapses cannot be studied; lastly the pathological changes cannot be correlated to behavioral changes (Rodrigues et al., 2011).

A major drawback in the EAE model is that the site and size of the lesions are unpredictable, which make comparison difficult and necessitate a large number of animals to be reliable. In this respect, a real improvement in the MOG-EAE model has been the targeting of EAE lesions to a predetermined axonal tract. To generate a new localized animal model of MS, the authors have taken advantage of the limited susceptibility of the Lewis rat to (MOG-EAE) and have combined subthreshold immunization with MOG with local injections of two proinflammatory cytokines (TNF-alpha and Interferon gamma) into the spinal cord, which induce local immune cell infiltration (Kerschensteiner et al., 2004). More recently the model has been elegantly adapted to the mouse (Tepavčević et al., 2011).

1.6.1.2 Cuprizone

S. Ludwin has introduced cuprizone as an *in vivo* model of chemically induced demyelination, which can be controlled spatio-temporally (Ludwin, 1978). In these model C57BL/6 mice, 6 to 8 weeks old, are given 0.2% cuprizone (bis-cyclohexanone oxaldihydrazone) as a part of their diet. Cuprizone is a copper chaelator which causes dysfunction of the mitochondrial complex IV leading to the death of oligodendrocytes. Demyelination is first detected 3 weeks after starting cuprizone diet; important demyelination is seen after 6 weeks of cuprizone diet. Demyelination occurs globally, but is prominent in corpus callosum and posterior cerebellar peduncles. Optic nerves and spinal cord are never or seldom concerned. Remyelination begins once the cuprizone diet is replaced by the normal diet. Cuprizone model is suitable to study remyelination, which is a crucial area of study in MS.

A major advantage of cuprizone is that demyelination is mostly localized in the white matter of the cerebellar peduncles and the corpus callosum and the extent of demyelination in the corpus callosum, can be scored more easily and consistently. Cuprizone induces apoptosis of mature oligodendrocytes that leads to a robust demyelination and profound activation of both astrocytes and microglia. Phagocytosis and removal of damaged myelin seems to be one of the major roles of microglia in this

model and it is established that removal of myelin debris is a prerequisite of successful remyelination. Magnetic resonance imaging (MRI) has been used to determine the degree of demyelination in cuprizone fed mice (Merkler et al., 2005). Functional deficits were seen in cuprizone treated mice compared to mice that were given a normal diet in the Rotor rod test and open field test (Franco-Pons et al., 2007). The only draw back of the model is that immune involvement is moderate and this component of MS cannot be studied.

1.6.1.3 Lysolecithin

Lysophosphatidylcholine is a detergent like agent that solubilizes membranes. Lysolecithin 1% solution is injected into the dorsal funiculus of the spinal cord or caudal cerebellar peduncle (CCP) (Gregg et al., 2007; Girard et al., 2005) or corpus callosum. In fact any myelinated tracts can be investigated depending on where the lysolecithin is being injected. Oligodendrocyte precursor cells are spared while treated with lysolecihtin so remyelination is faster compared to other models.

Remeyelination begins only after the myelin debris are removed, 7 days post lysolecithin injection in the spinal cord of mice or young adult rats thin myelin sheath begin to appear. In rats with CCP lesion remyelination is slower compared to spinal cord, it takes 3 weeks for remyelination to occur, compact myelin appears 6 weeks post demyelination.

Lysolecithin treatment unlike ethidium bromide (another toxin used to demyelinate) does not affect astrocytes, OPC or macrophages; this facilitates faster remyelination. Lysolecithin lesion can be spatio-temporally controlled. The disadvantage of this model is similar to that of cuprizone, the immune aspect of MS cannot be studied with this model.

1.6.2 NON-HUMAN PRIMATE MODEL OF MS

Non-human primates provide useful models of MS due to their genetic and immunological proximity to humans. The two most investigated models are EAE in rhesus monkeys and common marmosets. EAE is a valid experimental model of MS and is also one of the most intensively studied experimental models in basic immunology. EAE has been successfully induced in rodents, but they lack the genetic similarity that non-human primates share with human patients. Another important advantage of the non-human primate model is that the patterns of neurological deficits are less stereotypical than in rodents and resemble more the clinical and neuropathological heterogeneity seen in MS patients. Experimental therapies very

effective in controlling EAE in rodents are only partially effective in MS patients and in some cases even detrimental (Hohlfeld and Wiendl, 2001). The non-human primate EAE models are of particular importance for the safety and efficiency testing of new therapeutics for MS because of their species-specificity.

The most common macaques EAE models is rhesus monkey (*M. mulatta*). The presence of similar major histocompatibility complex (MHC)-DR and MHC-DQ allelic lineages in humans and macaques has been described and is of great interest because products of both loci have been identified as major regulatory elements of susceptibility to MS in the human population (Francis et al.,1991; Wucherpfennig et al., 1991). EAE in myelin-immunized rhesus monkeys usually follows an acute course, although in some unpredictable cases an MS-like chronic disease pattern can be found. The characteristic histological aspect of the model is the presence of large lesions with infiltration of abundant neutrophils, and serious destruction of white matter, affecting both myelin and axons (Stewart et al., 1991, Ravkina et al., 1978). The severe inflammatory aspect suggests that the lesions in this model are formed by an acute pathological event causing severe inflammatory necrosis rather than selective demyelination. EAE in the rhesus monkey therefore most resembles the acute fulminant forms of MS, such as post- infectious leuco-encephalomyelitis, rather than the more common chronic forms of MS.
Common marmosets (*Callithrix jacchus*) are small neo tropical primates. Marmosets breed easily in captivity, giving birth to one or two non-identical sets of twin or triplet siblings per year. As fraternal siblings have shared the placental blood circulation in utero, bone-marrow-derived elements developing in a twin or triplet are equally distributed over the siblings. This natural chimerism induces in each monkey permanent tolerance towards its fraternal sibling's alloantigen. Hence, it is possible to test the pathogenic role of auto reactive T-cells by adoptive transfer experiments between such siblings (Massacesi et al., 1995).
In its clinical presentation and the radiological and pathological aspects of the lesions, EAE in the common marmoset is an excellent model of chronic MS (Genain et al., 1997, 't Hart et al., 2000). The characteristic lesion type resembles closely the pattern II of active MS lesions, which is the most prominent type in chronic MS (Lucchinetti et al., 2000; Lassmann, 1999; 't Hart et al., 2000). The common marmoset is highly susceptible to EAE. Upon a single immunization with human myelin or recombinant human MOG in complete Freund's adjuvant, each monkey tested thus far has developed EAE, although the individual disease course varies.

An as-yet unresolved issue is that rhesus monkeys immunized with myelin or myelin antigens develop a disease resembling acute forms of MS, whereas marmosets immunized following the identical protocols develop a disease resembling chronic MS. A detailed examination of the pathogenic mechanisms in these models will shed light on the mechanisms that cause the clinical and pathogenic heterogeneity in MS patients (Brok et al., 2001). The disadvantage of this model is that it is very expensive to maintain the animals.

Lysolecithin method of demyelination is also used in non-human primates; lysolecithin is injected into right centrum semiovale of adult male macaque monkeys Demyelination can be seen by magnetization transfer (MTR) by day 7 (Dousset et al., 1995). Focal demyelination in the CNS has been induced by microinjection of lysolecithin in the optic nerve and spinal cord of adult *Macaca fascicularis* (Lachappelle et al., 2005)

1.6.3 ZEBRA FISH (*Danio rerio*)

Zebra fish is a transparent model to screen potential therapeutic drugs for MS. The molecular and cellular organization of zebra fish is similar to that of humans, homologues for most human genes can be found in zebra fish (Barbazuk et al., 2000, Postlethwait et al., 2000). In terms of myelin, however, fishes are still too primitive to correctly match with mammals. Notably, in contrast with tetrapods there are only little differences between PNS and CNS myelin composition. As a major example the presence of protein zero (P0), a characteristic component of PNS myelin proteins, is also the predominant myelin protein in fish CNS rather than PLP as in mammals. The structural properties and cell lineage relationship of oligodendrocytes is highly comparable between zebra fish and mammals. Orthologous genes for the major mammalian myelin–associated genes have been found in zebra fish, such as Dm20, MBP, and P0. There are variations in expression pattern and sequence of gene between zebrafish and mammals. In zebrafish, myelin associated genes appear 2 days before the appearance of compact myelin (Brosamle and Halpern, 2002).
Embryogenesis in zebrafish is ex vivo, the larvae are a few millimeters in length and transparent which is conducive for live imaging. Myelination begins 3 days post fertilization (dpf) (Buckley et al., 2010), time taken to observe phenotype is less. In vivo investigation of myelin gene function through RNA overexpression and morpholino gene knockdown experiments are suitable for zebrafish as the time taken for myelination to begin is 3 days.

Developing transgenic line is relatively easy and cheap compared to rodents; there are many reporter lines for myelin protein available such as Tg(*Sox10:eGFP*); Tg(*Olig2:eGFP*); Tg(*Plp:eGFP*). The system to develop transgenic line is well established in zebrafish; tol2 transposon system, Bacterial artificial chromosomes (BAC) and the Gal4-UAS system have been used to generate transgenic animals; it has also been possible to control the expression of transgene spatio-temporally. Target-induced local lesions in genomes (TILLING) (MacCallum et al, 2000) are used to make gene specific mutations in plants.

Transcription activator-like effector nucleases (TALENS), which are synthetic restriction enzymes generated by fusing a TAL effector DNA binding domain to a DNA cleavage domain. These synthetic enzymes can be custom made to bind practically any desired DNA sequence. When these restriction enzymes are introduced into cells, they can be used for genome editing in situ and also develop locus-specific mutations in zebrafish genome (Timothy and Kazuyuki, 2012).

Myelin breakdown in MS leads to eventual axon degeneration causing disability associated with the progressive stages of MS. Remyelination prevents damage of axon and hence halt the progression of the disease (Franklin and ffrench-Constant, 2008). Myelination in zebrafish starts 3 dpf, this time period is used to screen for drugs that make the process faster. Myelin injury is not needed in this case. Tg (*olig2:eGFP*) line is used to screen for drugs that increase Olig2 cell population that migrate from the pMN domain of the spinal cord. These drugs were further used to check if they interfered with differentiation of OPC into mature oligodendrocytes by measuring relative level of *MBP* mRNA using real time PCR. Drugs that specifically increase OPC number and their differentiation and do not affect neuron or astrocyte cell number can then be used in rodents and mammalian system to verify their potential use as a drug (Ibanez et al., 2004;Penderis et al., 2003).

There are zebrafish model in which myelin loss can be produced, one such method is laser ablation of OL. The second system is expression of nitroreductase (NTR) in oligodendrocytes (Chung et al., 2013). NTR is an enzyme, which reduces the nitro radical of prodrug metronidazole (MTZ) to hydroxylamine derivative that causes death of cells that expresses NTR (Curado et al., 2007). Thus zebrafish serves as a realistic and economical start point towards developing therapy that could target CNS remyelination.

There are, however, few drawbacks to using zebrafish to screen drugs for remyelination; firstly, only drugs that are permeable to the zebrafish skin can be used; hence screen of some potential therapeutic drugs can be missed. Secondly, zebrafish larvae are used to study

remyelination instead of adults. Remyelination efficiency decreases in older animals (Sim et al., 2002; Woodruff et al., 2004); thirdly using developmental process of myelination rather than the regenerative process of remyelination allows for much faster screening of drugs, but there are differences in mechanisms and molecules involved in myelination and remyelination; lastly as stated above, in terms of control of expression of myelin components, in all fishes, including zebrafish, CNS and PNS myelin are still very similar in contrast to higher vertebrate. In this respect, amphibian look more promising, since most of the major myelin constituents are very similar to mammal's myelin, not only for the coding sequences, but also including the regulatory sequences.

1.6.4 AFRICAN CLAWED FROG (*Xenopus laevis*)

Tadpole of Xenopus is another transparent animal model to study myelination. The advantage of this model is that the myelin is remarkably similar to that of mammals. The myelin purified from the CNS of Xenopus laevis contained the same major lipid and protein components as human myelin. Peripheral and central nervous system myelin of rat and Xenopus is highly similar (Quarles et al., 1978). In the PNS the P0 sequence in Xenopus is similar to P0 sequences of higher vertebrates, suggesting that a common mechanism of PNS myelin compaction via P0 interaction might have emerged through evolution (Luo et al., 2008). The morphology of developing oligodendrocytes is comparable to that of rodents, and hence Xenopus is suitable for studying maturation of oligodendrocytes and myelination process (Yoshida, 1997). Small model organisms, such as amphibians and some teleosts, are increasingly being used at various stages of drug development and constitute highly cost-effective alternative models to mammals (Saito and van den Heuvel, 2002; De Smet et al., 2006; Giacomotto and Ségalat, 2010).

To study myelination, demyelination and remyelination, in collaboration with A. Mazabraud and F. Kaya from University Paris Sud, we have produced a transgenic Xenopus line, *pMBP-eGFP-NTR*, designed to specifically express in oligodendrocytes the fluorescent reporter GFP fused to the Escherichia Coli nitroreductase (NTR), under the control of the 1.9 kb (-1907bp/36bp) proximal portion of mouse *MBP* regulatory sequence. In the mouse, this portion of the proximal upstream regulatory sequence of *MBP* gene drives the expression of *LacZ* reporter transgene only in mature myelin-forming oligodendrocytes (Stankoff et al., 1996). Our team showed that similarly to the mouse, in our transgenic *Xenopus laevis* line the eGFP-

NTR transgene is expressed only in myeling-forming oligodendrocytes (Kaya et al., 2012). The GFP^+ fluorescent oligodendrocytes are easy to quantify in the optic nerve. Furthermore, in terms of chronology of development it has been shown that in the optic nerve mature myelin-forming oligodendrocytes start to be detected at stage 47-48 (Cima and Grant, 1982), which is 2 weeks post fertilization (when the embryos are maintained at 23 °C). This has been totally confirmed in our transgenic line, by detection of GFP^+ cells in the optic nerve. In this transgenic Xenopus line, thanks to the NTR transgene mature myelin-forming oligodendrocytes are specifically ablated following treatment with metronidazole (MTZ, an NTR substrate). Treatment of *pMBP-eGFP-NTR* tadpoles induces selective demyelination, which is reversible on MTZ withdrawal (Kaya et al., 2012). The optic nerve of the embryo is conducive for live imaging; unlike the spinal cord there is no obstruction by muscles tissue. The number of mature oligodendrocytes, GFP positive cells, in the optic nerve is consistent among embryo of the same stage. This model can be used to quantify demyelination and remyelination non-invasively. To screen therapeutics drugs for remyelination this transgenic line could serve as a medium throughput model, since A. Mannioui in our team has shown that he could easily screen 10 molecules per week.

There are many similarities between zebrafish and Xenopus, both are tetraploid, aquatic, and transparent with ex-vivo development. In some aspects Xenopus scores over zebrafish. As already mentioned above, the myelin in Xenopus is closer to mammals compared to zebrafish; the electron microscopic images of the myelin in zebrafish are not as compact as the myelin in Xenopus, and for reasons still unexplained, EM images are of much higher quality in Xenopus compared to zebrafish. There are about 3000 embryo per mating pair in Xenopus, whereas zebrafish produces 300 of embryos, so it is relatively easy to collect a large number of embryos for high sample numbers.

Apart from being a suitable model to screen for therapeutics, the *pMBP-GFP-NTR* line could be used to study the consequences of demyelination such as clearing of the debris; recruitment of progenitors to replace the ablated oligodendrocytes and the fate of nodal proteins. The *pMBP-GFP-NTR* line can be crossed with other transgenic lines that express nodal proteins in fusion with a fluorescent protein reporter or a reporter specifically expressed in oligodendrocyte precursor cells (OPCs), to study the changes in the nodal proteins and recruitment of OPCs in real time, following demyelination.

1.6.4.1 TRANSGENESIS IN AMPHIBIANS

Amphibian embryos remained the embryos of choice for experimental embryologists for many decades. Amphibian embryos are large, can be obtained in large numbers and can be maintained easily and inexpensively in the laboratory. They are relatively easy to manipulate with microsurgical instruments, and they heal readily after surgery. In case of *Xenopus laevis*, the South African Clawed Frog spawning can be induced by injecting the female with gonadotropic hormone, this allows for the availability of eggs throughout the year in comparison to the other amphibian species that are seasonal breeders. Xenopus has many advantages as a developmental model system, Nevertheless there are also a few set backs with respect to using it as a model for genetic manipulations.

Stable integration of foreign DNA into genome aimed at generating transgenic model animals or producing mutations of endogenous genes has been of interest to all biologists. However, *X. laevis* was left aside as a model for genetic manipulations, due to the difficulty in producing and analysing inheritable genomic modifications. The first limitation occurs due to the genomic duplication that has occurred several times in most fishes and amphibians. *X. laevis* the most used xenopus species in research is tetraploid and has a generation time of 1–2 years, which make traditional genetic studies impractical (Bisbee et al., 1977; Evans et al., 2004, 2005; Morin et al., 2006). *X. tropicalis* , the only diploid species of the *Xenopus* genus has a 6–9 months generation time and the genome of it is completely sequenced. X.laevis and X.tropicalis share high sequence conservation in a number of genes (Chalmers et al., 2005). The maintenance of tropicalis has been a problem in laboratory as it is easily vulnerable to infection.

Gain and loss-of-function experiments have been traditionally performed via microinjections of RNA, DNA or morpholinos at an early stage of development. The relative short half-life of injected products, their dilution and mosaic distribution limits us to analyze certain genes that act early in development. In addition, there were not many available tools to modify its genetic information for many years. However, there have been new technical innovations that allow classical experimental procedures to be combined with sophisticated genetic studies may re-establish the use of *Xenopus* as a model system. One such mechanism to develop non-mosaic transgenic is Restriction enzyme mediated integration (REMI). This method provided a first step towards the engineering of tools and reagents, which are compatible with genetic approaches (Kroll and Amaya, 1996). The aim of this method was to reduce mosaic

expression of the transgene through an integration step into the host genome occurring *in vitro* within isolated sperm nuclei.

The procedure involves the incubation of a linearized transgene and isolated sperm nuclei along with the Restriction enzyme to favor the generation of double-stranded breaks and egg extracts to promote genomic DNA decondensation. The foreign DNA is thought to incorporate randomly into the genomic DNA during a process of DNA repair. The manipulated nuclei are then transplanted into unfertilized eggs, thus generating transgenic embryos (Figure 4). The advantage of this method is 70% efficiency and non-mosiac expression of transgene. The advantage over transgenesis in mice is that one can make first generation transgenics; you don't need to wait until the next generation to examine the effects of the exogenous gene on development. The disadvantages of this line is the numerous developmental defects and low survival rate of the embryos compared to standard microinjection techniques (Sparrow et al., 2000; Smith and Mohun, 2005).

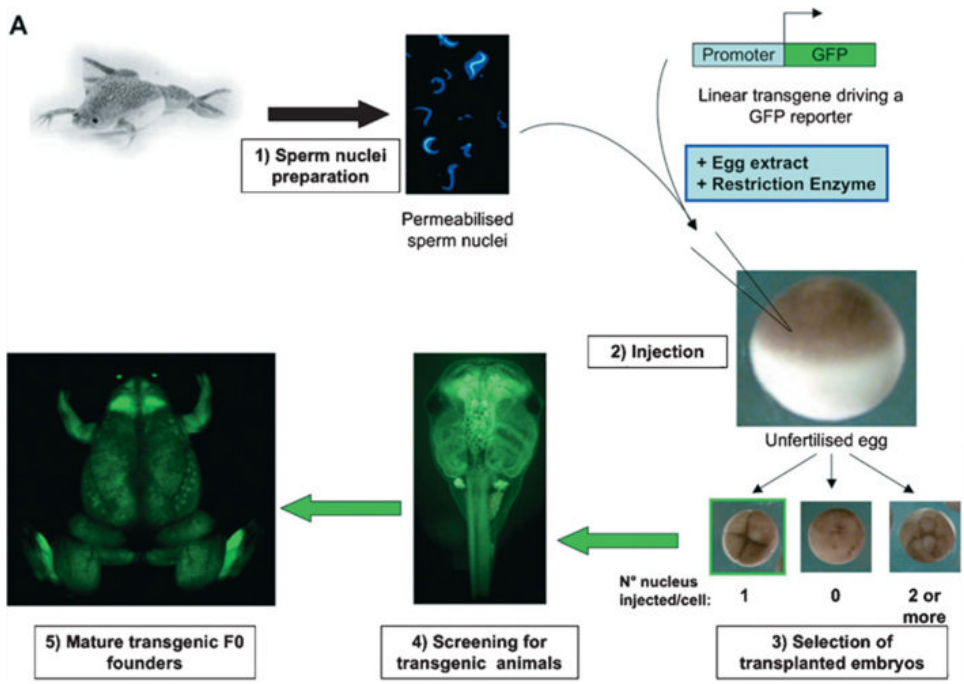

Fig 4 : A schematic showing REMI transgenesis procedure (Chesneau, 2008)

There are other new methods in Xenopus that are used to generate transgenics, Transposable system, phi-C31 integrase , I-SceI meganuclease and CRISPER are a few of them.

Transposons are mobile genetic elements that move in the host genome. Most DNA transposons are simply organized; they encode a transposase protein flanked by inverted terminal repeats (ITRs), which carry transposase binding sites. Any DNA flanked by the ITRs will be recognised by the transposase and will become enzymatically integrated into nuclear DNA. Transposons used in Xenopus transgenesis are Sleeping Beauty (SB) Piggyback and Tol2 (Hamlet et al., 2006). There is little or no abnormality among the transgenic Xenopus. The disadvantage is that the F0 transformants obtained exhibited a high degree of mosaic distribution.

The I-SceI meganuclease (meganuclease) is an endonuclease which recognizes an 18 bp sequence and was originally isolated from *Saccharomyces cerevisiae*. The meganuclease procedure requires only the I-SceI endonuclease, a commercially available meganuclease, and a transgene construct containing the 18 bp recognition site. The construct is digested with the meganuclease and the mixture is directly microinjected into fertilized eggs. Efficient integration requires an injection between the animal pole and the sperm entry site, thus in close proximity to the forming nucleus (Ogino et al., 2006b; Pan et al., 2006). The meganuclease method, a substantial number of non-mosaic embryos is generated (Pan et al., 2006). Significant advantages are the ease of manipulation, a good survival rate and efficiency.

Phi-C31-integrase-mediated transgenesis is developed to overcome random insertion of transgene in the genome. Phage DNA encodes the phi-C31 integrase that catalyses a site-specific recombination into the host genome. Two different short DNA sequences are needed to sustain integration by this integrase. The attP site in the phage DNA and the attB site in the bacterium genome are recombined to generate two new sequences (attR and attL). Transgenic approach involves the co-injection of mRNA encoding the integrase with a plasmid containing an attB site, using standard microinjection techniques, into fertilized eggs.
As the sequence requirements for attP sites can be relatively promiscuous, the integration event relies on the existence of pseudo-*attP* sites in the frog genome.
The integrase method offers a unique way to promote single-copy transgene insertion in a sequence-restricted manner.

A recent method in generating knock out in Xenopus is Transcription activator-like effector nucleases (TALENs), which are synthetic restriction enzymes generated by fusing a TAL

effector DNA binding domain to a DNA cleavage domain. These synthetic enzymes can be custom made to bind practically any desired DNA sequence. When these restriction enzymes are introduced into cells, they can be used for genome editing in situ, a technique known as genome editing with engineered nucleases.

The most recent method for targeted genome editing is CRISPR (clustered regularly interspaced short palindromic repeats)/Cas9 system. The system uses the Cas9 nuclease to facilitate RNA-guided site-specific DNA cleavage. The system consists of Cas9 protein carrying a nuclear localization and guide RNAs (gRNAs) that direct Cas9 protein to cleave the specific targeted DNA (Guo et al., 2014)

The new available techniques along with a diploid X.tropicalis species, with short generation time could prove very effective in generating transgenic Xenopus. This could help establish Xenopus as an effective model for genetic manipulation

1.7 AIM OF MY PROJECT

Demyelination is the pathological process in which myelin sheaths are lost from around axons. In the CNS demyelination is usually the consequence of a direct insult targeted at the oligodendrocyte, the cell that makes and maintains the myelin sheath. This type of demyelination is sometimes referred to as primary demyelination to distinguish it from secondary demyelination, in which myelin degenerates as a consequence of primary axonal loss (Wallerian degeneration).

Demyelination impairs function: the acute loss of a myelin internode is associated with conduction block, when, on a given axon, the demyelination process interests at least 3 to 5 consecutive internodes. Robust and rapid remyelination is needed to prevent transection of the axon. Therapeutics are now designed to protect the axon from inflammation and create a disease suppressive background in which remyelination could occur by recruitment of progenitors.

First part of my PhD was to examine recruitment of OPC in the optic nerve following demyelination. The optic nerve is a suitable system to study OPC recruitment migration

because it is devoid of neuronal cell and in our transgenic line the optic nerve can be imaged in real time. To image the recruitment of progenitors I have tried to develop a *sox10:td tomato* transgenic line.

Secondly I have tried to study the aggregation of the node during myelination, after demyelination and remyelination by immune labeling. I generated transgenic line that expresses β1 subunit of sodium channel in fusion with GFP under the control of the neuronal beta tubulin (NβT) promoter (*NβT- β1Nav-GFP*).

Finally, in collaboration with Dr Kurt Haas laboratory at University of British Columbia, I have analyzed the changes in the morphology of the retinal ganglion cell arbor post demyelination and remyelination.

Hence, in my PhD I have tried to use the *pMBP-GFP-NTR* transgenic line to address the following basic questions:

Part I

Origin of remyelinating cells after demyelination in the optic nerve and consequences of demyelination on nodal markers

Part II

Physiological consequences on bidirectional signals between oligodendrocytes and axons following demyelination and remyelination.

PART I

Origin of remyelinating cells after demyelination in the optic nerve and consequences of demyelination on nodal markers

INTRODUCTION

Remyelination is the process by which myelin sheaths are restored to demyelinated axons, facilitating them to recover the ability to carry action potentials by saltatory conduction. Cell adhesion molecules and ions channels at the node of Ranvier redistribution along the axon, similar to what was seen before myelination.

In the absence of Remyelination axonal transection could lead to permanent damage. In demyelinating disease such as MS there is an insufficiency of remyelination resulting in lesions that remain demyelinated and eventual lead to axonal loss. At the site of lesion there are macrophages, microglia and astrocytes, ready to clear the myelin debris and make the region conducive for recruitment of progenitors to differentiate and myelinated the demyelinated axon. This phase is very crucial for recovery, and treatments that are designed to enhance remyelination have this time window to focus on. Remyelination might fail if there is not sufficient amount of progenitors or failure of the recruited progenitors to differentiate. As an animal ages or when there is repeated demyelination the number of progenitor cell is reduced and they possibly not able to differentiate leading to demyelination (Sim et al., 2002; Shields et al., 1999).

Several strategies have been proposed to enhance remyelination in experimental models (Warrington et al., 2000), but the mechanism by which they are effective remains unknown (Stangel et al., 1999). Currently there is no explanation to why remyelination fails in MS, understanding the process better in the experimental models could shed more light enhancing remyelination case of MS.

We have established the Xenopus transgenic line p(*MBP-GFP-NTR*) as a suitable demyelinating model to screen to drugs. We had a few questions unanswered in our previous paper (Kaya et al., 2012) regarding the remyelination process. Recruitment of progenitors in the optic nerve after demyelination and the process of clearance of debris in our system were not examined. It is imperative to know the mechanism of repair in the demyelinating model. The p(*MBP-GFP-NTR*) line is used as a medium throughput model to screen drugs, the information regarding remyelination could help understand the effect of the drugs that are screened for remyelination.

Remyelination by resident oligodendrocyte precursor cells in a *Xenopus laevis* inducible model of demyelination.

S. Sekizar[1, 2, 3], A. Mannioui[1, 2, 3], L. Azoyan[1, 2, 3], C. Colin[1, 2, 3], D. Du Pasquier[4], M. Mallat[1, 2, 3] ,J-L Thomas[1, 2, 3] and B. Zalc[1, 2, 3, 5]

[1] Sorbonne Universités UPMC Univ Paris 06, UM-75, ICM-GHU Pitié-Salpêtrière, F-75013 Paris, France ;

[2]Inserm U1127, F-75013 Paris, France ;

[3]CNRS UMR 7225, F-75013 Paris, France ;

[4] Watchfrog, 91000 Evry, France

[5]AP-HP, Groupe Hospitalier Pitié- Salpêtrière, F-75013, Paris, France ;

Running title: Remyelination in a Xenopus model of demyelination

ABSTRACT

We have generated a *Xenopus laevis* transgenic line, *pMBP-eGFP-NTR,* allowing conditional ablation of myelin-forming oligodendrocytes. In this transgenic line the transgene is driven by the proximal portion of myelin basic protein (MBP) regulatory sequence, specific to mature oligodendrocytes. The transgene protein is formed by GFP reporter fused to the *E. coli* nitroreductase (NTR) selection enzyme. This enzyme converts the innocuous pro-drug metronidazole (MTZ) to a cytotoxin. Ablation of oligodendrocytes by MTZ treatment of the tadpole induced demyelination and here we show that myelin debris are eliminated by microglial cells. After cessation of MTZ treatment, remyelination proceeded spontaneously. We questioned the origin of remyelinating cells. Our data suggest that, $Sox10^{+}$ OPCs, which are already present in the optic nerve prior to the experimentally induced demyelination, are responsible for remyelination, and this required only minimal (if any) cell division.

Keywords: Oligodendrocyte, Myelin, Microglia, Multiple Sclerosis, Sox10, Isolectin B4.

INTRODUCTION

In the central nervous system (CNS), myelin, the membrane allowing saltatory nerve conduction, is synthetized by oligodendrocyte, a highly specialized glial cell. Saltatory conduction, a mechanism insuring a 50-100 fold increase in velocity of nerve impulse propagation, results by the regularly interspace wrapping of axon by myelin sheath, an acquisition of hinge-jaw vertebrates (Zalc et al., 2008). Death of oligodendrocytes leading to destruction of myelin has been described in various pathological conditions including the leukodystrophies and multiple sclerosis (MS) (Lucchinetti et al., 1996; Dowling et al., 1999; Feigenbaum et al., 2000). Once destroyed, myelin can be cleared from the tissue by professional phagocytes, such as microglial cells, the resident macrophages in the CNS (Kettenmann et al., 2011). Elimination of myelin debris is a key step for regeneration to take place. Remyelination a crucial repair mechanism in MS was hypothesized by Marburg, who first described shadow plaques (markschattenregeneration) a pathognomonic neuropathologic feature of MS demyelinated lesions (Marburg, 1906). Shadow plaques are explained by thinner myelin sheath during repair of demyelinated axons (Périer and Grégoire (1969). In experimental rodent models of demyelination it has been shown that remyelination results from activation and proliferation of endogenous oligodendrocyte precursor cells (OPCs) a large population of glial cells present in the adult brain (Levine and Reynolds, 1999). We have recently developed by transgenesis in *Xenopus laevis* an inducible model of oligodendrocyte ablation. In this *pMBP-eGFP-NTR* transgenic line, elimination of oligodendrocytes is accompanied by demyelination and then followed by spontaneous remyelination (Kaya et al., 2012). Here we have investigated the mechanism of clearance of myelin debris following demyelination, and the origin of remyelinating cells. We show that similar to higher adult vertebrate, in *Xenopus laevis* microglial cells are responsible for elimination of myelin debris and that remyelination is insured by resident OPCs.

MATERIALS & METHODS

Animals.

Xenopus tadpoles were raised and maintained as previously described (de Luze et al., 1993) and staged according to the normal table of *Xenopus laevis* (Daudin) of Nieuwkoop and Faber and developmental progress defined as NF stages (Nieuwkoop and Faber, 1994). Tadpoles of either sex were anesthetized in 0.05–0.5% MS222 (3-aminobenzoic acid ethyl ester; Sigma-Aldrich) before brain and spinal cord dissection. Animal care was in accordance with institutional and national guidelines.

Metronidazole preparation and use.

Metronidazole **(**MTZ) (Sigma-Aldrich) was dissolved in filtered tap water containing 0.1% DMSO (Sigma-Aldrich). Tadpoles were treated with MTZ (10mM) in the swimming water for 10 days. Control animals were kept in the same media without MTZ. Transgenic tadpoles were maintained in 600 ml of MTZ solution (maximum 10 tadpoles/600 ml) at 20°C in complete darkness (MTZ is light-sensitive) and changed every 2 days throughout the duration of treatment. For regeneration experiments, MTZ-treated animals were allowed to recover for up to 10 days in normal water in ambient laboratory lighting. Transgenic tadpoles were treated with drugs between stage NF 48 and 55. These stages correspond to pre-metamorphosis and represent stages in which myelination is ongoing. Myelination markers such as proteolipid protein (PLP) and myelin basic protein (MBP) are first immunodetected at stages 42/43 in the hindbrain and spread throughout the brain and spinal cord by stages 46/47 (Yoshida, 1997). In the optic nerve at the electron microscopic (EM) level myelination was reported to begin in the middle portion at stage 48/49 and the number of myelinated axons increases sevenfold between stage 50 and 57 (Cima and Grant, 1982).

Bromodeoxyuridine (BrdU) treatment.

BrdU at a final concentration of 500 ìM (Sigma-Aldrich) was diluted in aquarium water. One tadpole in 50ml of 500 ìM BrdU was maintained with tadpole food for 24h after MTZ treatment.

Antibodies.

The following antibodies required 4% paraformaldehyde at room temperature for 30 min: mouse anti-panNav (1:500,Sigma-Aldrich), rabbit anti-Ankyrin G (1:500, a gift from Dr. F. Couraud, UPMC, Paris), mouse anti-MBP (1:200, kindly provided by Dr. Saburo Nagata, Women's Tokyo University, Japan).

The following antibodies were used on tissue fixed in 4% paraformaldehyde over night. Mouse anti-MBP (directed against *Xenopus* MBP, 1:1000, kindly provided by Dr. Saburo Nagata), anti-pan-Neurofascin (NFC1) (1:1000; Zonta et al., 2008 a gift of Dr. P. Brophy, University of Edinburgh, UK), rabbit anti-Sox10 (raised against zebrafish Sox10, 1:5000 a gift of Dr. B. Appel, University Colorado Denver, USA) rabbit anti-PH3 (1:400, Millipore), mouse anti-PH3 (1:400, Millipore), mouse anti-BrdU (1:500, BD Biosciences), mouse anti-Nkx2.2 (1:10, mouse hybridoma, Developmental Studies Hybridoma Bank, Iowa City, IA), chick anti GFP (1:1000, Aves Lab, USA), chick anti-mcherry and rabbit anti-mcherry (1:500, EnCor Biotech, USA), rabbit anti Iba1 (1:400, Wako Chemicals), mouse anti-CD11b/c (OX42, 1:100), rat anti-CD11b (M1/70.15, 1:400), mouse anti-CD68 (ED1, 1:200), rat anti-CD68 (FA-11, 1:400), rat anti-F4/80 (1:100), all from Serotec.

Immunolabeling.

Tadpoles were fixed by immersion in 4% paraformaldehyde, the fixation varied according to the antibody used (see above).

Whole mount immunolabeling : Fixed tadpole brain and spinal cord were dissected and rinsed in Triton X-100 (0.1% in PBS 1x = PBT 0.1%) for 2 h with change in PBT 0.1% every 15 min. Samples were then incubated in blocking solution (normal goat serum diluted 10% in PBT 0.1%) for 1 h. Primary antibodies were added in the blocking solution and incubated for 48h on a gentle shaker at 4°C. The primary antibody was removed and the brain rinsed for 2 h in PBT 0.1%, with changes every 20min. Secondary antibodies, Alexa 350, Alexa 488, Alexa 594 and Alexa 647 (1: 1000, Invitrogen) were used in blocking solution, and incubated over night at 4 °C

on a gentle rotating shaker. The secondary antibody is removed and the labelled brains rinsed in PBT 0.1% for 2 h with changes every 20min. DAPI (Invitrogen) was used to label the nuclei and rinsed in PBT 0.1% for 2min and mounted on slide in FluorSave® Reagent mounting medium (Calbiochem).

Immunohistochemistry: Fixed brains were rinsed in PBS1x and cryoprotected in sucrose (20% in PBS1x). Cryoprotected brains were embedded in OCT® (Tissue Tek). Cryosections (12 µm thick) were blocked in normal goat serum (10% in PBS) containing 0.1% Triton X-100 and incubated overnight at 4°C with primary antibodies. Slides were rinsed in PBT 0.1% and secondary antibody added. The slides were mounted with DAPI coated Fluromount® (Sigma-Aldrich).

Immunohistochemistry for anti-BrdU: Cryosections were labelled for GFP and Sox10 as per the classic protocol and later fixed in paraformaldehyde 4% for 10min at room temperature and rinsed in PBT0.1%. These sections were denatured with 2 N HCl at 37 °C for 30 min, rinsed with PBT 0.1% and blocked with 10% normal goat serum in PBT0.1% at room temperature for 30 min. Tissue sections were then incubated with anti-BrdU antibodies overnight at 4°C.

Isolectin B4 staining.

Microglial cells were stained with *Bandeiraea Simplicifolia* isolectin B4 (Ib4) on fixed tissue sections or whole tadpole brain and spinal cord prepared as above. Tissue sections were incubated overnight at 4°C with Alexa Fluor 594-conjugated Ib4 (1:1000, Invitrogen) in PBT 0,1% supplemented with 1mM calcium, and then washed in PBT. For whole-mount staining, samples were incubated for 48h under gentle shaking. When combined to immunolabeling, tissue sections or whole samples were incubated with fluorescent Ib4 and washed before incubation in blocking solution and exposures to antibodies, as described above.

Two-photon observation.

For *in vivo* examination of GFP-expressing oligodendrocytes along the optic nerve, tadpoles were anesthetized in MS222 (Sigma-Aldrich) and placed in a POC-Chamber-System (H. Saur, Reutlingen, Germany), under a two-photon microscope. Mono-photon or two-photon excitation

was performed using Zeiss LSM 710 microscope system. The microscope was equipped with objective (20×, 1 NA). Calculated optical slice thickness was 2 µm. Each image presented is the 3D projection of 18–26 stacks of images. The settings (gain and aperture pinhole) were held constant within individual experiments. All images shown were processed with ImageJ software (NIH).

Image analysis and quantification.

Images were captured using a Nikon AZ100 fluorescence macroscope, a Zeiss AxioImager Z1 fluorescence microscope equipped with the Apotome® system and a Leica confocal SP2 microscope. Image analysis and quantification were performed using ImageJ software.

RESULTS

In the *pMBP-eGFP-NTR* transgenic *Xenopus laevis*, expression of the fusion protein eGFP-NTR occurs in myelin-forming oligodendrocytes.

As reported in the mouse (Stankoff et al., 1996), in *Xenopus laevis* the 1.9kb (-1907bp/36bp) proximal portion of mouse *MBP* regulatory sequence drives a cell type specific (oligodendrocyte) and developmental-selective (myelin-forming stage) expression of the transgene. In the optic nerve of *pMBP-eGFP-NTR* transgenic *Xenopus laevis*, GFP expressing oligodendrocytes are first detected at stage 47-48, which is in agreement with light and electron microscopy studies showing that myelination begins at stage 48 in the middle part of the optic nerve (Cima & Grant, 1982). In our transgenic construct GFP is cytoplasmic. Therefore the GFP fusion protein that diffuses into the cytoplasm of oligodendrocyte allowing oligodendroglial processes extending towards and along axons to be visible, but was excluded from compact myelin sheath, which in contrast was immunostained with anti-MBP antibodies (Figure 1).

In addition to GFP, the transgene fusion protein contains the E. Coli enzyme nitroreductase (NTR), which converts the nitro radical of prodrugs such as metronidazole (MTZ) to 2-(5-

(hydroxyamino)-2-methyl-1H-imidazol-1-yl-) ethanol, a hydroxylamine derivative highly cytotoxic. Thanks to the expression of GFP, in *pMBP-eGFP-NTR* transgenic oligodendrocytes can easily be quantified using a fluorescent macroscope or microscope. We have previously shown that the number of oligodendrocytes was halved following a 3 days exposure to 15 mM of MTZ (Kaya et al., 2012). In order to induce a more significant demyelination we increased the duration of the MTZ treatment. However, due to swelling, edema and several deaths among treated tadpoles, the concentration of MTZ was reduced from 15 to 10 mM and exposure length increased to 10 days (Fig. 2, D0 - D10). After 10 days, tadpoles were returned to normal water to recover and spontaneous remyelination occurred. Individual treated tadpoles were followed by repetitive two-photon microscopy examinations. For the same animal, oligodendrocyte cell death and recovery was monitored at the same position along the optic nerve (Fig. 2). During the length of the experiments, the numbers of oligodendrocytes per optic nerve were counted under a macroscope before treatment (D0), at the end of the MTZ treatment (D10) and then during recovery at 3 and 8 days (R3, R8)(Fig. 2B). After 10 days in the presence of MTZ, the number of GFP^+ oligodendrocytes dropped from 17.4 $\pm$ 0.4 to 3.8 $\pm$ 0.2. Recovery, however, occurred quite rapidly; numbers of detected oligodendrocytes per optic nerve was 8.3 $\pm$ 0.9 and 13.3 $\pm$ 1.5 at R3 and R8, respectively.

Redistribution of nodal proteins following demyelination.

In our previous study (Kaya et al., 2012) we have demonstrated that in the *pMBP-eGFP-NTR* transgenic tadpole the GFP-NTR transgene is expressed in oligodendrocytes and even in myelin-forming oligodendrocytes only and that elimination of myelinating oligodendrocytes following MTZ treatment resulted in demyelination. This was illustrated by loss of luxol fast blue staining as well as, at the EM level, on brain stem ultra thin tissue-sections (Kaya et al., 2012). Another method to illustrate demyelination is labeling of node of Ranvier and/or components of paranodal region. On tissue sections of *pMBP-eGFP-NTR* transgenic tadpoles, staining of myelinated axons with anti-MBP antibodies showed regularly spaced interruptions of the labeling

corresponding to nodes of Ranvier (Fig. 3A, C, G, I), which are clearly labeled with either anti-ankyrinG (Fig. 3B, C) or pan-sodium voltage-gated channel (pan-Na_v Fig. 3 E, F) antibodies. Immunostaining with pan-antineurofascin (panNFC) antibodies labeled both the node itself and the paranodal region corresponding to the two neurofascin isoforms of 186 kDa and 155 kDa, respectively (Fig. 3 H, I). Following MTZ treatment, the myelin sheath is largely damaged (Fig. 3J, L, P, R) and paranodal structure disappeared. As a consequence, nodal protein ankyrin G (Fig. 3K, L) or Na_v channel (Fig. 3N, O) are no longer aggregated but are more or less homogeneously redistributed along the axons. Similarly localization of neurofascin is disturbed as illustrated by the presence of hemiparanodes (Fig. 3 M, O) and also elongated aggregates (Fig. 3 Q, R). Altogether these alteration of nodal and paranodal structures illustrate demyelination consecutive to myelinating oligodendrocytes death.

Elimination of myelin debris.

A 10 days treatment with MTZ of stage 50 *pMBP-eGFP-NTR* transgenic tadpoles induced a nearly complete elimination of myelinating oligodendrocytes. As shown in the above paragraph ablation of myelin-forming oligodendrocyte is accompanied by a rapid demyelination. Three days after withdrawal of MTZ from swimming water myelin-forming oligodendrocytes (GFP expressing cells) reappeared in the optic nerve. We questioned how was the myelin debris eliminated during such a short period. An obvious candidate are microglial cells. In a first series of experiments we tested different antibodies known to label microglial cells in the mouse or the rat. Probably due to species differences, immunostaining with anti-CD11b, anti-CD68, anti-F4/80 , or anti-Iba1 antibodies were negative**.** In contrast, microglial cells were clearly labelled after incubation of optic nerve tissue sections with Ib4 isolectin (Fig. 4A). Of note, Ib4 labeled cells had the typical multi processes morphology of microglia in the normal CNS. After MTZ treatment the number of Ib4+ microglial cells was increased by a factor of 2.6 (Fig. 4C). This increase in number was accompanied by a change in cell morphology, typical of microglial cell activation and marked by enlargement of cell bodies and shortening of cell processes, (Fig. 4A middle panel). Three days

after recovery, a few GFP+ cells had reappeared and the number of microglial cells had nearly returned to normal (Fig. 4 A right panel). Activated microglial cells were also observed in concomitance with the MTZ-triggered loss of GFP cells, in the hindbrain and the spinal cord. The detection of Ib4+processes spreaded over GFP + cell bodies (Fig. 4B) strongly suggested that activated microglia were engaged in the phagocytosis of dying oligodendrocytes By performing double staining with Ib4 and anti MBP antibodies, we could observe MBP-positive particles engulfed by microglia, indicating that myelin fragments are cleared by phagocytosis (Fig. 4B)

Origin of remyelinating cells.

In rodent as in birds, it has been established that oligodendrocytes myelinating the optic nerve are generated in the supra chiasmatic area, a focal region at the ventral midline of the third ventricle, from where they migrate towards the optic nerve, which they colonize from the chiasmatic towards the retinal end (Small et al., 1987; Giess et al., 1992; Ono et al., 1997). As illustrated above, in our transgenic *Xenopus* model spontaneous remyelination occurs rapidly following demyelination, which raises the question of the origin of the cells responsible for myelin repair. To address the question of the source of remyelinating cells, we use immunolabeling with anti-Sox10 antibodies. The transcription factor Sox10, which belongs to the high-mobility-group protein transcriptional regulator, has been shown to be expressed very early during development in the oligodendroglial lineage already at the stage of progenitor and its expression is maintained throughout their differentiation and maturation including in myelin-forming oligodendrocytes (Kuhlbrodt et al., 1998; Stolt et al., 2002). By immunolabeling of stage 55 optic nerve of *pMBP-eGFP-NTR* Sox10 expressing cells were either isolated or aligned in rows of 4-5 cells, typical of interfascicular glia (Fig. 5). Among the Sox10 expressing cells, some were $Sox10^{+}/GFP^{-}$ and other $Sox10^{+}/GFP^{+}$. Being GFP^{+}, the later are myelin-forming oligodendrocytes, and the former were identified as oligodendrocyte precursor cells (OPCs) (Fig. 5). After 9 days of MTZ-induced

demyelination, most of GFP+ cells have disappeared (Fig. 6), but Sox10+ OPCs are intact. Only very few Sox10+ cells have incorporated BrdU (12.9 $\pm$ 3.9 n=4), which was not statistically significantly different from control animals (n=4) of same stage (7.8 $\pm$ 1.8; p value 0.28). After 4 days of recovery new $Sox10^{+}/GFP^{+}$ cells are detected and were uniformly distributed along the optic nerve, eliminating the possibility of an invasion of newly generated OPCs from the supra chiasmatic area. Therefore we concluded that GFP^{+} cells (i.e., remyelinating cells) are generated from $Sox10^{+}$ OPCs already present in the optic nerve.

DISCUSSION

Microglial cells are responsible for clearance of myelin debris

Here we show that in the optic nerve, of developing *Xenopus laevis*, cell autonomous-triggered elimination of myelinating cells is followed by a prompt remyelination, which is already significant 3 days after inactivation of the cell death process. This recovery is likely to implicate cellular mechanisms insuring rapid elimination of myelin debris that are thought to prevent OPC differentiation into myelinating cells (Robinson and Miller, 1999; Kotter et al., 2006). In the CNS of mammals affected by demyelination, resident microglia play a key role in the clearance of myelin debris owing to their phagocytic behavior, although the scavenging efficiency may strongly vary according to the type of lesions or pathologies responsible for myelin disruption (Nielsen, 2009; Gaudet et al., 2011, Gudi et al., 2014). Culture studies have allowed to identify a set of microglial receptors implicated in the capacity of rodent microglia to recognize and ingest myelin particles (Smith et al., 2011).

In the current study using an isolectin B4 (Ib4) staining procedure that labels microglia in mammal species including human and rodents (Kaur et al., 1992), we could observe resident microglia in the optic nerve and other CNS regions of the *Xenopus* tadpole at stage 50 and

onward. Similar cells were previously revealed in section from stage 54/56 *Xenopus* using a monoclonal antibody raised against tadpole retinal cells (Goodbrand and Gaze, 1991). Although the embryologic origin of *Xenopus* microglia has not been formally established, investigations in birds, fish and rodents indicate that microglia stem from macrophage progenitors, which are generated in the yolk sac and infiltrate the CNS during early stages of neurogenesis (Cuadros et al., 1993, Herbomel et al., 2001, Ginhoux et al., 2010, Schulz et al., 2012). Microglia are highly plastic and motile cells that swiftly react to CNS cell death or damage. The spectrum of microglial responses may cover cell migration, mitosis and changes in microglial cell shape accompanied by upregulation or modulation of functional capacities, among which phagocytosis (Kettenmann et al., 2011). We found that in the optic nerve of *MBP-eGFP-NTR Xenopus* tadpoles undergoing demyelination induced by MTZ treatment, the microglial response is marked by accumulation of Ib4+ cells and enlargement of microglial cell bodies. The local recruitment of reactive microglia is likely to be fuelled by microglial chemotaxis toward GFP^+ dying cells. In support of this assumption, we have shown that MTZ treatment triggers caspase 3-dependent apoptosis in GFP^+ cells (Kaya et al., 2012), whereas apoptotic cells are known to release chemoattractants sensed by microglia, including ATP (Hochreiter-Hufford and Ravichandran, 2013, Corriden and Insel, 2012, Honda et al., 2001). Furthermore, apoptosis is known to trigger cell surface externalization or unmasking of ligands called "eat me signals", the best characterized being phosphatidyl serine. Eat me signals are recognized by engulfment receptors expressed by professional phagocytes and thereby promote phagocytosis of apoptotic cells (Nagata et al., 2010). Microglial expression of engulfment receptors and propensity to engulf apoptotic cells is well documented in rodent species (Marin Teva et al., 2004, Sierra et al., 2013). Accordingly, we propose that in Xenopus tadpole undergoing demyelination, dying GFP cells express eat me signals, which trigger their engulfment by activated microglia, as illustrated by spreading contacts between microglial processes and GFP^+ cell bodies (Fig 4B). In addition to microglial cell redistribution, morphological changes and engulfing behaviors, we could detect short-lived events

such as the presence of MBP^+ material in microglial phagosome. Altogether our observations indicate that in *Xenopus* tadpole, the mobilization of engulfing microglia directly participates in the elimination of dying cells and myelin debris resulting from targeted apoptosis in myelinating cells.

In the optic nerve resident OPCs are responsible for remyelination

Unlike in mammals, in the optic nerve of Xenopus laevis only a small percentage of axons are myelinated as shown by counting on EM sections (Gaze & Peters, 1961). In the larvae, between stage 51 to 57, the ratio of unmyelinated to myelinated fibers was in the average of 20:1. For instance, on stage 51 tadpoles, 6 000 fibers were unmyelinated and 300 were myelinated (Gaze & Peters, 1961). Since we have shown that on animal of same development stage the number of myelinating oligodendrocyte was 25 ± 3, we can infer that each oligodendrocyte myelinates in the average 12 internodes. During this period the total number of axons increases and by stage 58, the number of myelinated axons was reported 420 (Gaze & Peters, 1961). To accommodate this increase in axons to be myelinated new oligodendrocytes needs to be generated from OPCs, which is what we observed by immunolabeling with the anti-Sox10 Ab. Therefore, when tadpoles optic nerve are demyelinated at stage 50 or 55, there are already plenty of $Sox10^+$ OPCs present and therefore there is no need to have additional OPC migrating into the ON nor division of existing OPCs as shown by the absence of PH3 labeling and the modest increase in BrdU incorporation. How remyelination during development can be compared with the situation in adulthood? We have not found in the literature data on remyelination in adult Xenopus. However, in mammals, including human, adult OPCs are present in the myelinated tract and the parenchyma. These adult OPCs, initially reported by Wolswijk and Noble M (1989), constitute in the rat between 5 to 8 % of total brain cells (Dawson et al., 2003). There is a body of studies reporting that in experimental model of demyelination in adult animals, these adult OPCs migrate towards the lesion and remyelinate (Levine and Reynolds, 1999; Chari and Blakemore, 2002;

Fancy et al., 2004). However, in addition to adult OPCs, cell lineage tracing experiments have shown that SVZ progenitor cells can give rise to oligodendrocytes in demyelinated lesions, contributing potentially to remyelination, and that mobilisation of SVZ progenitors also occurs in MS patients (Nait Oumesmar et al., 2007). The respective contribution of either adult OPC or SVZ progenitor cells to remyelination is not clear, but one likely possibility is that it may depend on the localisation of the lesion to be remyelinated.

ACKNOWLEDGEMENTS

We thank Dr F. Kaya and A. Mazabraud for their contribution to the early steps of this work, Dr B. Appel for the gift of anti-Sox10 antibody and Dr. S. Nagata for the gift anti-*Xenopus* MBP antibody. This work was supported by the program "Investissements d'Avenir" ANR-10-IAIHU-06, and NeuRATRIS.

REFERENCES

Chari DM, Blakemore WF. Efficient recolonisation of progenitor-depleted areas of the CNS by adult oligodendrocyte progenitor cells. Glia. 2002; 37(4): 307-13.

Cima C, Grant P. Development of the optic nerve in Xenopus laevis. II. Gliogenesis, myelination and metamorphic remodelling. J Embryol Exp Morphol. 1982; 72: 251-67.

Corriden R, Insel PA.New insights regarding the regulation of chemotaxis by nucleotides, adenosine, and their receptors. Purinergic Signal. 2012; 8(3): 587-98.

Cuadros MA, Martin C, Coltey P, Almendros A, Navascués J. First appearance, distribution, and origin of macrophages in the early development of the avian central nervous system. J Comp Neurol. 1993; 330(1): 113-29.

Dawson MR, Polito A, Levine JM, Reynolds R. NG2-expressing glial progenitor cells: an abundant and widespread population of cycling cells in the adult rat CNS. Mol Cell Neurosci. 2003; 24(2):476-88.

Dowling P, Ming X, Raval S, Husar W, Casaccia-Bonnefil P, Chao M, Cook S, Blumberg B Up-regulated p75NTR neurotrophin receptor on glial cells in MS plaques. Neurology 1999; 53: 1676–1682.

Fancy SP, Zhao C, Franklin RJ. Increased expression of Nkx2.2 and Olig2 identifies reactive oligodendrocyte progenitor cells responding to demyelination in the adult CNS. Mol Cell Neurosci. 2004; 27(3): 247-54.

Feigenbaum V, Gélot A, Casanova P, Daumas-Duport C, Aubourg P, Dubois-DalcqM Apoptosis in the central nervous system of cerebral adrenoleukodystrophy patients. Neurobiol Dis. 2000; 7: 600–612.

Gaudet AD, Popovich PG, Ramer MS. Wallerian degeneration: gaining perspective on inflammatory events after peripheral nerve injury. J Neuroinflammation. 2011; 8: 110.

Gaze RM and Peters A. The development, structure and composition of the optic nerve of Xenopus laevis (Daudin). Q J Exp Physiol Cogn Med Sci. 1961; 46: 299-309.

Giess MC, Soula C, Duprat AM, Cochard P. Cells from the early chick optic nerve generate neurons but not oligodendrocytes in vitro. Brain Res Dev Brain Res. 1992; 70(2): 163-71.

Ginhoux F, Greter M, Leboeuf M, Nandi S, See P, Gokhan S, Mehler MF, Conway SJ, Ng LG, Stanley ER, Samokhvalov IM, Merad M. Fate mapping analysis reveals that adult microglia derive from primitive macrophages. Science. 2010; 330(6005): 841-5.

Goodbrand IA, Gaze RM. Microglia in tadpoles of Xenopus laevis: normal distribution and the response to optic nerve injury. Anat Embryol (Berl). 1991; 184(1): 71-82.

Gudi V, Gingele S, Skripuletz T, Stangel M. Glial response during cuprizone-induced de- and remyelination in the CNS: lessons learned. Front Cell Neurosci. 2014; 8: 73.

Herbomel P[1], Thisse B, Thisse C. Zebrafish early macrophages colonize cephalic mesenchyme and developing brain, retina, and epidermis through a M-CSF receptor-dependent invasive process. Dev Biol. 2001 Oct 15;238(2):274-88.

Honda S, Sasaki Y, Ohsawa K, Imai Y, Nakamura Y, Inoue K, Kohsaka S. Extracellular ATP or ADP induce chemotaxis of cultured **microglia** through Gi/o-coupled P2Y receptors. J Neurosci 2001; 21(6): 1975-82.

Hochreiter-Hufford A, Ravichandran KS. Clearing the dead: apoptotic cell sensing, recognition, engulfment, and digestion. Cold Spring Harb Perspect Biol. 2013; 5(1): a008748.

Kaur C, Chan YG, Ling EA. Ultrastructural and immunocytochemical studies of macrophages in an excitotoxin induced lesion in the rat brain. J Hirnforsch. 1992;33(6):645-52.

Kaya F, Mannioui A, Chesneau A, Sekizar S, Maillard E, Ballagny C, Houel-Renault L, Dupasquier D, Bronchain O, Holtzmann I, Desmazieres A, Thomas JL, Demeneix BA, Brophy PJ, Zalc B, Mazabraud A. Live imaging of targeted cell ablation in Xenopus: a new model to study demyelination and repair. J Neurosci. 2012; 32(37): 12885-95.

Kettenmann H, Hanisch UK, Noda M, Verkhratsky A. Physiology of microglia. Physiol Rev. 2011; 91(2): 461-553.

Kotter MR, Li WW, Zhao C, Franklin RJ. Myelin impairs CNS remyelination by inhibiting oligodendrocyte precursor cell differentiation. J Neurosci. 2006; 26(1): 328-32.

Kuhlbrodt K, Herbarth B, Sock E, Hermans-Borgmeyer I, Wegner M. Sox10, a novel transcriptional modulator in glial cells. J Neurosci. 1998; 18(1): 237-50.

Levine JM, Reynolds R. Activation and proliferation of endogenous oligodendrocyte precursor cells during ethidium bromide-induced demyelination. Exp Neurol. 1999; 160(2): 333-47.

Lucchinetti CF, Bru¨ck W, Rodriguez M, Lassmann H. Distinct patterns of multiple sclerosis pathology indicates heterogeneity on pathogenesis. Brain Pathol. 1996; 6: 259 –274.

Marburg O. Die sogenannte "akute multiple Sklerose". Publisher: F. Deuticke (Leipzig und Wien) 1906, pp. 37 and 47

Marín-Teva JL, Dusart I, Colin C, Gervais A, van Rooijen N, Mallat M. Microglia promote the death of developing Purkinje cells. Neuron. 2004; 41(4): 535-47.

Nagata S, Hanayama R, Kawane K. Autoimmunity and the clearance of dead cells. Cell 2010; 140(5): 619-30.

Nait-Oumesmar B, Picard-Riera N, Kerninon C, Decker L, Seilhean D, Höglinger GU, Hirsch EC, Reynolds R, Baron-Van Evercooren A. Activation of the subventricular zone in multiple sclerosis: evidence for early glial progenitors. Proc. Natl. Acad. Sci. USA. 2007; 104(11): 4694-9.

Nielsen HH, Ladeby R, Fenger C, Toft-Hansen H, Babcock AA, Owens T, Finsen B. Enhanced microglial clearance of myelin debris in T cell-infiltrated central nervous system. J Neuropathol Exp Neurol. 2009; 68(8): 845-56.

Nieuwkoop PD, Faber J (1994) Normal Table of Xenopus laevis (Daudin). New York: Garland Publishing.

Ono K, Yasui Y, Rutishauser U, Miller RH. Focal ventricular origin and migration of oligodendrocyte precursors into the chick optic nerve. Neuron 1997; 19(2): 283-92.

Périer O, Grégoire A. Electron microscopic features of multiple sclerosis lesions. Brain 1965; 88(5): 937-52.

Robinson S, Miller RH. Contact with central nervous system myelin inhibits oligodendrocyte progenitor maturation. Dev Biol. 1999 Dec 1;216(1):359-68.

Schulz C, Gomez Perdiguero E, Chorro L, Szabo-Rogers H, Cagnard N, Kierdorf K, Prinz M, Wu B, Jacobsen SE, Pollard JW, Frampton J, Liu KJ, Geissmann F. A lineage of myeloid cells independent of Myb and hematopoietic stem cells. Science 2012; 336(6077): 86-90.

Sierra A, Abiega O, Shahraz A, Neumann H. Janus-faced microglia : beneficial and detrimental consequences of microglial phagocytosis Front Cell Neurosci. 2013 `Jan 30;7:6.

Small RK, Riddle P, Noble M. Evidence for migration of oligodendrocyte--type-2 astrocyte progenitor cells into the developing rat optic nerve. Nature 1987; 328(6126): 155-7.

Smith AJ, Liu Y, Peng H, Beers R, Racke MK, Lovett-Racke AE. Comparison of a classical Th1 bacteria versus a Th17 bacteria as adjuvant in the induction of experimental autoimmune encephalomyelitis. J Neuroimmunol. 2011; 237(1-2): 33-8.

Stankoff B, Demerens C, Goujet-Zalc C, Monge M, Peyron F, Mikoshiba K, Zalc B, Lubetzki C. Transcription of myelin basic protein promoted by regulatory elements in the proximal 5' sequence requires myelinogenesis. Mult Scler. 1996 Oct;2(3):125-32.

Stolt CC, Rehberg S, Ader M, Lommes P, Riethmacher D, Schachner M, Bartsch U, Wegner M. Terminal differentiation of myelin-forming oligodendrocytes depends on the transcription factor Sox10. Genes Dev. 2002; 16(2): 165-70.

Wolswijk G, Noble M. Identification of an adult-specific glial progenitor cell. Development 1989; 105(2): 387-400.

Yoshida M. Oligodendrocyte maturation in Xenopus laevis. J Neurosci Res. 1997 Oct 15;50(2):169-76.

Zalc B, Goujet D, Colman D. The origin of the myelination program in vertebrates. Curr Biol. 2008; 18(12): R511-2.

Legend to the figures

Figure 1: **Whole-mount confocal microscopy of optic nerve of a stage 49 *pMBP-GFP-NTR* transgenic *Xenopus* tadpole double labeled for GFP and MBP.**

In the *pMBP-eGFP-NTR* transgenic tadpole mouse *MBP* regulatory sequence drives expression of the transgene into myelin-forming oligodendrocytes. Immunolabeling for GFP (green) and MBP (red), a specific marker of myelin. The myelin around axons is stained by the anti-MBP antibodies (in red) and myelinating oligodendrocyte cell body and processes are in green (GFP^+). There is no overlap of GFP and MBP staining, because both RNA encoding *MBP* and MBP protein migrate out of the cell body to accumulate in the myelin sheath, while GFP stains oligodendrocyte cell body and processes, but is excluded from compact myelin. Note the clearly visible GFP^+ oligodendrocyte processes aligning along the myelinated axons (MBP^+ red) representing the most external spiral turn of the myelin sheath. Scale bar: 10 μm.

Figure 2: Live imaging of oligodendrocytes ablation during MTZ exposure and spontaneous recovery following cessation of treatment.

Successive observations for a period of 18 days of the same region of the optic nerve on a stage 52 tadpole by two-photon microscopy (D0 - R8). Images were taken with the same acquisition parameters. Tadpole was treated for 10 days with MTZ (10 mM) (observed on D0, D3 and D10), then returned to normal water for 8 days and observed after 3 and 8 days (R3, R8). The number of oligodendrocytes decreased progressively during MTZ treatment. During recovery period, new myelin-forming oligodendrocytes appeared. The graph shows the number of oligodendrocytes per optic nerve before treatment (D0) at the end of MTZ-treatment (D10 MTZ) and at 3 and 8 days of recovery (D3, D8). (n = 12; Scale bar: 20 μm).

Figure 3: Disruption of nodal structures following MTZ-induced demyelination.

Sections of control (A-I) of MTZ treated (J-R) stage 50 *pMBP-GFP-NTR* transgenic *Xenopus* tadpole optic nerve were doubly immunostained with anti-MBP A, C, G,I, J, L, P, R or either anti-ankyrin G (B, C, K, L) or anti-panNeurofascin (H, I, Q, R). Other sections were doubly immunolabeled with anti-panNeurofascin (D, F, M, O) and anti-panNav (E, F, N, O). Nodal constituants ankyrinG and panNav, which are aggregated, forming the node of Ranvier, are redistributed along the axons following demyelination. Note that pan-Neurofascin antibodies label both the node (D, F) corresponding to Neurofascin 186kDa and the paranode (D, F), corresponding to Neurofascin 155kDa. Scale Bar: 1µm

Figure 4: Mobilization and activation of microglia following MTZ-induced demyelination.

A) Stage 50 *pMBP-GFP-NTR* transgenic *Xenopus* tadpole were treated for 10 days with 10mM of MTZ. Optic nerve tissue sections of stage 50 *pMBP-GFP-NTR* transgenic *Xenopus* tadpole were triply stained with anti-GFP, conjugated-isolectin B4 (Ib-4), and DAPI. Stained optic nerves were dissected from animals either treated for 10 days with 10mM of MTZ before recovery (MTZ-treated) or after 8 days recovery (recovery) or non-treated animals (control). Note the impressive increase in numbers and change in morphology of Ib4+ microglial cells in MTZ-treated animals compare to control. Scale bar : 10 µm

B) Higher magnification of sections of MTZ treated tadpole doubly stained for GFP and Ib-4 (upper panel) or MBP and Ib-4 (lower panel). Upper panel: Ib-4^+ microglial cells engulfing a GFP^+ oligodendrocyte, small arrows point to contacts between $Ib4^+$ cells and GFP^+ labeled debris or cell body; z-stack, confocal microscopy. Lower panel: $Ib4^+$ cell in the process of phagocytose of MBP^+ myelin debris (arrow head). Scale bar : 10 µm.

C) Quantification of the number of Ib-4^+ microglial cell under the three experimental conditions examined.

Figure 5: Detection of Sox10$^+$ OPCs in the optic nerve of stage 50 *pMBP-GFP-NTR* transgenic *Xenopus* tadpole, before MTZ-treatment.

Whole-mount of optic nerve were immunolabeled with anti-GFP (A, C) and anti-Sox10$^+$ (B, C). Myelin-forming oligodendrocytes (GFP$^+$) are also Sox10$^+$, while OPCs are Sox10$^+$ but GFP$^-$. Note the aligned-in-rows disposition, typical of interfascicular glia, containing both GFP$^+$/ Sox10$^+$mature myelin-forming oligodendrocytes and GFP$^-$ /Sox10$^+$ OPCs. Scale bar: 10 µm

Figure 6: Detection of BrdU$^+$ cells in *pMBP-GFP-NTR* transgenic *Xenopus* tadpole before and after MTZ-treatment.

Stage 50 tadpoles were treated (or not: Control) for 10 days with MTZ (10mM) before being left for 24h in the presence of BrdU. Optic nerve sections performed either at the end of BrdU treatment or 8 days later were triple labeled with antibodies raised against GFP (green), Sox10 (purple) and BrdU (red). All myelinating oligodendrocytes (GFP$^+$; small and large arrows) observed before treatment and after recovery were also Sox10$^+$, some had incorporated BrdU (large arrows), but others were BrdU$^-$ (small arrows). Similarly some OPCs (Sox10$^+$, GFP$^-$) had incorporated BrdU (thin arrows) but others were BrdU$^-$ (arrow head). In the middle panel (MTZ-treated) arrowhead points to a Sox10+ cell which had not incorporated BrdU. Brdu$^+$ cells that do not belong to the oligodendroglial lineage are indicated by a white asterix. Scale bar: 10 µm

Figure 1

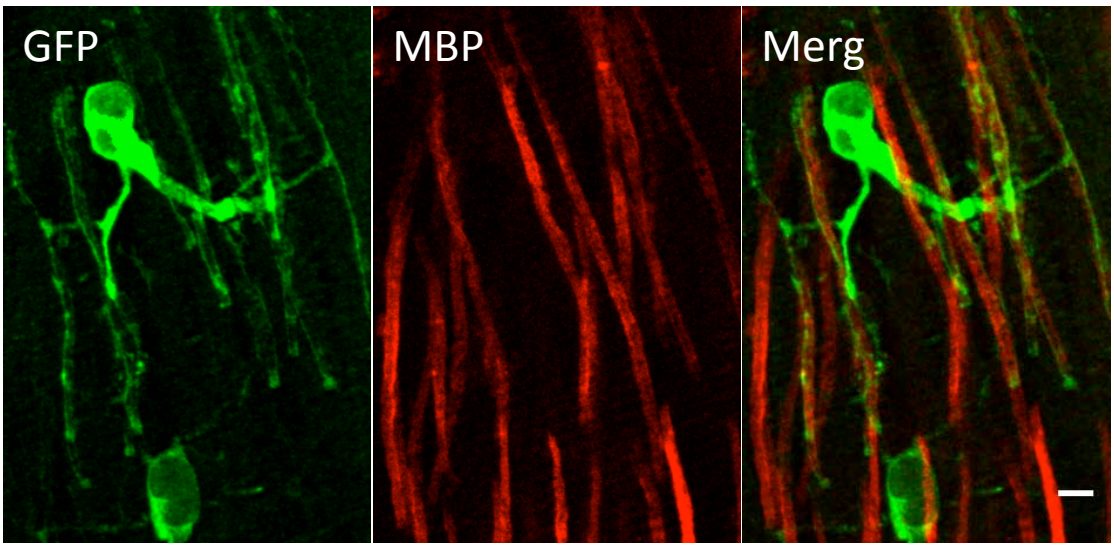

Figure 2

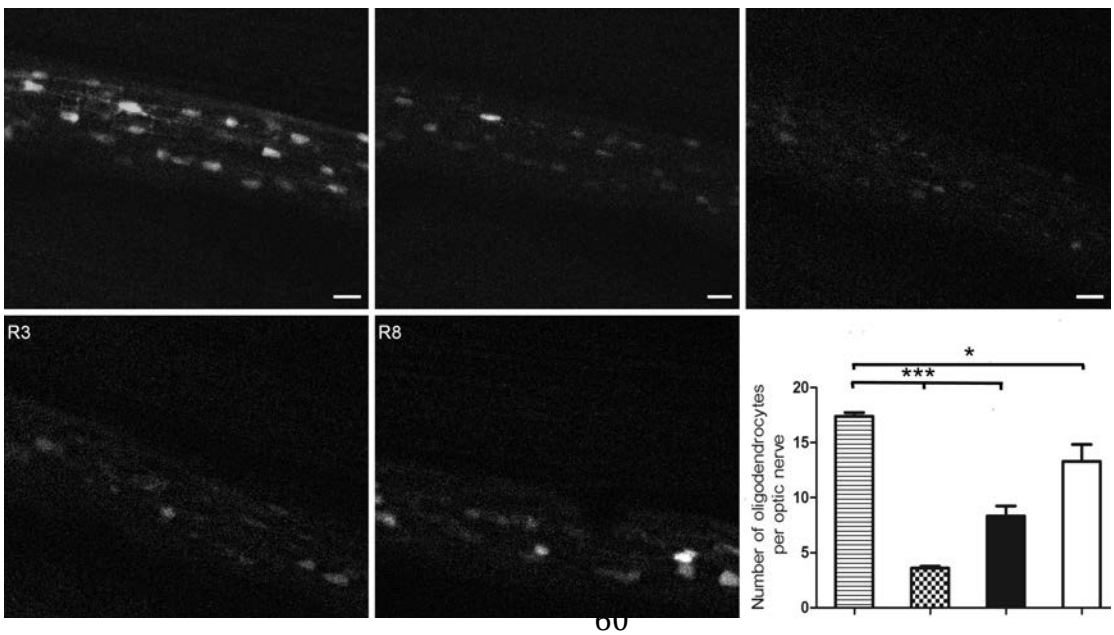

Figure 3

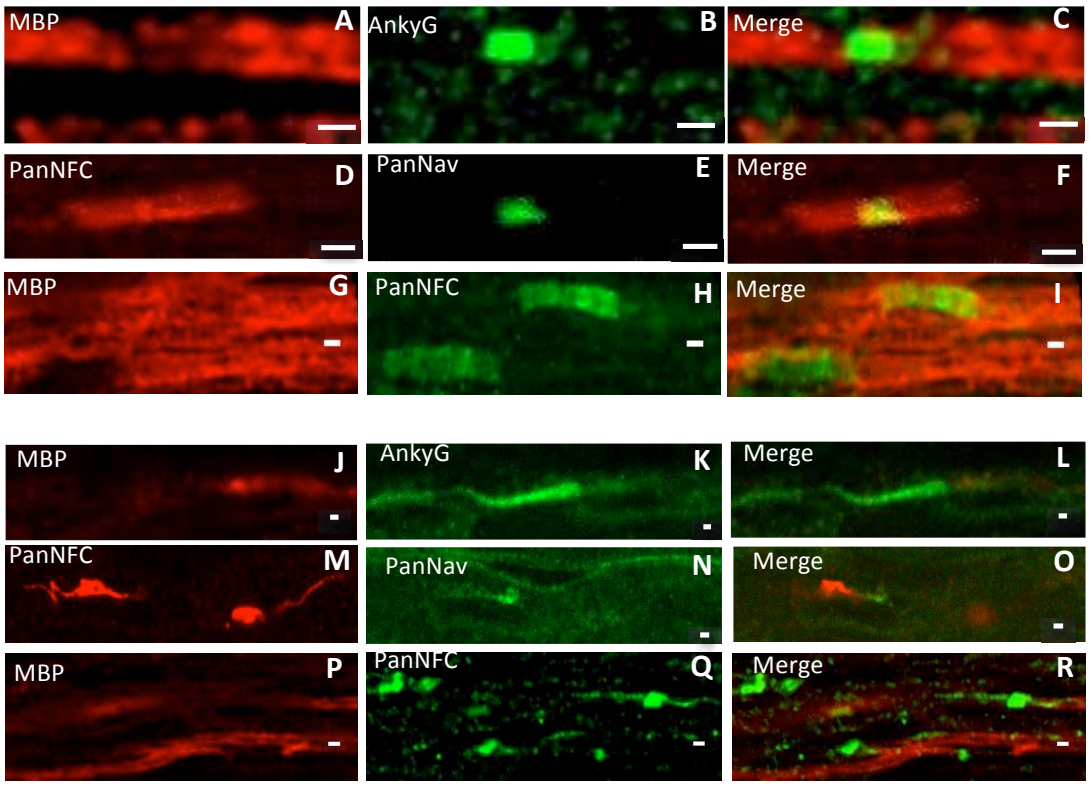
MBP
A
AnkyG
B
Merge
C
PanNFC
D
PanNav
E
Merge
F
MBP
G
PanNFC
H
Merge
I
MBP
J
AnkyG
K
Merge
L
PanNFC
M
PanNav
N
Merge
O
MBP
P
PanNFC
Q
Merge
R

Figure 4

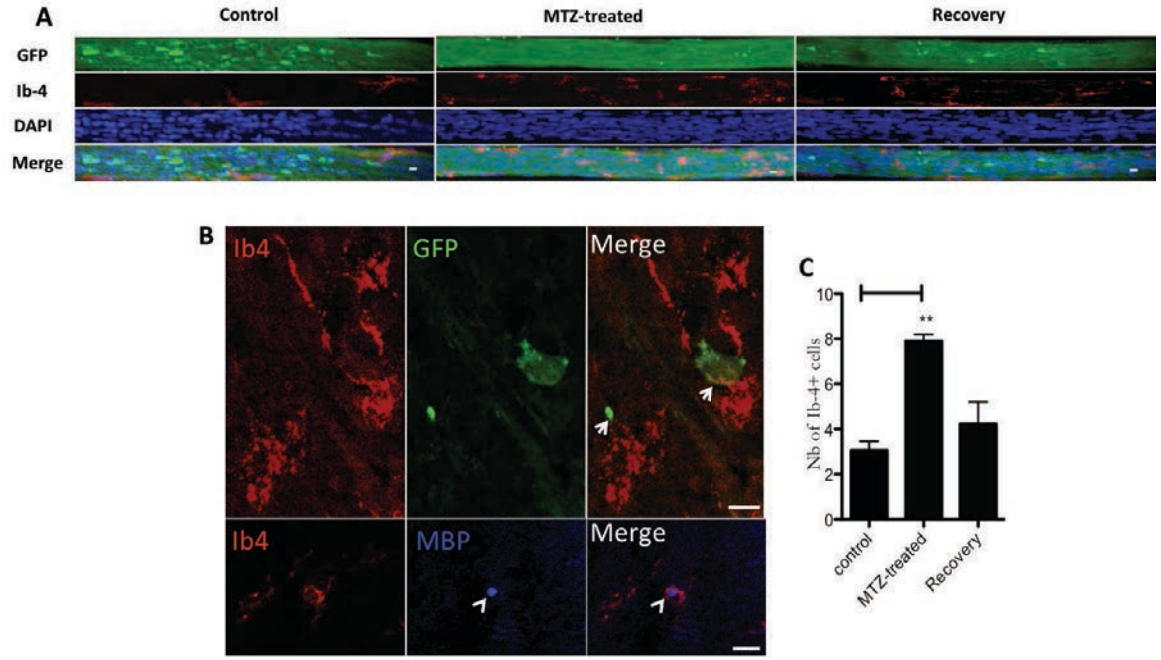
A
Control
MTZ-treated
Recovery
GFP
Ib-4
DAPI
Merge
B
Ib4
GFP
Merge
Ib4
MBP
Merge
C
Nb of Ib-4+ cells
10
8
6
4
2
0
**
control
MTZ-treated
Recovery

Figure 5

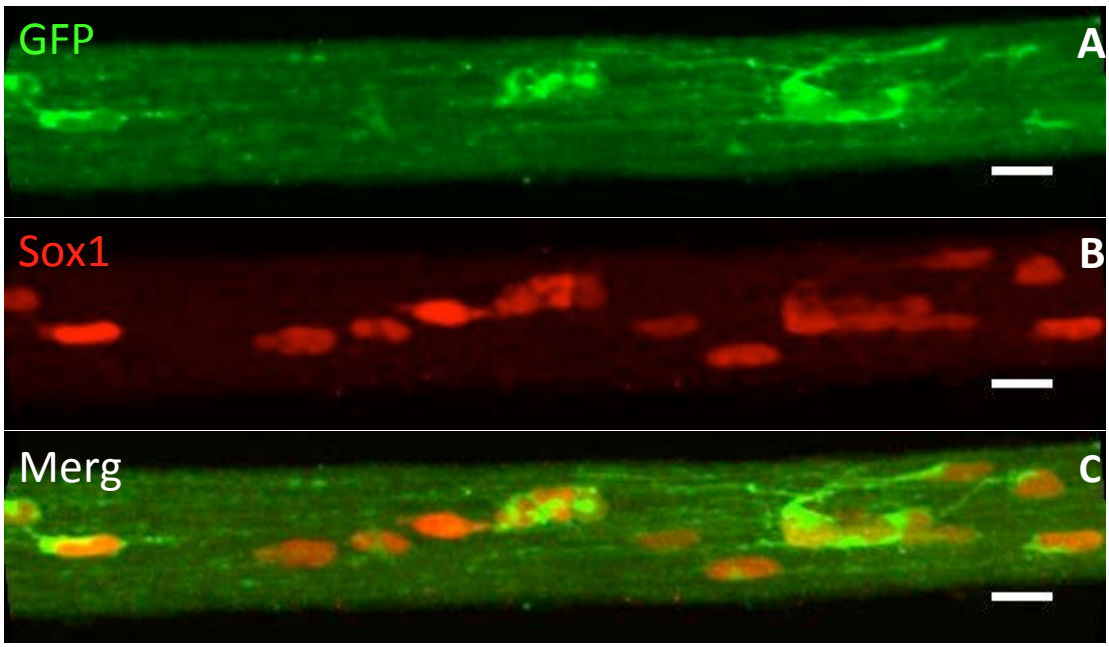

Figure 6

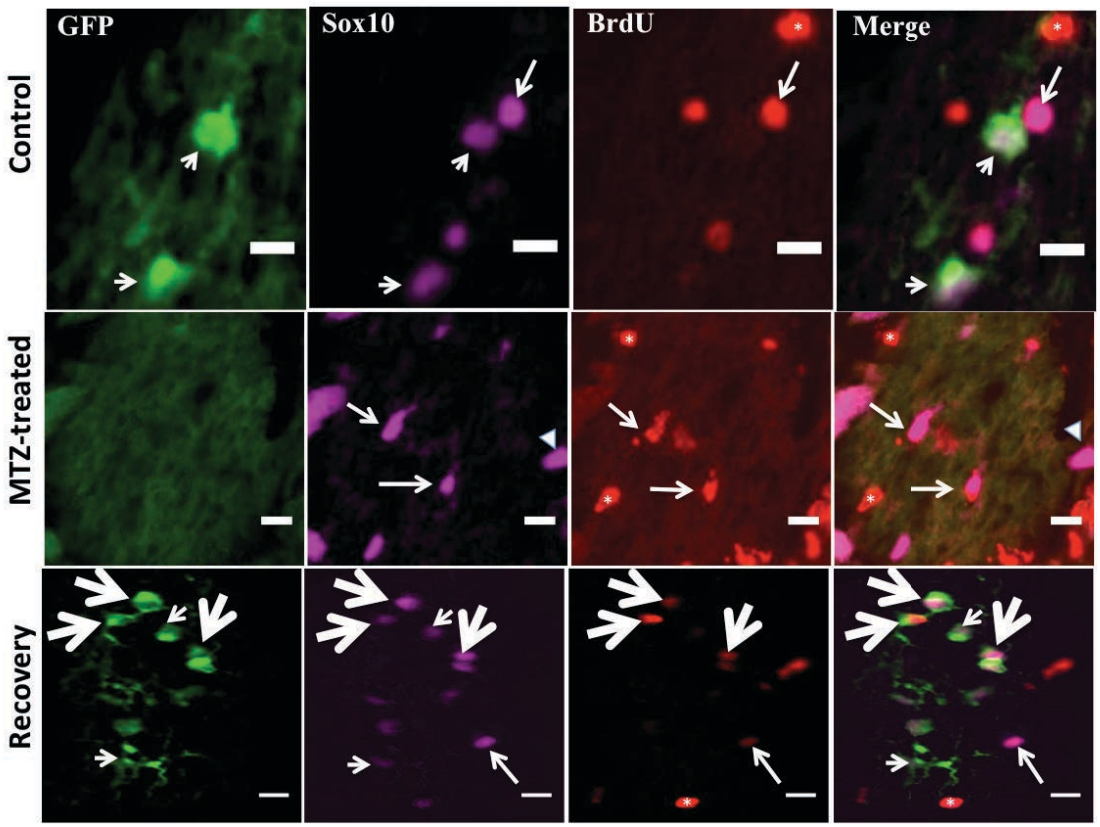

Part II

Physiological consequences on bidirectional signals between oligodendrocytes and axons following demyelination and remyelination.

PART II

Physiological consequences on bidirectional signals between oligodendrocytes and axons following demyelination and remyelination.

The survival of an organism depends on its ability to successfully interact with the environment, to a large part this depends on the nervous system in developing animals. As an organism grows the neural circuits and electrical properties of neurons within the circuit undergo activity dependent and activity independent changes and help refine immature neural circuit. The changes in neural circuit continue in adult brains.

Myelin is shown to control neuronal properties such as conduction velocity, spike frequency by controlling the internode length and the density of ion channels at the node and paranode (Dupree et al, 2004). The shape of the action potential, amplitude and firing frequency can be modulated by myelin. In addition to controlling the action potential myelin also plays an important role in synapse formation. Myelin proteins Nogo-A, MAG and OMgp cause the tips of growing axons to collapse and prevent axonal sprouting and could help prune the synapses (Chen, 2000 and Mckerracher , 1994).

When Nogo-66 is knocked out in mice, the critical period of ocular plasticity is extended (McGee et al, 2005). In mice loss of Erb recptor in oligodendrocytes leads to downregulation of dopamine recptor 1. In these mice branch points on cellular process, myelin thickness and conduction velocity decreases. The mice exhibit behavioural deficits similar to schizophrenia. The exact correlation between erb recptor loss and D1 is not known. Never the less it can be concluded that, by attenuating level of expression of myelin proteins, morphology of synpase and hence synaptic plasticity of neurons can be can be altered.

Neurons also have an effect on myelination, this reciprocal interaction is crucial and very little is known about it. Prematurely opening the eyes of rabbits increases myelination (Tauber et al, 1980). Activity dependent enhancement of myelination and myelin dependent synaptic plasticity function should function synchronously to foster a healthy nervous system.

Under pathological conditions, established complexes of axons and oligodendrocytes can break down, resulting in demyelination. The consequence of demyelination to neural circuit structure and function are also not well understood. While demyelination has been shown to slow axonal conduction, the effects of altered signaling and loss of interactions between axons

previously myelinated by the same OL on information processing through a central circuit has not been tested.

The visual system of Xenopus laevis has been as well-established model to study stimulus induced plasticity and morphology change **(Figure 1).** Retinal ganglion cells (RGC) extend axons from the retina to their target in the contralateral tectum. The RGC arborize and form synapse with tectal neurons dendrites. The effect of visual stimulus on the RGC arbor dyanamics is well studied in xenopus. I have used this system to study the morphology changes in the RGC arbor after demyelination.

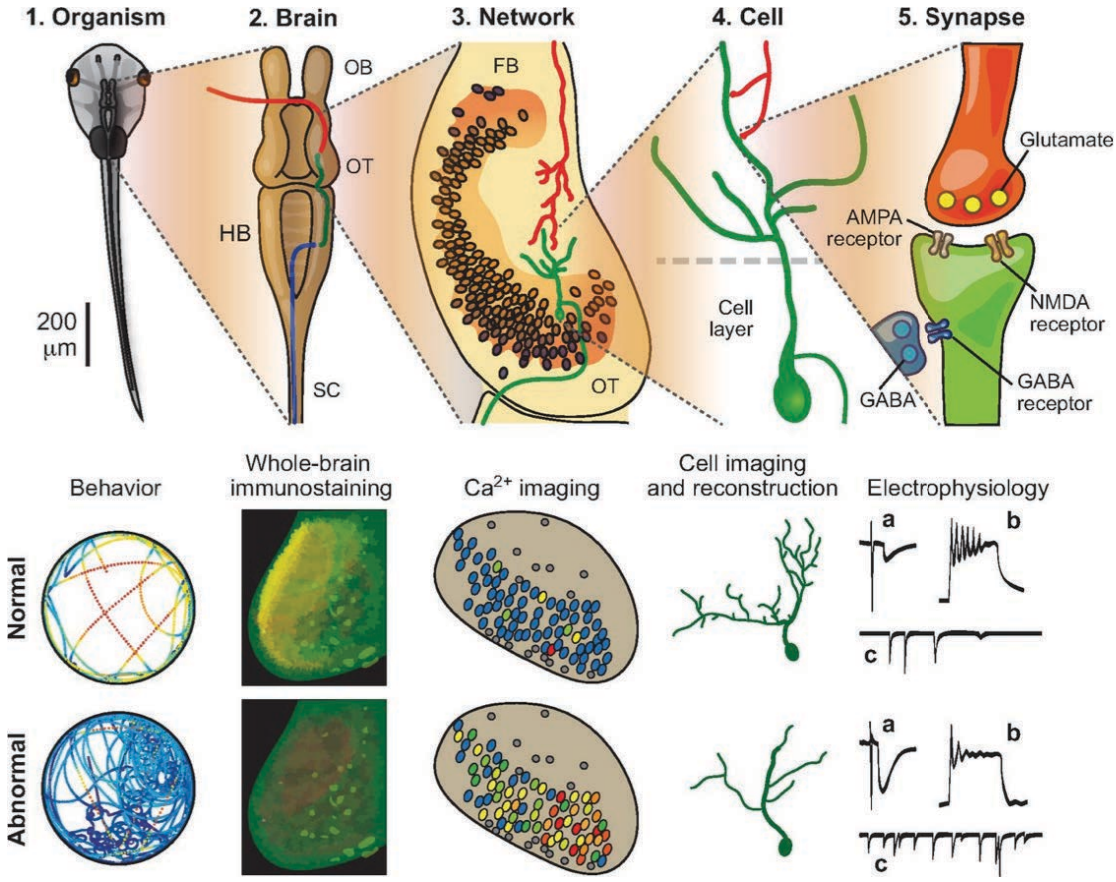

(Kara, 2013)

Fig1: The *Xenopus* tadpole as a versatile research model, shown with key experimental techniques that are used.

(1) Top view of the animal 3 weeks post-fertilization. Several behavioral tests can be used to assess brain development: for example, wild-type animals usually swim along the sides of the container (represented by a circle; bottom), whereas animals with altered excitation/inhibition

balance tend to circle in the middle of it. (2) General view of the brain. OB, olfactory bulbs; OT, optic tectum; HB, hindbrain: SC, spinal cord; red, projections from the retina; green, tectal projections to the hindbrain; blue, descending projections to the spinal cord. An isolated brain provides an accessible *in vitro* preparation, and whole-brain immunostaining (bottom) can be used to quantify global alterations in brain biochemistry (an exaggerated staining for GABA is shown). (3) Horizontal section of the optic tectum (OT) and caudal forebrain (FB); at this level, Ca^{2+} imaging can be used to detect abnormal seizure-like patterns of activity (bottom). (4) At the neuron level, *in vivo* or *ex vivo* imaging allows assessment of cell morphology development. (5) At the synaptic level, electrophysiology offers a way to quantify maturation of synaptic and intrinsic properties of the cell through recordings of (a) evoked synaptic responses, (b) spiking in response to current injections and (c) spontaneous synaptic activity. The figure is taken from (Kara,2013)

SUMAMRY

In *X laevis* tadpole the ability to visualize synapses in real time provides insights about the dynamic mechanisms underlying synaptogenesis. It has been shown that visual stimulation enhanced the stability of the RGC arbor, while concurrently inducing the retraction of exploratory branches with few or no synaptic (Ruthazer, 2006). Dendrites of tectal neurons form synapses with RGC arbor, it has been demonstrated in single tectal neurons visual stimulation induces coordinated changes to neuronal responses and dendritogenesis (Chen, 2010)

In my final year of my PhD in collaboration with Kurt Haas laboratory in University of British Columbia at Vancouver we planned to study the morphogenetic changes in the RGC arbor after demyelination by live imaging within the intact and unanesthetized tadpole.

The aim of my experiment is to study the effects of optic nerve demyelination on RGC axonal morphology in the MBP-GFP-NTR transgenic line. We use electroporation to transfect RGC and directly image RGC axonal morphology within its terminal field in the optic tectum. We propose to examine the effects of demyelination and re-myelination on RGC axonal morphology, growth dynamics and activity-dependent growth plasticity

I hypothesize that demyelination will lead to changes in the developmental refinement of RGC projections in the tectum. The processes at the arbor would be more dynamic, retract and extend at a higher rate to make new synapses, compared to control.

METHODS AND MATERIALS

Animals

Female albino X. *laevis* frogs were primed with 750ul of gonadotropin hormone and transgenic pMBP-GFP-NTR (Kaya.F, 2012) males were primed by injecting 300ul of gonadotropin, the frogs were left in a tank overnight, the eggs were collected the next day. Freely swimming tadpoles were housed at 19°C in 0.1x Steinberg's solution (10 mM HEPES, 60 mM NaCl, 0.67 mM KCl, 0.34 mM $(CaNO3)2$, 0.83 mM $MgSO4$, pH 7.4) and maintained on a 12-h light/ dark cycle. Experiments were conducted on Stage 55 tadpoles (Nieuwkoop and Faber, 1994) and fed nettle powder. Experiments were performed within guidelines set by the Canadian Council on Animal Care. The Animal Care Committee of the Faculty of Medicine at the University of British Columbia approved protocols that were used.

Metronidazole preparation and use

MTZ (Sigma Aldrich) was dissolved in filtered tap water containing 0.1% DMSO (Sigma Aldrich). MTZ was used at concentrations of 10mM for 10 days. Control animals were kept in the same media without MTZ. Furthermore, transgenic tadpoles were maintained in 600 ml of MTZ solution (maximum 10 tadpoles/600 ml) at 20°C in complete darkness (MTZ is light-sensitive) and changed every 2 days throughout the duration of treatment. For regeneration experiments, MTZ-treated animals were allowed to recover for up to 6 days in normal water in ambient laboratory lighting. Transgenic tadpoles were treated with drugs at stage NF 55. In the optic nerve at the electron microscopic (EM) level myelination was reported to begin in the middle portion at stage 48/49 and the number of myelinated axons increases sevenfold between stage 50 and 57 (Cima and Grant, 1982).

Electroporation Protocol

Embryos stage 33/34 were placed in fresh 0.1X steinberg. Embryo anaesthetized in 0.01% MS222. Anaesthetized embryos were individually transferred into the transfection chamber (Julien et al 2007) in a drop of 1x steinberg, placed into the main channel of the chamber and excess medium was gently removed. Homemade flat-ended 0.5 mm wide platinum electrodes (Sigma, 26788-1G) were placed into the transverse channel of chambers. Cmv-tdTomato (Addgene, AY678269) was injected (10nl) into the retina at a concentration of 2mg/ml. Electroporation parameters are 20v, 8 pulses, 10ms pulse duration and at a frequency of 1Hz. The electroporated tadpole was transferred to 0.1X Steinberg to recover.

Chamber

All the chambers and its holders were designed on CAD software. A 3-d printer (leapfrog 3D printer, 871880127001) was used to print the design using poly lactic acid.

There are two main chambers made:

1) Electroporation chamber: A mould for stage 33/34 was made and sylgard (sigma, 761028-5EA) was poured into it and allowed to polymerize at 60^{o} C. The hardened plastic was used as electroporation chamber, with electrodes. The dimensions for the chamber are the same as used in the article Julien et al, 2007.

2) Chamber to hold NF 55 embryo for imaging: There are 3 parts to the chambers **(Figure2)**. The inner most chamber (green in color) hold the tadpole; the middle piece (grey in color) is portion where the green piece with the tadpole in it rest along with the perfusion system; the last part is the frame (yellow color) that hold the inner and middle chamber along with the LED/projector (black in color) and is made of plastic and can be screwed into the stage of the two-photon.

The other parts of the chamber are the red ‘L’ shaped plastic to hold the glass cover slip. The magenta screen is where the visual stimulus is presented.

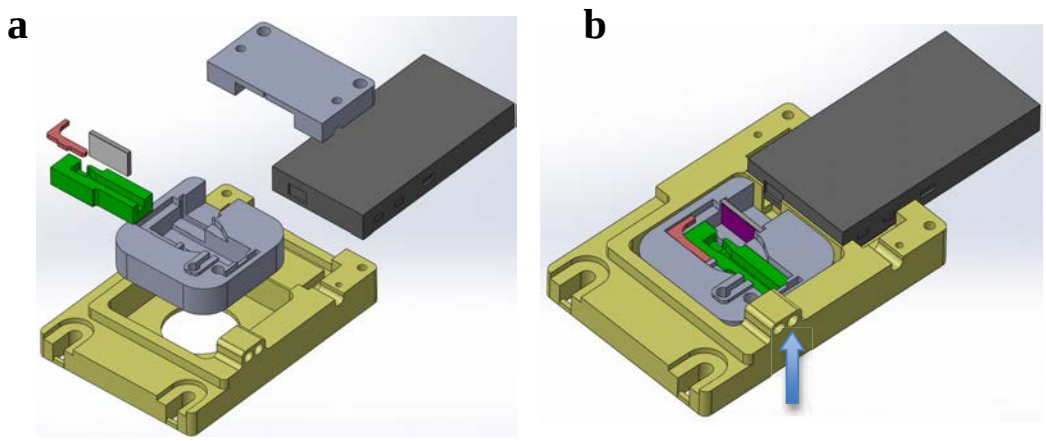

Fig 2: 3-D drawing of the chamber

a). Shows the 3 parts that made up the entire chamber. The grey square adjacent to the green piece is the screen on which the stimulus was projected.

b) After assembly of the 3 parts the chamber was connected to perfusion system. Pipes were connected at position shown by arrow. In most cases the projector was replaced by a standard 5mm LED (470nm).

Visual stimulation

To apply light stimulus, a diode (470nm) was projected onto the eye. A Continous stimulus of 50 ms OFF stimuli presented every minute for 60 min with interstimulus ON light stimulation (Dunfield et al, 2010), this stimulus paradigm was run using matlab (Matlab, The mathworks Inc, Natick,MA). The stimulus was put off during image acquisition due to bleed through into the imaging channel. Image was acquired every 15min.

Screening tadpoles for imaging.

Tadpoles electroporated at stage NF 32/33 with Cmv-td tomato were screened at stage 48, only transgenic tadpoles (GFP positive) that have myelinated RGC electroporated were raised to stage 55 (Leica fluorescence stereomicroscope) The tadpoles were allowed to grow to reach stage 55. We planned all our experiments at this stage because the axons are fully myelinated and there are no axons, which have only stretches of myelin. It should also be noted that a large number of axons are myelinated at this stage and I choose only the RGC that are myelinated to image. The transgenic MBP-GFP-NTR tadpoles are not albino so to image them we had to remove the skin covering the tectum. Tadpoles were paralyzed and the skin over the tectum was removed in sterile condition, care was taken not to rupture the blood vessel that runs over the midline and temporal edge of tectum **(Figure 3)**. The tadpole was placed in the chamber to image and was constantly perfused with oxygenated 0.1x steinberg. A glass cover slip was placed over the brain and held in place with a plastic holder. Tadpoles with single RGC that had strong expression of td-tomato were chosen for imaging. If there were more than one RGC labeled and the arbor overlapped then it could not be used. This level of screening was done on the two-photon. The laser power was maintained as low as possible to avoid bleaching and blebing of the arbor. The tadpoles that matched the criterion for imaging were 1 in 20 of the stage NF 45 screened tadpoles.

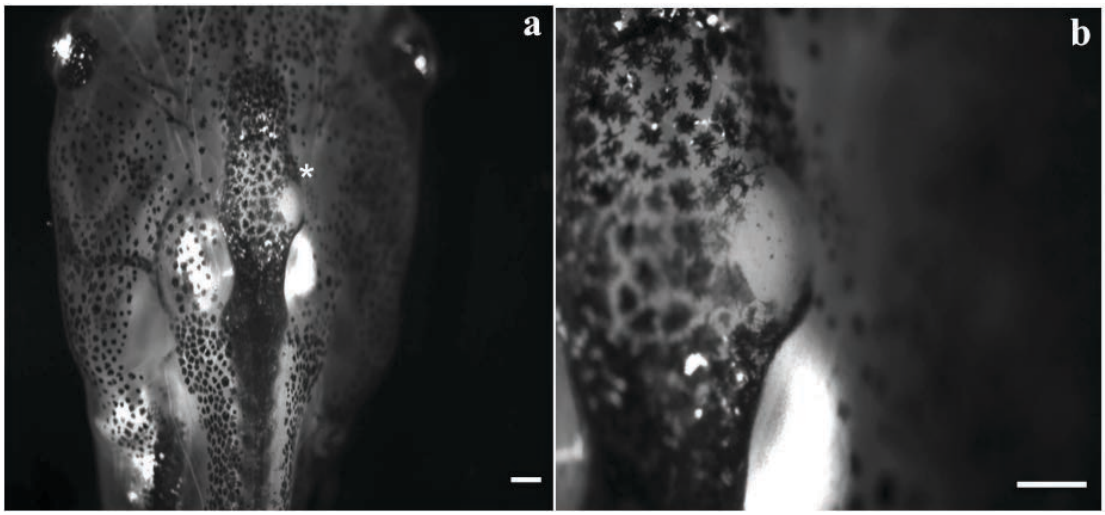

Fig 3: Skin removed over the tectum of stage 55 tadpoles.
Scale bar: a=500um, b=500um

In Vivo Time-Lapse Two-Photon Imaging in the Unanesthetized Brain

In order to image dynamic neuronal growth in vivo without the confounding effects of activity blockade from anesthetics, awake tadpoles were immobilized with the reversible paralytic pancuronium dibromide (PCD, 3 mM, Tocris).

The tadpole skin on the tectum onto which the RGC projected was removed in sterile condition carefully to avoid rupture of blood vessel. The tadpole was mounted on a custom-built imaging chamber. The tadpole was continuously perfused with oxygenated 0.1X Steinberg's solution. Images of fluorescently labeled neurons were acquired using a custom-built two-photon microscope consisting of a modified Olympus FV 300 confocal microscope (Olympus, Center Valley, PA) and a laser (Coherent, Santa Clara, CA). The optic tectum was imaged at a resolution of 512x512 pixels and zoom factor of 1.5x or 2x.Three- dimensional stacks of images of the retinal ganglion cell arbor were captured using a 60x, 1.1 NA, water immersion objective (Olympus). The effort was made to capture the entire extent of the arbor. When the arbor covered the entire tectum and could not be captured in its entirety, the densest region of the arbor was imaged. Optical sections were acquired at a distance of 1.5um on the z- axis. Stacks of images encompassing RGC arbor were taken at 15 min intervals for 1 hr. Following imaging, tadpoles were fixed in 4%paraformaldehyde.

Whole mount immune labelling:

Fixed tadpole brain and spinal cord was dissected and rinsed in PBS 1x containing 0.1% Triton X-100 (PBT 0.1%) for 2 hrs with change in PBS1X 0.1% triton every 15minutes. Blocking in 10% normal goat serum in PBT 0.1% for 1 hr. Primary antibodies used are Chicken anti-GFP (1:2000, aves lab), rabbit anti-m-cherry (1:500,encore technology) and mouse anti-MBP (1:1000, kindly provided by Saburo Nagata, Women's Tokyo University, Japan). Primary antibody were added in the blocking solution and incubated for 48hrs on a gentle shaker at 4 °C. The primary antibody was removed and the brain rinsed for 2 hrs in PBT 0.1%, with changes every 20min. Secondary antibodies, alexa 488, alexa 594 and alexa 647 (1: 1000, Invitrogen) were used in blocking solution, and incubated over night at 4 °C on a gentle shaker. The secondary antibody is removed and the labelled brains rinsed in PBT 0.1% for 2 hrs with changes every 20min. DAPI (Invitrogen) was used to label the nuclei and rinsed in PBT 0.1% for 2min and mounted on slide in FluorSave Reagent mounting medium (Calbiochem).

A

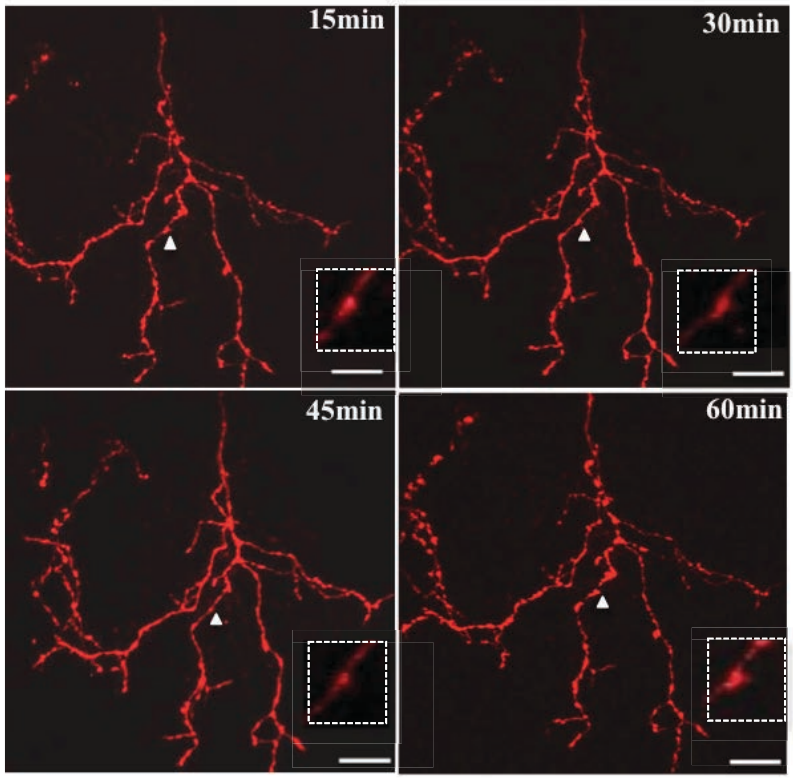

B

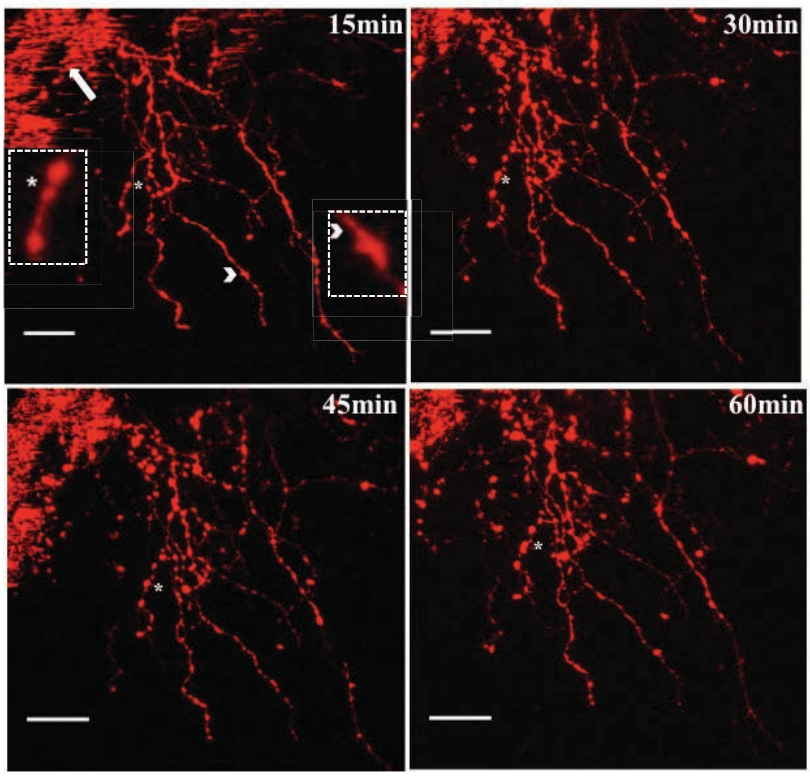

Fig 4: Time lapse Imaging of RGC arbor in pMBP-GFP-NTR tadpole

A) Time lapse of CMV-tdTomato transfected RGC arbor. Z project of stack of mages taken every 15min when constantly visual stimulated with 50ms OFF stimulus and interstimulus ON stimulus. Inset shows a process that retracts and reappears, it is labeled with an arrow head (B) Demyelinated RGC arbor, * indicates blebbing (inset). Arrow indicates skin that is covering the rest of the tectum; Arrowhead (inset) shows a process that appears. Scale bar 10um.

RESULTS

Morphology of RGC arbor after demyelination

The aim of the experiment was image RGC arbor before demyelination and after demyelination and after recovery. The tadpoles that were suitable for imaging were imaged every 5min for an hour. The arbor was bleached during the last few time points and developed blebs. The images were analyzed by making a movie (Image J) of the stack of images taken at 5min interval for an hour. It was noticed that there was no change in morphology of the arbor. As there was no change in the morphology of the arbor at every 5min (n=5), we decided to increase the time interval of imaging to 15min reducing the exposure to laser which would help reduce bleaching blebbing.

The chance of an animal imaged for 1hr (either imaged every 5 or 15min) to survive was low (1 in 10 tadpole survived). The tadpoles that did survive were treated with 10mM MTZ for 10 days and control tadpoles were treated with 0.1%DMSO and maintained in dark. The tadpoles after 10 days of MTZ treatment were again paralyzed, the skin removed and imaged in the same manner as mentioned. In both the MTZ treated and Control tadpoles there was a scar at the site of skin removal, the tectum at this region did not look healthy it looked swollen. In both cases there was absence was fluorescence, the arbor was not visible even at high laser power. As there was absence of fluorescence in control and MTZ treated tadpoles, the absence cannot be attributed to demyelination.

To over come this practical difficulty we choose not to use the same animal to image before and after demyelination. We treated animals with 10mM MTZ for 10 days and this tadpole was imaged every 15min for 1 hr. Control animals that were maintained in 0.1% DMSO was also imaged. We continued to use the 15min interval, as there was no difference between images taken at 5min interval. Tapoles were fixed after imaging and immune labeled to verify demyelination of the RGC imaged.

The MTZ treated tadpoles arbor was more amenable to bleaching and blebing compared to control **(Figure 4)**. In conclusion there was no arbor retraction and elongation for the 1 hr the arbor was imaged n=5. As there was no change after demyelination, we did not look at the arbor after re-myelination.

DISCUSSION

In vivo imaging studies in Xenopus system have revealed that the RGC axon terminal and tectal dendritic arbor are remarkably dynamic structures especially in developing stages. It has been shown that synaptophysin and synaptobrevin are localized at a higher concentration at processes that are dynamic in immature retinotectal system (Ruthazer, 2006).In tadpoles at mid larval stages (46-50) there is an apparent decrease in size of arbor with respect to the tectum. This is shown to be due to rapid growth of tectal neuropil and not due to retrataction of the arbor (Sakaguchi, 1985). In axon regeneration experiments during the early phase of regeneration the axon sprouts several branches, which retracts, and degenerates resulting in an ordered projection of the arbor unto the tectum (Fujisawa, 1982).

In our experiment we do not see changes in the morphology of the arbor at stage 55 in control animals even though the eye is continuously stimulated. The arbor may be at its mature state and has developed ways to be plastic which does not include change in morphology. It can be speculated that in the static arbor there could be a change in density of ion channel and neurotransmitter release vesicles. It could be interesting to live image distribution of ion channels, AMPA and NMDA receptors after demyelination at the postsynaptic end.

The postsynaptic tectal neuron dendrites have not been imaged in this study. The tectal neurons dendritic arbor could become dynamic after demyelination and leave the RGC arbor with no changes in morphology. I electroporated tectal cell in my experiment to study morphometrics of the tectal neuron dendrites, but they were at a depth that could not be captured by the two-photon. Another approach to study these cells at stage 55 could be an ex vivo approach, remove the brain and image the tectum in a sterile medium.

PARTIII

CONCLUSION AND PERSPECTIVES

The work presented in this thesis has aimed towards providing insight into the remyelination process in p (MBP-GFP-NTR)

In my PhD project I examined the origin of progenitors that repopulate the demyelinated optic nerve. The data suggest that, $Sox10^{+}$ OPCs, which are already present in the optic nerve prior to the experimentally induced demyelination, are responsible for remyelination. There was no drastic increase in cell proliferation in the optic nerve or the supra chiasmatic region following demyelination.

The experiments were performed on stage 55 tadpoles, this is prior to metamorphosis and the ability of the tadpole to regenerate is high. The metamorphic changes of frog development are all brought about by the secretion of the hormones thyroxine (T_4) and triiodothyronine (T_3) from the thyroid during metamorphosis. It is known that T3 induces OPC maturation (Gao et al., 1998). If the tadpole is demyelinated in the pre- metamorphosis period there will be an effect of T3 in inducing rapid differentiation and remyelination. Inability of OPC to differentiate at the site of lesion leads failure of remyelination.

It would be interesting to look at Remyelination in adult Xenopus (post metamorphosis); it has been shown in zebra fish that in older fishes the optic nerve fails to remyelinate with increasing age (Münzel et al., 2014). To check if repeated demyelination would lead to inability of the optic nerve to remyelinate, we could treat the tapdole with the pro-drug and let is recover for a a few days and repeat the process to check if the resident progenitors are depleted what is the source of progenitors.

Myelin debris is removed by microglia; contact of myelin debris with OPC inhibits differentiation (Robinson and Miller, 1999). To facilitate differentiation of OPC at the site of lesion, the environment should be non-hostile. The nodal and paranodal proteins are dis-assembled after demyelination, these features are very similar to that found in rodent and mammalian model after demyelination.

The second project in my PhD is the oligodendrocytes and neuronal interaction after demyelination in the optic nerve of xenopus. This project was a collaboration with Dr Kurt Haas lab in University of British Columbia, Canada. I used the demyelinating line *p(MBP-GFP-NTR)* and electroporated the retina with *CMV-tdTomato* plasmid. Tapoles with single RGC electroporated and myelinated by the GFP positive cells were taken for treatment with the prodrug MTZ. I observed no change in the morphology of the arbor after demyelination. The arbor that was treated with MTZ were more sensitive to imaging and developed blebs. In our previous paper (Kaya et al., 2012) we have shown that there is no axonal damage after

demyelination. Nevertheless it appears that the demyelinated axons are more sensitive to the manipulation done to the tectum prior to imaging.

As shown in chapter one the node proteins and ion channels disassemble after demyelination. There could be a similar event at the axon arbor, where the presynaptic proteins and synaptic vesicles could modify its distribution and accommodate the change due to demyelination. It would be interesting to label presynaptic proteins by immune labelling or electroporation to examine if there are changes.The possible changes in the post synaptic end, that is the dendrites of the tectal neurons were not examined. If synaptic contacts between the RGC arbor and the denrites of tectal neurons are lost, there could be changes in the morphology of the dendrites.

Due to lack of time I could not carry out experiment to check changes in the receptive field of the tadpoles post demyelination, I think these experiments could be very interesting to study how the visual system changes after demyelination. In MS the optic nerve is region which is affected and leads to vision loss. The retino-tectal system in Xenopus is a simple model to study changes after demyelination.

APPENDIX

TRANSGENIC ANIMALS GENERATED

INTRODUCTION

Transgenesis has become a major technique in basic research and has multiple applications. Transparent animal models such as zebrafish and xenopus larvae are preferable for transgenesis for practical reasons such as, large number of eggs laid, fertilization and development is external. The larvae of these models are transparent hence screening transgene expressing animal is easy, if the transgene is fused to a fluorescent protein. Small model organisms, such as amphibians and zebrafish are increasingly being used at various stages of drug development and are a economical model compared to rodents and nonhuman primates.

Xenopus is a very suitable non-mammalian model to study myelination. Myelin in Xenopus is remarkably similar to that of mammals. The morphology of developing oligodendrocytes is comparable to that of rodents. To study myelination, demyelination and remyelination, we have produced a transgenic Xenopus line, *pMBP-eGFP-NTR*, (Kaya, 2006, in collaboration with A Mazabraud and F Kaya from University Paris Sud. This transgenic line has been shown to be a reliable model for demyelination, remyelination and also serves as medium throughput model for screening therapeutics.

In demyelinating disease such as multiple sclerosis it is of paramount importance to initiate remeylination rapidly to prevent axonal damage. To initiate remyelination, the crucial step is to repopulate the area of demyelination, these cells could come from cells already present in the demyelianated area or be recruited from the surrounding white matter or subventricular zone. We plan to study recruitment of progenitors after demyelination in our transgenic line. Understanding the process of remyeliantion is this model system will permit us to test potential therapeutics that could enhance the recruitment of OPC. To study the recruitment of progenitors in real time we need a reporter line for OPC. Having a reporter line for progenitors that could be crossed with the *pMBP-GFP-NTR* line would enable us to study the effect of therapeutics on oligodendrocytes precursor cell (OPC) recruitment.

The interaction between oligodendrocytes and neurons is an important factor to initiate myelination as well as to remyelinate a demyelinated axon. The node of Ranvier and the axon initial segments are the non-myelinated region along the length of a myelinated axon where the neuron is exposed to the external milieu. The aggregation of sodium channel and adhesion

molecules at the nodes have been studied in rodents, but the mechanism of assembly of the node and the factors that initiate the formation of node in CNS is a topic that is being actively researched currently.

To study the assembly of node of Ranvier and live image the formation of the node during myelination, we wanted to generate transgenic lines that express the beta1 subunit of sodium channel in fusion with fluorescent proteins, we choose the beta1 subunit as it is small in size compared to the pore-forming alpha subunit. Larger the size of the transgene it is difficult to insert the transgene in to the genome. we have had success only with a maximum of 11-12kb plasmids. These lines that when generated can be crossed with *p(MBP-GFP-NTR)* line to study the dynamics of these molecules after demyelination.

MATERIAL AND METHODS

Plasmid construction

MCS4-tdtomato

An 819bp enhancer to *Sox10,* present 5' to the mouse *Sox10* coding sequence. This sequence is highly conserved across species and is referred as MCS4 (multiple species conserved sequence)(Anthony Antonellis et al, 2008). 819bp sequence was PCR amplified from the pDONR221 vector and cloned into a vector at BamH1 site of the membrane tagged td-tomato UAS gal4 vector that has thymidine kinase (tk) minimal promoter. The membrane targeting sequence is lyn kinase.

Neuronal-β-tubuline-β1Nav-GFP (*Nβt-β1Nav-GFP) and Nβt-β1Nav-dsRED*

Mice sequence of β1 subunit of voltage gated sodium channel (*β1Nav)* 656bp cDNA ORF (Origene,MG202467) was purchased in a vector with CMV promoter and a C-terminal GFP. The *β1Nav* portion was PCR amplified and digested with SacII and cloned using two flanking primers containing SacII restriction sites at their 5′ end, and the product was inserted into the unique SacII site in frame to eGFP in the Neuronal-β-tubulin-eGFP plasmid (Cohen et al, 2001). The orientation of *β1Nav* insertion was check by sequencing. I also generated a *Nβt-*

β1Nav-dsRED plasmid, the *CMV-ds red* was purchased from clontech (632412). The animals and transfected cell cultures were not healthy, so we did not proceed to use it for trangensesis.

Trangenesis

The MCS-4-tdtomato plasmid was linearized with SacII, *Nβt-β1Nav-GFP* was linearized with ApaL1.Linearized plasmid was run on a gel to confirm the absence of undigested plasmid. The linear plasmid was purified (Qiagen plasmid purification kit) and dissolved in endotoxin free water provided in the kit. The DNA was quantified, aliquoted and stored at -20°C. The linearized plasmid was used at a concentration of 200ng/ul. Simplified restriction enzyme-mediated integration (REMI) procedure (Kroll and Amaya, 1996; Sparrow et al, 2000; Chesneau et al, 2008) was used to generate the Sox10 reporter line and *Nβt-β1Nav-GFP transgenic tadpole*. To generate double transgenic xenopus that express both the sox10-tdtomato and MBP-GFP-NTR at the F0 generation, I mixed the two linearized plasmids after purification, at a concentration of 200ng/ul of each. MBP-GFP-NTR plasmid was linearized using EcoRI. The fluorescence was detected directly in live embryos using an AZ100 Nikon Zoom fluorescence Microscope.

RESULTS

Sox10 reporter line

To verify transgene expression, the tadpoles were screened for fluorescence in live under a fluroscence screeing scope. A few F0 positive animals were taken to verify transgene expression on two photon and later fixed for immune labeling (**Figure 1,A-C**). The rest of the animals (7 founders) were allowed to reach maturity, after 1 whole year I choose 2 F0 mature transgenic animals to be crossed with wild type xenopus (due to shortage of time). The animals were labeled B and C. The line B is a double transgenic is also expresses the GFP-NTR fusion protein in mature oligodendrocytes.

In Figure1, A we see td-tomato $^{+}$ cells myelinating axons, the paranodes show high expression of tdtomato. The td-tomato has a membrane targeting sequence lyn kinase at its N-terminal, this directs the td-tomato to pranodes that are rich in lipid rafts.

The F1 tadpole from these two lines has varied expression of td-tomato. In line B the td-tomato is expressed in radial glia like cells **(Figure 1, B).** These cells are Nkx2.2 positive; the white arrow in B' shows the end feet of these cells. Mature myelinating GFP $^{+}$ cells do not express td-tomato.

In animal C, there was variation in expression of transgene among the tadpoles of the same mating pair. In some tadpoles the expression of td-tomato was found at the ventricle (Figure 1, C) and in some tadpoles the expression was found only in mature oligodendrocytes that myelinate the mauthner (Figure 1,D).
The two animals (B and C) td-tomato co-localizes with Nkx2.2.

A

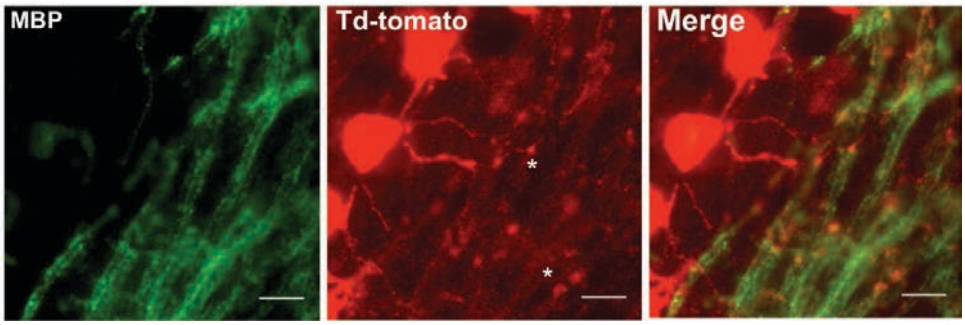
MBP
Td-tomato
Merge

B

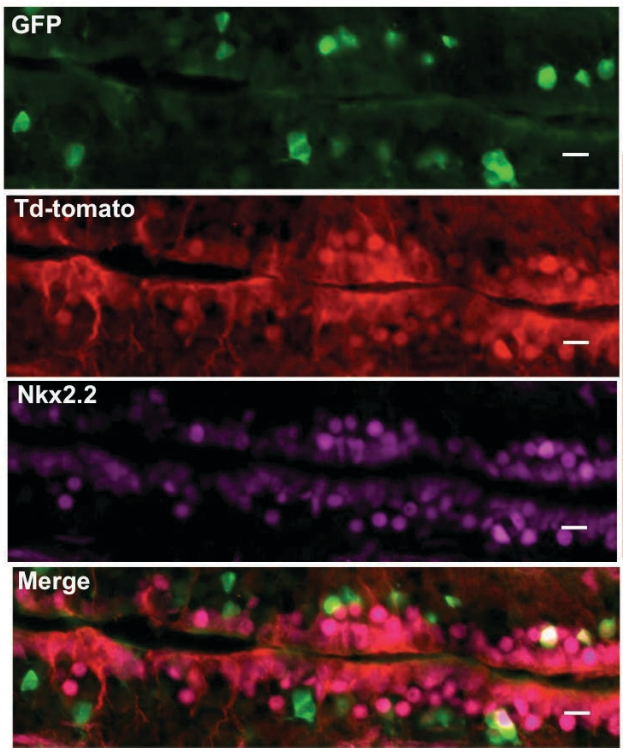
GFP
Td-tomato
Nkx2.2
Merge

B'

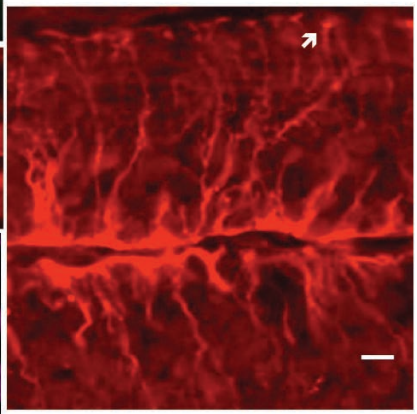

C

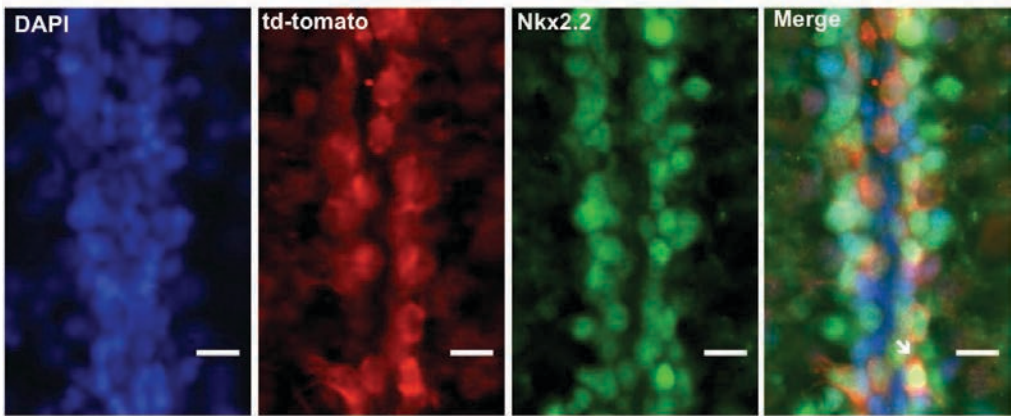
DAPI
td-tomato
Nkx2.2
Merge

D

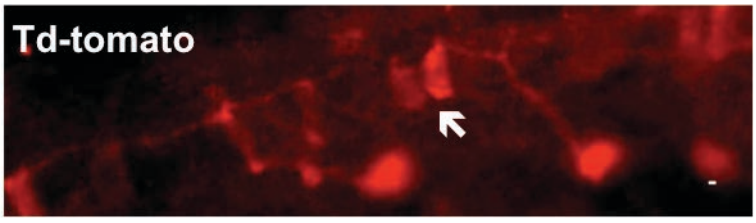
Td-tomato

Figure 1:Immuno labeling of *Sox10-tdtomato*

A) Cryosecction of F0 transgenic tadpole immuno labeled with MBP and td-tomato. White star indicates the paranode. Stage 53

B) Cryosection of F1 generation from founder B.(B') shows the end feet of the td-tomato positive cells, which are Nkx2.2 $^{+}$. Stage 49

C) Cryosection of F1 generation from founder C. Stage 49

D) Whole mount immunolabelling of F1 generation from founder C, in this tadpole there was expression of transgene only in mature oligodendrocytes. Stage 49

Scale= Scale=1µ

Nβt-β1Nav-GFP transgenic line

To verify transgene expression, the tadpoles were screened for fluorescence in live under a fluroscence screeing scope. A few F0 positive animals were taken to verify transgene expression on two photon and later fixed for immune labeling (**Figure 2,A**). The rest of the animals (4 founders) were allowed to reach maturity, after 1 whole year I choose 2 F0 mature transgenic animals to be crossed with wild type xenopus.

In Figure 2,A the *β1Nav-GFP* fusion protein is expressed at the node and is flanked by strong neurofascin 155 and very weak neurofascin 186 labelling (PanNFC antibody)

In Figure B, the expression of *β1Nav-GFP* is localised at the node of myelinated mauthner axon. Mauther axon is myelinated early in development.

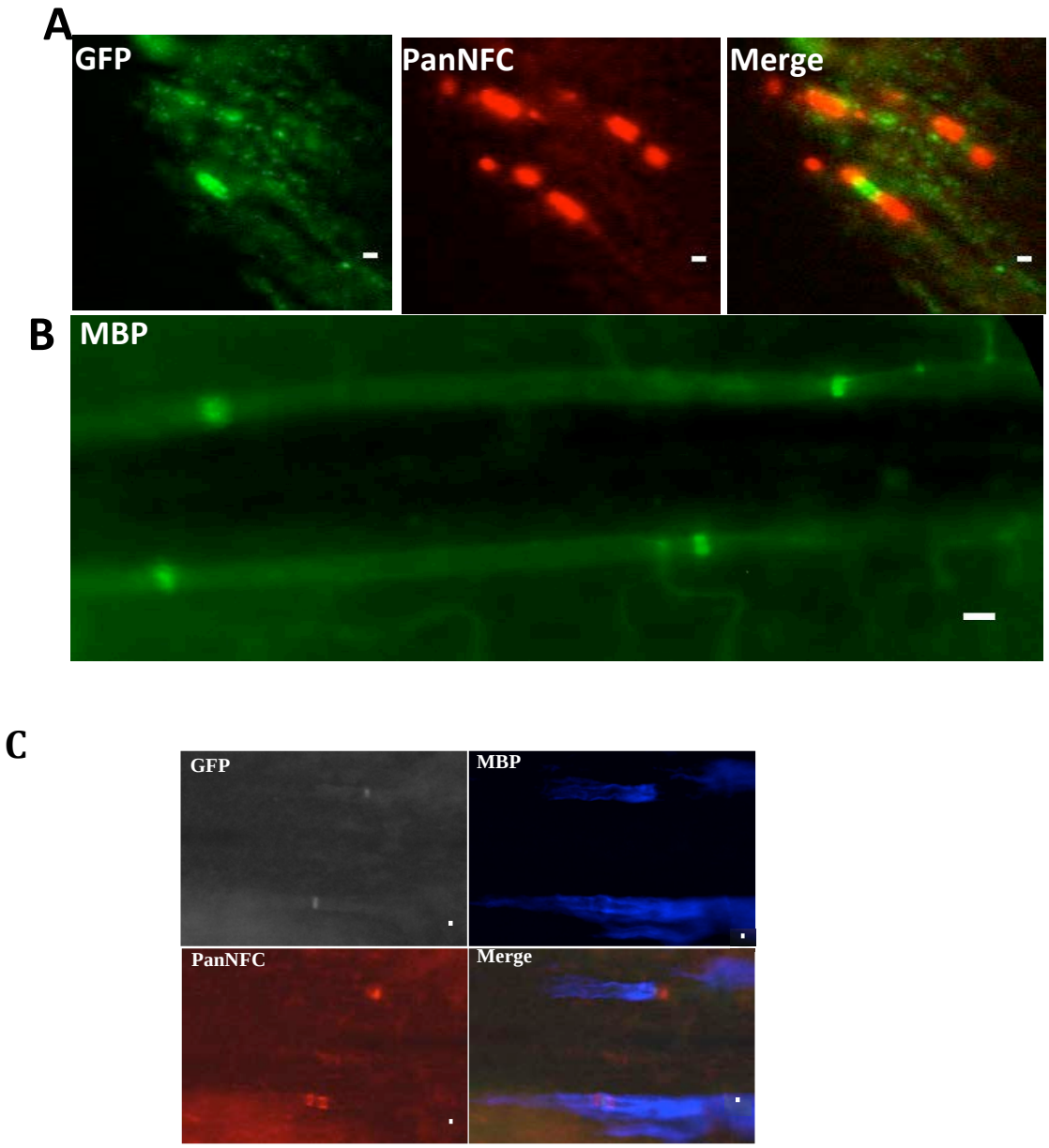

Figure 2: **Immuno labeling of *Nβt-β1Nav-GFP***

A) Cryosecction of F0 transgenic tadpole (stage 53) immuno labeled with GFP and Pan NFC. Scale=1µm.

B) Endogenous GFP expression is a dissected brain of F1 generation. Mauthner axon (stage 49) Scale=10µm.

C) Whole mount immunolabelling with MBP,GFP and PanNFC STAGE 49 . Scale=1µm.

DISCUSSION

The transgenic lines generated are in the process of screening for founders that express the transgene in the optic nerve, as that is the region in tadpoles amenable to live imaging. In the F0 lines that I have had the opportunity to examine, we see expression of the transgene, *β1Nav-GFP* only in the mauthner. The promoter used is pan neuronal (*NβT)* we expect to see expression in the PNS and the CNS (Coen et al., 2001). We surmise that the GFP expression could be low and to notice structures that are small in size like the *β1subunit* of the sodium channel we need a higher expression. The fact that we see expression at the node in the mauthner axon could be because of the large amount of the protein aggregated.

The expression of the *Sox10 –td tomato* reporter line is not consistent among the founders examined. The expression of td-tomato is not seen in the optic nerve OPC. This variation could be due to the position of insertion of the transgene in the genome. In transgenesis procedure REMI, there is random insertion of transgene and a large copy number of insertions, mostly as concatomers. This could be useful in some cases to enhance the expression of the fluorescent protein but in case of enhancer it could affect the pattern of expression. Transgenesis methods like CRISPER target the transgene at specific sites.

The enhancer could also work based on the time of development, they could have different patterns. Enhancer could also work differently based on the minimal promoter used. These aspects should be taken care of while developing plasmids and transgenic lines.

The founders I have screened have not met the requirements that we had to live image. Nevertheless I think they are interesting to study in a tissue culture system or live image the mauthner myelination early in development. The F2 generation could have more stable expression of the transgene and should be examined. I have examined only 4 lines for my thesis, I should analyse the other founders I have.

Development/Plasticity/Repair

Live Imaging of Targeted Cell Ablation in *Xenopus*: A New Model to Study Demyelination and Repair

Ferdinand Kaya,[1]* Abdelkrim Mannioui,[2,3,4]* Albert Chesneau,[1] Sowmya Sekizar,[2,3,4] Emmanuelle Maillard,[1] Chantal Ballagny,[1] Ludivine Houel-Renault,[9] David DuPasquier,[8] Odile Bronchain,[1] Isabelle Holtzmann,[1] Anne Desmazieres,[2,3,4] Jean-Léon Thomas,[2,3,4,7,10] Barbara A. Demeneix,[5] Peter J. Brophy,[6] Bernard Zalc,[2,3,4,7]* and Andre Mazabraud[1]*

[1]CNRS UPR 3294, Neurobiology and Development, Université Paris Sud XI, 91405 Orsay, France, [2]Université Pierre-et-Marie-Curie-Paris 6, Centre de Recherche de l'Institut du Cerveau et de la Moelle épinière, 75013 Paris, France, [3]Inserm UMR_S 975, 75013 Paris, France, [4]CNRS UMR 7225, 75013 Paris, France, [5]CNRS UMR 7221, Muséum d'Histoire Naturelle, 75005 Paris, France, [6]Centre for Neuroregeneration, University of Edinburgh, Edinburgh EH16 4SB, United Kingdom, [7]Assistance Publique-Hôpitaux de Paris, Groupe Hospitalier Pitié-Salpêtrière, 75013 Paris, France, [8]WatchFrog, 91000 Evry, France, [9]Centre Commun de Microscopie Electronique, Université Paris Sud XI, 91405 Orsay, France, and [10]Department of Neurology, Yale School of Medicine, New Haven, Connecticut 06511

Live imaging studies of the processes of demyelination and remyelination have so far been technically limited in mammals. We have thus generated a *Xenopus laevis* transgenic line allowing live imaging and conditional ablation of myelinating oligodendrocytes throughout the CNS. In these transgenic *pMBP-eGFP-NTR* tadpoles the myelin basic protein (MBP) regulatory sequences, specific to mature oligodendrocytes, are used to drive expression of an eGFP (enhanced green fluorescent protein) reporter fused to the *Escherichia coli* nitroreductase (NTR) selection enzyme. This enzyme converts the innocuous prodrug metronidazole (MTZ) to a cytotoxin. Using two-photon imaging *in vivo*, we show that *pMBP-eGFP-NTR* tadpoles display a graded oligodendrocyte ablation in response to MTZ, which depends on the exposure time to MTZ. MTZ-induced cell death was restricted to oligodendrocytes, without detectable axonal damage. After cessation of MTZ treatment, remyelination proceeded spontaneously, but was strongly accelerated by retinoic acid. Altogether, these features establish the *Xenopus pMBP-eGFP-NTR* line as a novel *in vivo* model for the study of demyelination/remyelination processes and for large-scale screens of therapeutic agents promoting myelin repair.

Introduction

The myelin sheath was a transformative vertebrate acquisition, enabling at least a 50-fold increase in efficiency and velocity of action potential propagation along axons without increase in diameter (Zalc and Colman, 2000; Zalc et al., 2008). In the CNS, myelin is synthesized by the oligodendrocyte. Multiple sclerosis (MS) is an inflammatory and demyelinating CNS disease of the young adult. Within MS plaques demyelination is associated with loss of oligodendrocytes and often with axonal damage resulting in neurological deficit. To date, available treatments for MS can treat inflammation, but have little, if any, efficacy on remyelination. One way to facilitate repair of demyelinated lesions would be to promote endogenous oligodendrocytes development and their migration to the lesion sites. Unfortunately, the existing mammalian models of MS are not ideally suited to follow *in vivo* the process of demyelination and remyelination or for developing large-scale screens of compounds that promote myelin repair *in vivo* (Miller and Fyffe-Maricich, 2010). Therefore, there is a critical need for alternative animal models allowing live imaging and monitoring of oligodendrocytes during the demyelination and remyelination processes.

Small model organisms, such as amphibians and some teleosts, are increasingly being used at various stages of drug development and constitute highly cost-effective alternative models to mammals (Saito and van den Heuvel, 2002; De Smet et al., 2006;

Received May 9, 2012; revised July 6, 2012; accepted July 25, 2012.

Author contributions: B.Z. and A. Mazabraud designed research; F.K., A. Mannioui, A.C., S.S., E.M., C.B., L.H.-R., D.D., I.H., and A.D. performed research; D.D. and P.J.B. contributed unpublished reagents/analytic tools; F.K., A. Mannioui, D.D., A.D., J.-L.T., B.D., P.J.B., B.Z., and A. Mazabraud analyzed data; O.B., J.-L.T., B.D., P.J.B., B.Z., and A. Mazabraud wrote the paper.

This work was supported by the CNRS (B.D., A. Mazabraud, B.Z.), Inserm (B.Z., J.-L.T.), UPMC (B.Z., J.-L.T.), the Ville de Paris, Région Ile de France, Medicen, and the Ministry of Industry through the AMBRe consortium (B.D., B.Z. and A. Mazabraud). F.K. was supported by a fellowship from the Fondation ARSEP (Fondation pour l'Aide à la Recherche sur la Sclérose En Plaques) and A. Mazabraud by a fellowship from the Fondation pour la Recherche Médicale. P.J.B. was on sabbatical leave and supported by a grant provided by the Ecole des Neurosciences de Paris and the Wellcome Trust. We thank Dr. S. Nagata for the gift of monoclonal antibody against *Xenopus* MBP and Dr. A. Gow for providing us with the pMG2 plasmid. The Nkx2.2 antibody, developed by T. M. Jessell and S. Brenner-Morton, was obtained from the Developmental Studies Hybridoma Bank developed under the auspices of the NICHD and maintained by the University of Iowa, Department of Biological Sciences, Iowa City, IA.

This paper is dedicated to the memory of the late Pr. David R. Colman and of Pr. Maurice Wegnez who initiated this work. We Are grateful to Dr. François Tiaho for introducing and encouraging us to use two-photon microscopy for live imaging of tadpoles, Aurelien Dauphin from our imaging facility, PICPS, for his precious help, Chistophe De Medeiros for animal care, and Muriel Perron for helpful discussions.

*F.K., A. Mannioui., B.Z., and A. Mazabraud contributed equally to this work.

Dr. Barbara Demeneix is a founder of the company WatchFrog and Dr. David DuPasquier is an employee of WatchFrog.

This article is freely available online through the *J Neurosci* Open Choice option.

Correspondence should be addressed to Dr. André Mazabraud, CNRS UPR 3294, Neurobiology and Development, Université Paris Sud XI, Bâtiment 445, 91405 Orsay, France. E-mail: andre.mazabraud@u-psud.fr.

DOI:10.1523/JNEUROSCI.2252-12.2012
 0270-6474/12/3212885-11$15.00/0

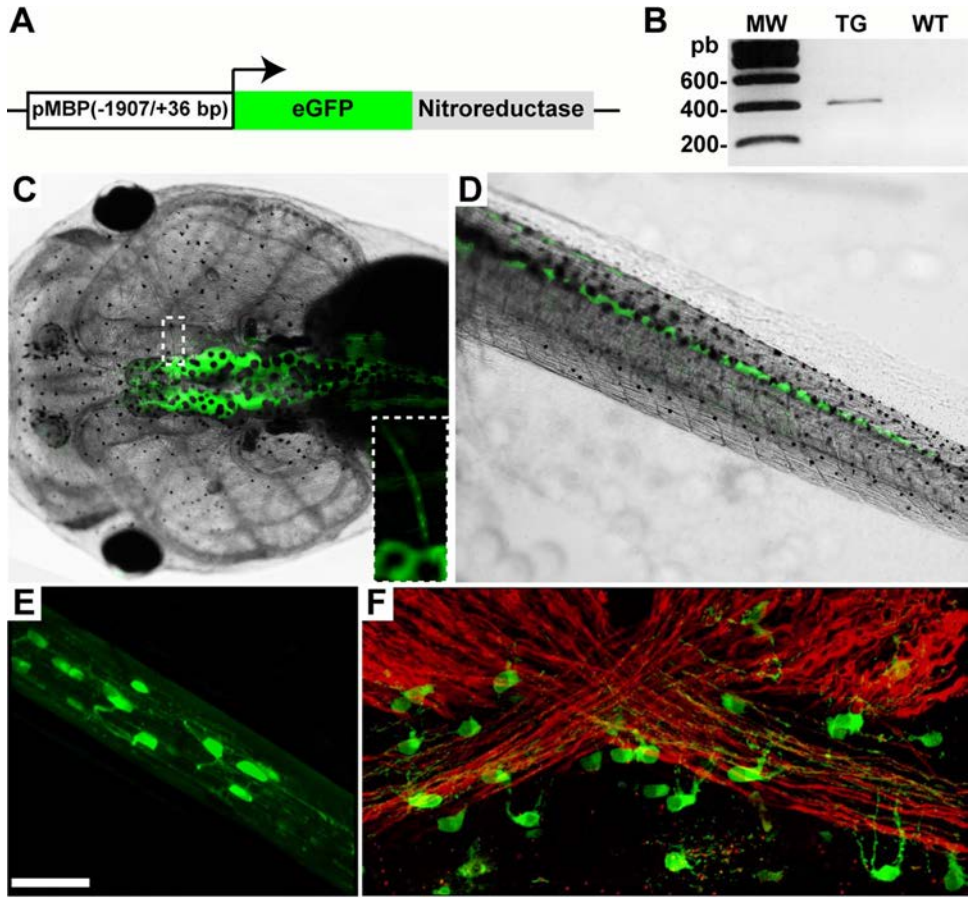

Figure 1. Structure and expression of the *pMBP-eGFP-NTR* transgene. ***A***, Schematic diagram of the *pMBP-eGFP-NTR* construct. The transgene contains the *eGFP* open reading frame fused to that of *E. coli* NTR placed under the control of the DNA regulatory sequence of the murine *MBP* gene (−1907 bp and +36 bp). ***B***, RT-PCR performed on RNA extracted from brains of transgenic (TG) or wild-type (WT) tadpoles used to amplify a 394 bp fragment corresponding to the junction of eGFP/NTR sequence. ***C–F***, Transgene expression as assessed by GFP fluorescence (***C–E***) or immunolabeling (***F***) in a *pMBP-eGFP-NTR* transgenic tadpole at stage 55. Dorsal view of the head (***C***) and sagittal view of the tail (***D***). Expression is only observed in the CNS (brain and spinal cord) but not in the peripheral nervous system. Inset in ***C*** is a higher magnification to illustrate the detection of GFP in the optic nerve. ***E***, *In vivo* stack of images of the optic nerve obtained by two-photon microscopy. Note the fluorescent processes of the GFP^+ cells. ***F***, Confocal image of a whole mount of the optic chiasm immunostained for MBP (red) and GFP (green). Note the GFP^+ cell bodies extending their processes toward the strongly MBP^+ myelinated fibers. Scale bar (in ***E***) ***C***, ***D***, 2 mm; ***E***, ***F***, 50 μm; inset (***C***), 1 mm.

Giacomotto and Ségalat, 2010). Zebrafish and *Xenopus* embryos are transparent and develop as free-living larvae and therefore are particularly suited to investigate developmental processes at all stages. To study myelination, demyelination and remyelination, we have produced a transgenic *Xenopus* line (*pMBP-eGFP-NTR*) designed to specifically express in oligodendrocytes the fluorescent reporter GFP fused to the *Escherichia coli* nitroreductase (NTR), under the control of the 1.9 kb proximal portion of mouse *MBP* regulatory sequence. Here, we show that the GFP reporter is faithfully expressed in mature myelin-forming oligodendrocytes that are specifically ablated following treatment with metronidazole (MTZ, an NTR substrate). Treatment of *pMBP-eGFP-NTR* tadpoles induces selective demyelination, which is reversible on MTZ withdrawal. Two-photon microscopy allows tracking of GFP expression and thus the processes of demyelination and remyelination *in vivo* on the same transgenic specimen. Finally, using this *in vivo* model we show that spontaneous remyelination is dramatically increased upon exposure to retinoic acid, a molecule recently shown to play an essential role in myelin formation (Joubert et al., 2010; Latasa et al., 2010; Huang et al., 2011). Thus, the *pMBP-eGFP-NTR Xenopus* line offers a novel model to study demyelinization/remyelinization processes and is ideally suited for *in vivo* large-scale screening of pro-remyelinating drugs.

Materials and Methods

Animals. Xenopus tadpoles were raised and maintained as previously described (de Luze et al., 1993) and staged according to the normal table of *Xenopus laevis* (Daudin) of Nieuwkoop and Faber and developmental progress defined as NF stages (Nieuwkoop and Faber, 1994). Tadpoles of either sex were anesthetized in 0.05–0.5% MS222 (3-aminobenzoic acid ethyl ester; Sigma-Aldrich) before brain and spinal cord dissection. Animal care was in accordance with institutional and national guidelines.

Generation of the pMBP-eGFP-NTR construct and transgenic Xenopus *lines.* The bacterial *Nfs*B gene encoding NTR was directly amplified by PCR from *E. coli* using the following oligos: 5′-ATGCTCGAGCCATG GATATCATTTCTGTCGCCTTA-3′ and 5′-GGGGATCCGATCGATC TCAATACCCGCTAAATA-3′, as previously described (Curado et al., 2007). The amplification product was digested by XhoI and BamHI and cloned in frame to *eGFP* in the *peGFP-C1* vector (Clontech) to produce the *CMV-eGFP-NTR* construct. This vector was used to amplify the *eGFP-NTR* fusion cDNA using two flanking primers containing BamHI restriction sites at their 5′ end, and the product was inserted into the unique BamHI site of the pMG2 plasmid containing the 1.9 kb proximal portion of mouse *MBP* regulatory sequence (Gow et al., 1992) to produce the final *pMBP-eGFP-NTR* vector (Fig. 1*A*). The *pMBP-eGFP-NTR* plasmid was linearized with EcoRI and used to generate stable transgenic *Xenopus laevis* embryos using a simplified restriction enzyme-mediated integration (REMI) procedure (Kroll and Amaya, 1996; Sparrow et al., 2000; Chesneau et al., 2008). F0 animals were crossed to wild-type *Xenopus* to generate lines, one of which was selected that carry a single trans-

gene integration site. Transgenic embryos were genotyped by assessing the presence of *eGFP/NTR* fusion transcripts by reverse transcriptase (RT)-PCR using the forward primer 5′-ACGTCTATATCATGGCCG ACAAG-3′ and reverse primer 5′-TGCAGTAGCGTTTTGATCTGCT C-3′ located on either side of the *eGFP/NTR* junction to amplify a 394 bp fragment. To this end, 2 μg of total RNA extracted from brains were reverse transcribed using the SuperScript II kit (Invitrogen) according to the manufacturers' instructions and used as template for the PCR. The fusion protein (GFP/NTR) was detected directly by fluorescence in live embryos using an AZ100 Nikon Zoom Microscope.

Metronidazole preparation and use. MTZ (Fluka) was dissolved in filtered tap water containing 0.1% DMSO (Sigma Aldrich). Preliminary experiments demonstrated that high concentrations (> 20 mM) of MTZ were toxic. Therefore, MTZ was used at concentrations of 10 or 15 mM and exposure time ranged from 3 to 11 d. Control animals were kept in the same media without MTZ. Furthermore, transgenic or nontransgenic sibling tadpoles were maintained in 600 ml of MTZ solution (maximum 10 tadpoles/600 ml) at 20°C in complete darkness (MTZ is light-sensitive) and daily changed throughout the duration of treatment. For regeneration experiments, MTZ-treated animals were allowed to recover for up to 6 d in normal water in ambient laboratory lighting.

Transgenic tadpoles were treated with drugs between stage NF 48 and 55. These stages correspond to pre-metamorphosis and represent stages in which myelination is ongoing. Myelination markers such as proteolipid protein (PLP) and myelin basic protein (MBP) are first immunodetected at stages 42/43 in the hindbrain and spread throughout the brain and spinal cord by stages 46/47 (Yoshida, 1997). In the optic nerve at the electron microscopic (EM) level myelination was reported to begin in the middle portion at stage 48/49 and the number of myelinated axons increases sevenfold between stage 50 and 57 (Cima and Grant, 1982).

Immunohistochemistry. Tadpoles were fixed by immersion in 4% paraformaldehyde, rinsed in 1× PBS, cryoprotected in 30% sucrose (1× PBS) and frozen embedded in OCT (Tissue Tek). Cryosections (12 μm) were blocked in 10% normal goat serum in 1× PBS containing 0.1% Triton X-100 and incubated overnight at 4°C with primary antibodies. For whole-mount immunolabeling, dissected fixed brains were first incubated for 2 d at 4°C in primary antibody and then overnight at 4°C with secondary antibody. The brains were rinsed extensively in 0.1% Triton X-100 following antibody incubations and before mounting. The following primary antibodies were used for immunostaining: mouse anti-GFP (1:1000, Invitrogen), rabbit anti-activated-caspase3 (1:250, BD PharMingen), mouse anti-APC (Ab7) (1:500, Calbiochem), anti-Nkx2.2 (1:10, mouse hybridoma, Developmental Studies Hybridoma Bank, Iowa City, IA), mAb to phosphorylated neurofilaments (mouse IgG1 SMI 31; 1/500, Covance), mouse anti-MBP monoclonal antibodies (directed against *Xenopus* MBP, 1:1000, kindly provided by Saburo Nagata, Women's Tokyo University, Japan), anti-pan-neurofascin (NFC1) (1:1000; Zonta et al., 2008), and anti-Hu (1:10,000 Human serum, kindly provided by Dr. Jean-Yves Delattre, Centre de Recherche de l'Institut du Cerveau et de la Moelle épinière, Groupe Hospitalier Pitié-Salpêtrière, France). Specific binding sites were visualized using anti-mouse or anti-rabbit fluorescent secondary antibodies (1:1000 Alexa 488 or 594, Invitrogen) and for Hu Ab, anti-human IgG F(c) coupled to Texas Red (1:400, Rockland). Sections were stained in Hoechst solution (Sigma-Aldrich) and mounted in FluorSave Reagent mounting medium (Calbiochem).

Electron microscopy. Tadpoles were fixed in 2% paraformaldehyde, 2% glutaraldehyde, 1% potassium ferricyanide in 0.1 M cacodylate buffer, pH 7.4 and 0.002% calcium chloride overnight at 4°C, washed in 0.1 M cacodylate buffer, and postfixed in 1% osmium tetraoxide, 1% potassium ferricyanide in 0.1 M cacodylate buffer. After washing in cacodylate buffer and water, tadpoles were incubated in 1% uranyl acetate aqueous solution at 4°C overnight. After rinsing twice in water, tadpoles were dehydrated in increasing concentrations of ethanol, washed in increasing concentrations of 2-hydroxypropyl methacrylate (Electron Microscopy Sciences) dissolved in 90% ethanol, infiltrated, and embedded in Epon-BDMA solution (Epon, benzyl dimethylamine; Electron Microscopy Sciences). Blocks were heated at 70°C for 72 h. Ultrathin sections (70 nm) were examined on an EM208 electron microscope (Philips).

Histology and Luxol fast blue staining. Tadpoles were fixed for 48 h at room temperature in 3.8% formaldehyde in water. Paraffin sections (6 μm) were stained with Luxol fast blue as previously described (Geisler et al., 2002). Briefly, rehydrated sections were immersed in a Luxol fast blue-0.1% ethanol solution at 60°C for 24 h and washed in distilled water. The slides were differentiated in 0.05% lithium carbonate solution for 30 s and then in 70% ethanol for 30 s. Slides were counterstained in cresyl violet solution for 30–40 s. After rinsing in distilled water, the slides were differentiated in 95% ethanol for 5 min in 100% ethanol and mounted with Eukitt medium (Sigma Aldrich). As a result of these staining procedures, myelinated fibers are stained blue, and neuronal cell bodies are stained pink to violet.

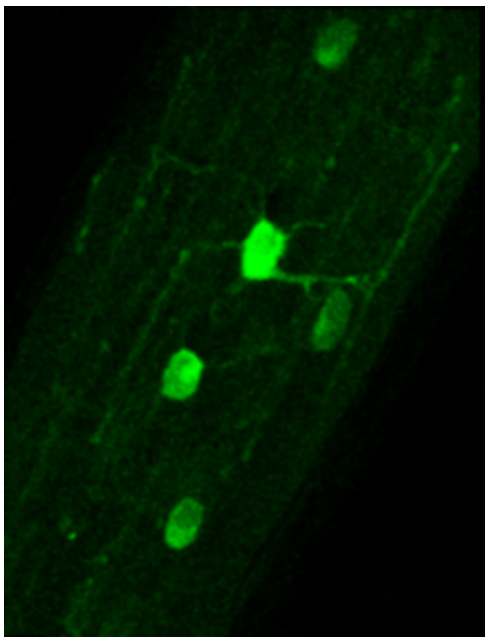

Movie 1. Faint detection of GFP in myelin along optic nerve axons of stage 50 *pMBP-eGFP-NTR* transgenic tadpole. At this early developmental stage, the wrapping process is ongoing, therefore myelin is still not completely compact and this allows diffusion of GFP in the myelin cytoplasmic compartment. This movie represents the *Z*-projection of 17 successive optical sections across the thickness of the optic nerve imaged by two-photon microscopy.

Two-photon observation. For *in vivo* examination of GFP-expressing oligodendrocytes along the optic nerve, tadpoles were anesthetized in MS222 and placed in a POC-Chamber-System (H. Saur), under a two-photon microscope. Mono-photon or two-photon excitation was performed using Zeiss LSM 710 microscope system. The microscope was equipped with objective (20×, 1 NA). Calculated optical slice thickness was 2 μm. Each image presented is the 3D projection of 18–26 stacks of images. The settings (gain and aperture pinhole) were held constant within individual experiments. All images shown were processed with ImageJ software (NIH).

Quantification of GFP$^+$ cells. In the optic nerve, the total number of GFP$^+$ cells was counted, from the emergence of the nerve to the retinal end before and after MTZ treatment on the same embryos and data were compared with control untreated animals of the same developmental stage. On medulla preparations, quantification of GFP$^+$ cells was per tissue sections and each data point is the mean value of six sections from one tadpole. Data presented are the mean ± SEM of number of GFP$^+$ cells counted on 6 tadpoles ($n = 6$).

Statistical analysis. Prism v5 software (GraphPad) was used for statistical analyses. Results are expressed as means ± SEM. Data were compared using Student's *t* test. Statistical significance was set at $p < 0.05$.

Results

Oligodendrocyte-restricted expression of a dual reporter/selection transgene in *Xenopus laevis*

The proximal regulatory sequences of the murine myelin *MBP* gene contain enhancer and promoter elements localized between

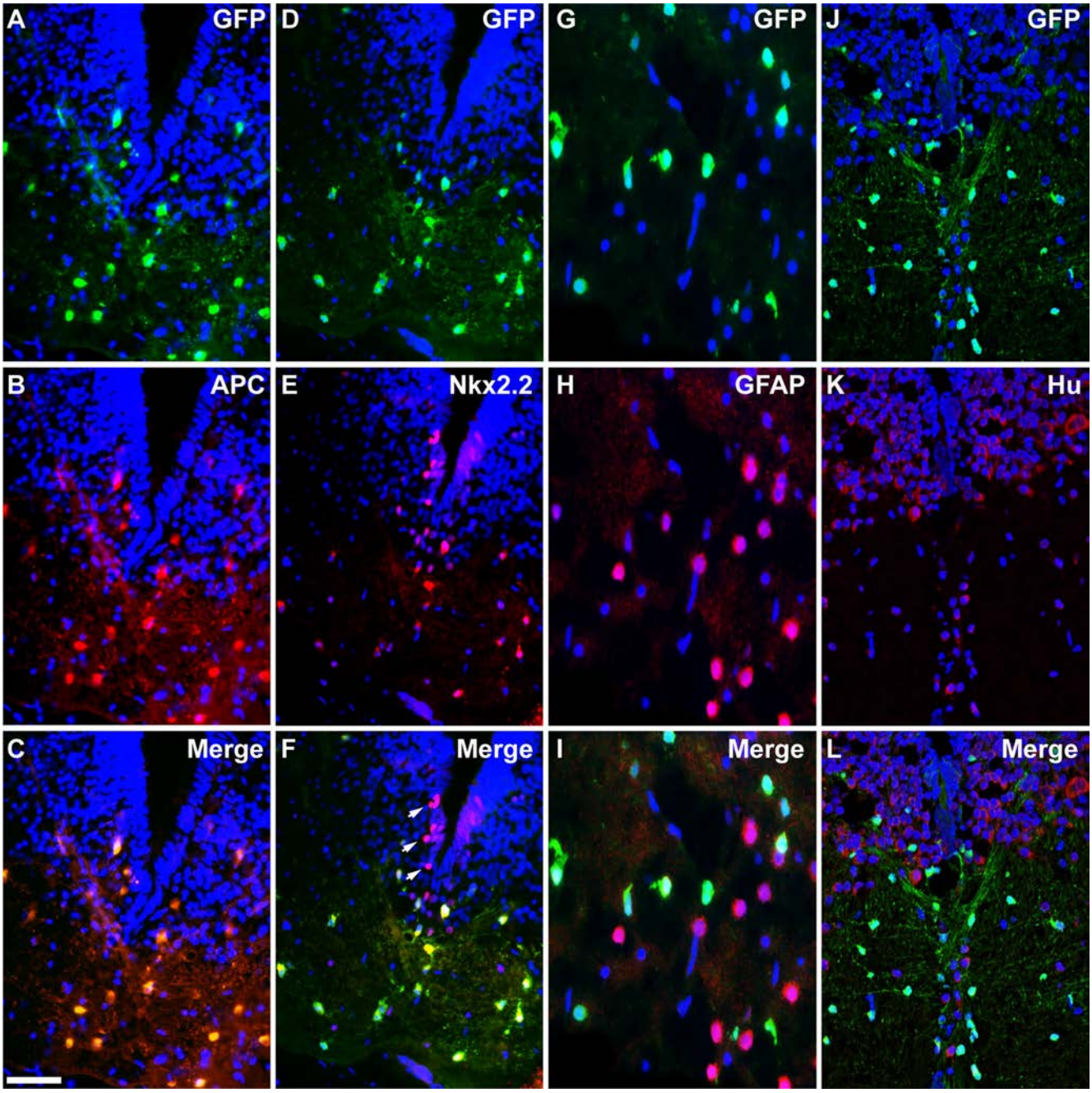

Figure 2. The *pMBP-eGFP-NTR* transgene drives expression in mature oligodendrocytes. Coronal tissue sections across the medulla of *pMBP-eGFP-NTR* tadpole at stage 55 coimmunostained for GFP and successive markers of different cells types. ***A–C***, GFP and APC, a specific marker of mature oligodendrocytes. Note the complete overlap of GFP labeling with that of APC. ***D–F***, GFP and Nkx2.2, a marker of progenitor of oligodendrocytes and mature oligodendrocytes. Note that cells doubly labeled for GFP and Nkx2.2 are localized in the white matter tract, with no GFP detection in Nkx2.2$^+$ progenitors in the ventral ventricular layer (white arrows in ***F***). ***G–I***, GFP and GFAP, a marker of astrocytes. ***J–L***, GFP and Hu, a pan-neuronal marker. Note the complete exclusion of GFP labeling with either GFAP (***I***) or Hu (***L***). Scale bar (in ***C***) ***A–F***, ***J–L***, 50 μm; ***G–I***, 25 μm.

position +36 and −1907, which are sufficient for a strong and specific expression in mature oligodendrocytes (Gow et al., 1992; Stankoff et al., 1996). As shown in Figure 1*A*, this 1.9 kb proximal regulatory sequence is used to drive expression of a dual reporter/selection transgene (*eGFP-NTR*) composed of the enhanced green fluorescent protein (*eGFP*) reporter gene fused in frame with the bacterial *nfs*B gene encoding the NTR enzyme for MTZ-dependent cell ablation (Curado et al., 2007). The *pMBP-eGFP-NTR* vector was used for REMI transgenesis in *Xenopus laevis*. Several transgenic founders (F0) were generated and crossed to wild-type animals to obtain F1 progenies. F1s were then genotyped by RT-PCR to confirm the expression of the fusion GFP/NTR transcript and to characterize the number of integration sites for each line (Fig. 1*B*).

Indicative of transgene expression in the *pMBP-eGFP-NTR* tadpole the first GFP$^+$ cells were detected at stage 41–42 within the brainstem (data not shown). At stage 55, GFP$^+$-expressing cells were detected exclusively in the brain (Fig. 1*C*), spinal cord (Fig. 1*D*) and optic nerve, where fluorescence was clearly confined to cell bodies extending thin processes, highly reminiscent of oligodendrocytes (Fig. 1*E*,*F*). It should be noted that, as GFP is cytoplasmic, fluorescence was not detected in the myelin sheath.

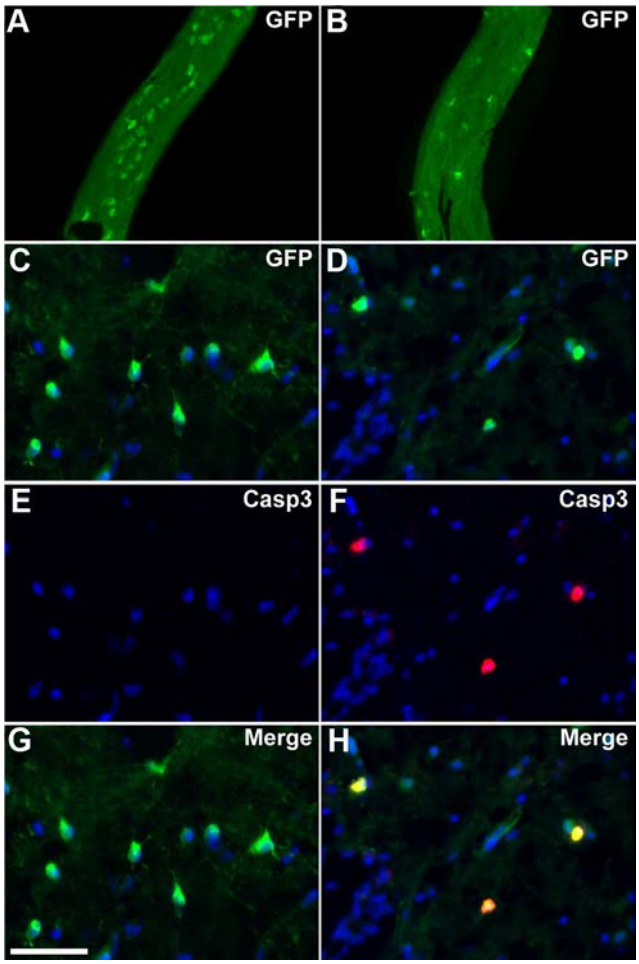

Figure 3. Oligodendrocyte depletion and apoptosis in transgenic tadpoles following MTZ treatment. ***A***, ***B***, Whole-mount two-photon microscopy of the optic nerve at stage 55 showing GFP $^+$ cells in transgenic animals untreated (***A***) or MTZ-treated for 3 d (***B***). MTZ induced a severe depletion of GFP $^+$ cells in the optic nerve. ***C–H***, Immunolabeling for GFP and activated caspase3 (Casp3) on coronal sections across the medulla in untreated (***C***, ***E***, ***G***) or MTZ-treated (***D***, ***F***, ***H***) transgenic animals. In MTZ-treated animals, activated caspase3 is detected in GFP $^+$ cells. Scale bar (in ***G***) ***A***, ***B***, 150 μm; ***C–H***, 50 μm.

Figure 1*F* shows a whole mount of the chiasm double-labeled with anti-GFP and -MBP antibodies. GFP $^+$ cells extend processes toward the internode region of axons where MBP expression is mostly concentrated in the myelin sheath (Ainger et al., 1997). However, during the process of wrapping before myelin compaction, GFP can diffuse in the cytoplasmic compartments of myelin and it was possible to detect early myelination *in vivo*. Indeed, at stage 50, i.e., at a stage when myelination is ongoing, oligodendrocyte processes extending along axons were clearly visible as illustrated on a stack of 17 optical sections of the optic nerve (Movie 1). As development proceeds, the distribution of GFP $^+$ cells extends from the brainstem, caudally to the spinal cord and rostrally to the forebrain, following the expected pattern of myelination in mammals (Kanfer et al., 1989). We could not detect expression of the transgene in the peripheral nervous system (PNS). This result is in agreement with the observation that the 1.9 kb MBP regulatory sequence drives *MBP* expression in oligodendrocytes, while in Schwann cells, *MBP* expression is controlled by a different 422 bp enhancer −9 kb upstream of the transcriptional initiation site (Denarier et al., 2005).

To confirm the specific expression of the *eGFP/NTR* transgene in mature oligodendrocytes, cryosections from *pMBP-eGFP-NTR* transgenic tadpoles at stage 55 were double labeled with antibodies against GFP and cell type-specific markers, i.e., APC (adenomatous polyposis coli) for mature oligodendrocytes (Bhat et al., 1996), Nkx2.2 transcription factor for oligodendrocyte precursor cells and mature oligodendrocytes (Soula et al., 2001; Yoshida and Macklin, 2005), GFAP (glial fibrillary protein) for astrocytes (Eng et al., 1971), and Hu RNA-binding protein for neurons (Graus and Ferrer, 1990; Fig. 2). All sections examined showed a complete superimposition of GFP and APC labeling, with all GFP $^+$ cells expressing APC and all APC $^+$ cells expressing eGFP (Fig. 2*A–C*). This observation bolsters the argument that GFP/NTR expression is restricted to oligodendrocytes. In the ventral ventricular domain of the medulla, Nkx2.2 $^+$ progenitor cells did not express GFP. In contrast, white matter tracts showed a vast majority of Nkx2.2 $^+$/GFP $^+$ cells, which are likely mature oligodendrocytes (Fig. 2*D–F*). In addition, GFP expression was detected neither in GFAP-expressing astrocytes (Fig. 2*G–I*) nor in Hu $^+$ neurons (Fig. 2*J–L*), These data demonstrate the strict oligodendroglial expression of the *eGFP-NTR* transgene in tadpoles and suggest that, both in mice and *Xenopus*, the 1.9 kb regulatory sequence of *MBP* selectively drives transgene expression in mature myelin-forming oligodendrocytes.

Movie 2. Live imaging of an oligodendrocyte cell death caused by MTZ treatment. A stage 55 tadpole was treated with MTZ for 5 d. The optic nerve was visualized by two-photon microscopy between one and four times a day for 5 d. On day 6, when the pattern of fluorescence of one oligodendrocyte (arrow) in the field of observation changed dramatically, indicative that the cell was entering apoptosis, we imaged four times at 90 min intervals.

MTZ treatment induces oligodendrocyte depletion and demyelination in a MTZ-dependent manner

We next tested the ability of NTR to render oligodendrocytes susceptible to drug-dependent ablation by treating transgenic tadpoles with increasing concentrations of MTZ. Preliminary experiments showed that treatment of stage 55 tadpoles with 20 mM MTZ (or higher concentrations) was toxic. Hence, tadpoles were treated with 10 or 15 mM MTZ for 3 or 6 d. The number of GFP $^+$ cells per optic nerve was highly reproducible and increased progressively as a function of development (7 $\pm$ 2, 25 $\pm$ 3, and 31 $\pm$ 2 at stages 48, 50, and 55 respectively). Progressive MTZ-induced oligodendrocyte cell death in transgenic tadpoles was monitored

on live embryos by successive examinations of the optic nerve of the same animal under either a fluorescent macroscope or a two-photon microscope.

In vivo examination of the optic nerve of MTZ-treated stage 55 tadpoles (10 mM for 3 d) resulted in a 50% depletion of GFP$^+$ cells per optic nerve (Fig. 3*A*,*B*). Quantification showed that this reduction was highly significant: 31 ± 2 in controls versus 16 ± 2 after 72 h MTZ treatment ($p < 0.001$ $n = 6$ tadpoles). A similar depletion of GFP$^+$ oligodendrocytes was observed in medulla sections (Fig. 3*C–H*): 42 ± 2 in controls vs 22 ± 1 after MTZ treatment, number of GFP$^+$ cells per tissue section ($p < 0.0001$, $n = 6$ tadpoles). Oligodendroglial cell death following MTZ treatment occurred by apoptosis as double immunostaining showed that most GFP$^+$ cells were also positive for anti-caspase 3 staining in MTZ-treated tadpoles (Fig. 3*D*,*F*,*H*). This result contrasted with the absence of caspase3$^+$/GFP$^+$ cells in untreated tadpoles (Fig. 3*C*,*E*,*G*). Apoptosis was also confirmed at an earlier developmental stage by TUNEL (terminal deoxynucleotidyl transferase-mediated biotinylated UTP nick end labeling) assays (data not shown). Live imaging in the optic nerve of the death of an oligodendrocyte consecutive to MTZ treatment of a stage 55 tadpole is illustrated in Movie 2.

Since GFP$^+$ cells are mature myelinating oligodendrocytes, ablation of these cells should lead to a severe demyelination. As illustrated on medulla sections, MTZ-treated tadpoles showed a marked decrease in the density of Luxol fast blue-stained fibers compared with untreated controls (Fig. 4*A*,*B*). It was previously shown that disorganization of nodes of Ranvier is a good indicator of demyelination (Howell et al., 2006; Pernet et al., 2008). To confirm that demyelination occurred in MTZ-treated *pMBP-eGFP-NTR* tadpoles, we analyzed the nodes of Ranvier organization using pan-neurofascin antibodies directed against neurofascin isoforms NF155 and NF186, which are expressed at the paranodal and nodal domains, respectively (Zonta et al., 2008, 2011). Immunolabeling of tadpole optic nerve sections with pan-neurofascin antibodies showed, as in the mouse, an intense staining at the paranodal domains (probably corresponding to glial NF155) and a weaker, although clearly detectable, staining (axonal NF186) of the node (Fig. 4*C*, inset).

To determine the extent of demyelination process induced by MTZ treatment, we next examined whole mounts of optic nerves, isolated from control and MTZ-treated *pMBP-eGFP-NTR* tadpoles, stained with both pan-neurofascin and anti-neurofilament (SMI-31) antibodies. Following 3 d of MTZ treatment, SMI-31$^+$ axons do not appear to be altered (Fig. 4*G*,*H*), while numerous neurofascin$^+$ hemiparanodes (Fig. 4*F*, inset) were observed, indicative of a partial demyelination (Fig. 4*F*,*H*). In contrast, untreated transgenic tadpoles showed a complete neurofascin$^+$ nodal staining, i.e., two paranodes on either side of each node of Ranvier (Fig. 4*C*,*E*).

The characteristics of demyelination were further investigated using electron microscopy. We counted the number of myelinated axons in the dorsal medulla of control and MTZ-treated transgenic tadpoles at stage 55. Controls showed ap-

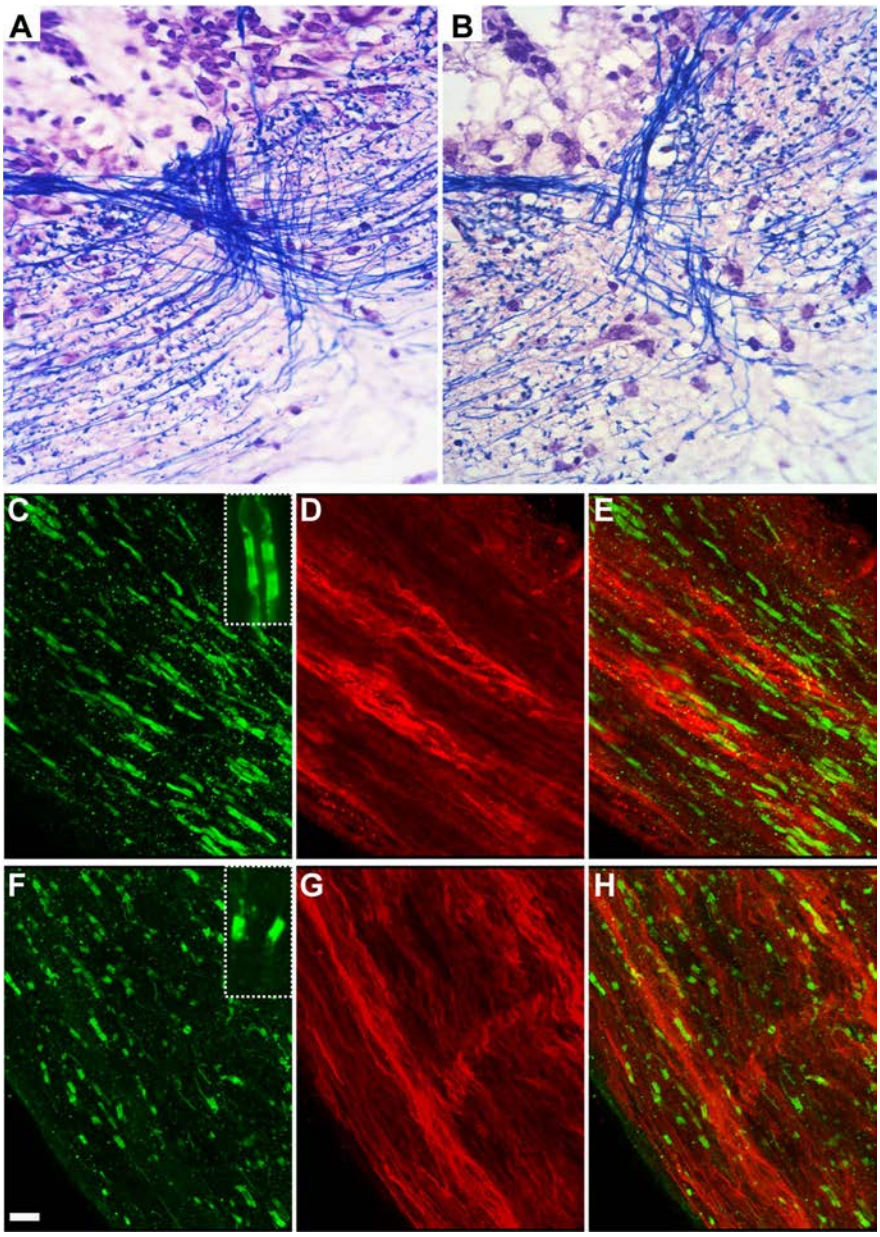

Figure 4. MTZ treatment induces demyelination without axonal damage. ***A***, ***B***, Myelinated fibers staining with Luxol fast blue on coronal sections across the medulla at stage 55 in untreated (***A***) or MTZ-treated (***B***) transgenic animals. ***C–H***, Whole mount of optic nerve at stage 55 immunostained for neurofascin (green) and SMI-31 (red) in untreated (***C–E***) or MTZ-treated (***F–H***) transgenic animals. Insets in ***C*** and ***F*** are high magnifications of nodes of Ranvier showing a strong signal for NF 155 in the paranodal domain and a weaker signal in the node (NF186) in a control animal (***C***), where in case of partial demyelination, only hemiparanodes are labeled (***F***). MTZ treatment induced demyelination, characterized by disorganization of the neurofascin$^+$ nodes of Ranvier (***F***, ***H***) with numerous heminodes compared with control (***C***, ***E***). In MTZ-treated tadpoles, SMI-31 axons had a normal appearance (***G***, compared with ***D***), suggesting that MTZ-induced demyelination does not affect the axons. Scale bar (in ***F***) ***A***, ***B***, 17 μm; ***C–H***, 5 μm; insets (***C***, ***F***), 2 μm.

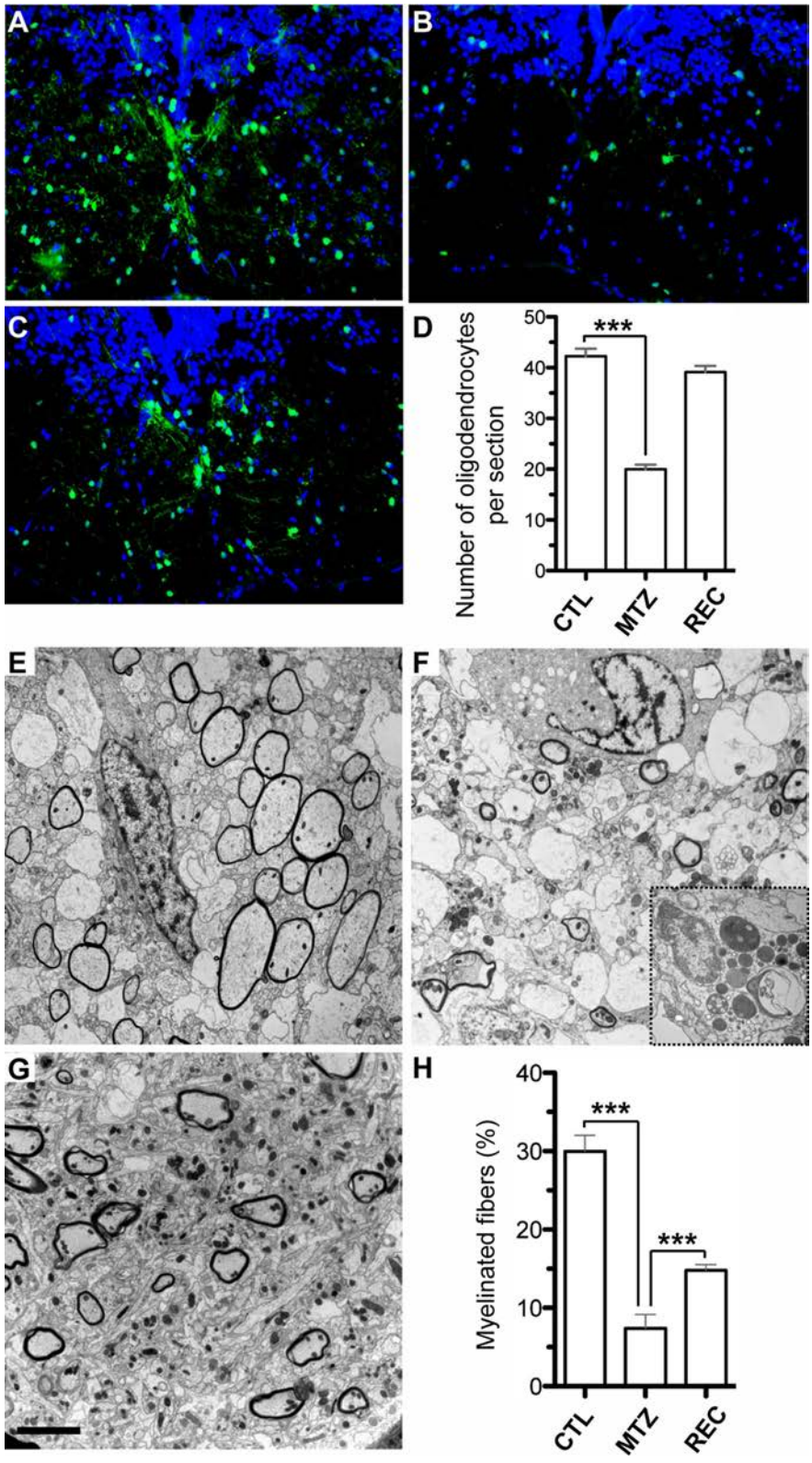

Figure 5. Quantification of oligodendrocyte depletion, demyelination and recovery after cessation of MTZ treatment. ***A–D***, GFP immunostaining of coronal sections across the medulla of stage 55 *pMBP-eGFP-NTR* tadpoles untreated (***A***), treated for 6 d with 10 mM MTZ (***B***), and after 6 d of recovery following treatment cessation (***C***). ***D***, Quantification of the number of oligodendrocytes (GFP^+ cells) per section in control (CTL) MTZ-treated (MTZ) and after recovery (REC) ($n = 6$ tadpoles for each condition, $^{***}p < 0.0001$). ***E–H***, Electron micrograph across the medulla of stage 55 transgenic tadpole untreated (***E***) or MTZ-treated for 6 d (***F***). Following MTZ treatment, most of the myelinated fibers disappeared and the demyelinated areas were invaded by macrophages filled with lipid droplets and myelin debris (inset in ***F***). Note the normal morphological appearance of axons in MTZ-treated tadpoles. ***G***, Six days after treatment cessation a large number of axons are remyelinated. ***H***, Quantification of myelinated axons expressed as percentage of total axons ($n = 3800$ fibers scored per animal, $^{***}p < 0.0001$). Scale bar (in ***G***) ***A–C***, 50 μm; ***E–G***, 4 μm; inset (***F***), 0.4 μm.

proximately one third of their axons myelinated (31 ± 2% of axons per section, $n = 3800$ fibers counted per animal; Fig. 5*E*,*H*). In contrast, after 6 d of MTZ treatment, only 7 ± 2% of axons remained wrapped by a myelin sheath (Fig. 5*F*,*H*). Tissues from MTZ-treated transgenic tadpoles were also infiltrated by macrophages displaying lipid droplets and phagocyted-myelin debris (Fig. 5*F*, inset). The morphology of naked axons was however normal, confirming our observation following immunolabeling with SMI31 antibody (Figs. 4*G*, 5*F*). Therefore, MTZ treatment of *pMBP-eGFP-NTR* tadpoles respects axonal integrity, but induces demyelination by apoptotic cell death of oligodendrocytes. This finding led us to analyze the potential for spontaneous repair of oligodendrocytes and myelin in *pMBP-eGFP-NTR* tadpoles after interruption of the MTZ treatment.

Spontaneous remyelination after interruption of the MTZ treatment

Stage 55 *pMBP-eGFP-NTR* tadpoles were treated for 3 d with 10 mM MTZ and then returned to normal water for 6 d. Animals were then killed for examination of medulla sections either by immunolabeling with anti-GFP antibody or using electron microscopy. As described above, 3 d of MTZ treatment reduced by half the number of oligodendrocytes (Fig. 5*A*,*B*,*D*). After 6 d of recovery, the population of GFP^+ cells had however strongly increased and was nearly restored ($n = 6$ tadpoles, $p < 0.0001$; Fig. 5*C*,*D*). EM examination of tadpoles following 6 d of recovery confirmed a partial remyelination of MTZ-induced demyelinated axons (Fig. 5*G*,*H*), in agreement with the return to nearly normal level of the number of GFP^+ cells (Fig. 5*D*). To investigate the potential of spontaneous repair *in vivo*, stage 55 tadpoles received the same treatment (MTZ 10 mM for 3 d then 6 d in normal water). Each treated tadpole was submitted to repetitive two-photon microscopy examinations. The disappearance and reappearance of GFP^+ oligodendrocyte cells was monitored in the same specimen and at the same location along the optic nerve (Fig. 6). Before treatment, in the field illustrated in Figure 6 we focused our observation on 6 GFP^+ cells (Fig. 6, T1). After 3 d of MTZ treatment, 3 cells were no longer observed (Fig. 6, T3) and a fourth cell had disappeared on the following observation (Fig. 6, R3). Two cells resisted the MTZ treatment (asterisks). After 3 d of recovery, new GFP^+ cells appeared (Fig. 6, R3), and their number progressively increased (Fig. 6, R6).

After 6 d of recovery, the number of GFP$^+$ cells was approximately similar to control conditions, indicative of a spontaneous recovery mechanism.

***pMBP-eGFP-NTR* tadpole as a tool for screening of remyelinating compounds**

We then questioned whether we could use this model to screen for molecules favoring *de novo* oligodendrogenesis and ultimately remyelination. As a proof of concept, we tested the efficiency of retinoic acid (RA), since it has previously been shown to increase myelination and remyelination both in *in vivo* and *ex vivo* models (Joubert et al., 2010; Latasa et al., 2010; Huang et al., 2011). In a first set of experiments, *pMBP-eGFP-NTR* tadpoles at stage 48 were treated with 13-*cis*-retinoic acid (100 nM). After 3 d of RA treatment, the number of GFP$^+$ cells per optic nerve (16 ± 3, $n = 10$) was doubled compared with untreated controls (7 ± 2, $n = 10$), suggesting a strong promoting effect of this retinoid X receptor agonist on oligodendrogenesis. RA acted in a dose-dependent manner, 10 and 50 nM RA resulting in 15 and 20% increase in the number of oligodendrocytes, respectively. Finally, we tested the effect of RA on *in vivo* remyelination potency. To induce an extensive demyelination, stage 50 *pMBP-eGFP-NTR* tadpoles were treated with 10 mM MTZ for 11 d. Tadpoles were then treated for 72 h with either 13-*cis*-retinoic acid (100 nM) or vehicle added to the aquarium water. The effects of MTZ followed by RA treatment were assessed by counting the number of GFP$^+$ oligodendrocytes in the optic nerve (Fig. 7). This longer exposure to MTZ induced a drastic deletion of myelinated oligodendrocytes in the optic nerve, which was further aggravated after 3 d in normal water. In contrast, the number of optic nerve GFP$^+$ cells was increased following a 3 d treatment with RA.

Together these results lead us to propose the *pMBP-eGFP-NTR* transgenic *Xenopus* line as a new, reliable and convenient model for monitoring the process of oligodendrogenesis *in vivo*.

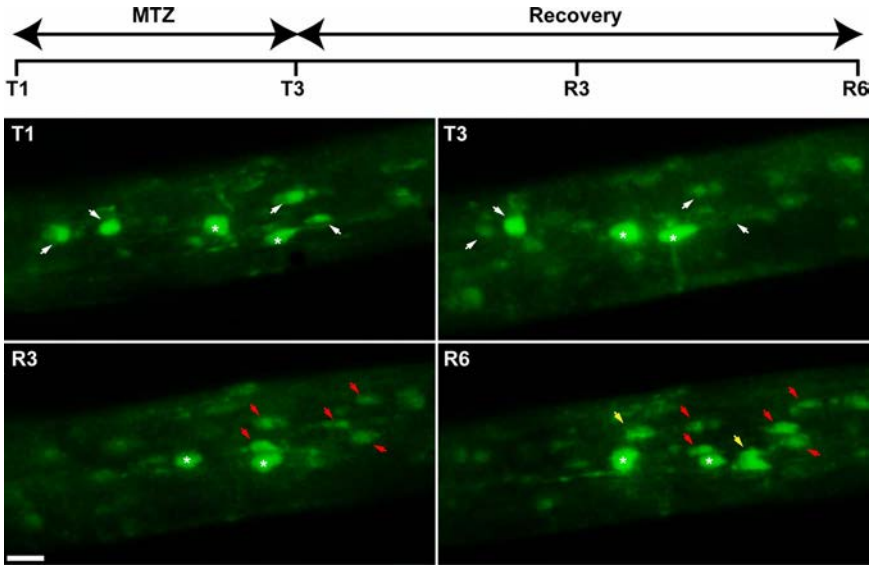

Figure 6. Live imaging of oligodendrocyte depletion and reappearance following MTZ treatment and cessation. Successive observation of the optic nerve of the same transgenic tadpole by two-photon microscopy. Transgenic tadpoles at stage 55 were treated for 3 d with MTZ (10 mM) (T1, T3), then returned to normal water for 6 d. Observations were before treatment (T1), after 3 d in the presence of MTZ (T3) and during recovery at 3 and 6 d in normal water (R3, R6). White arrows in T1 and T3 point to oligodendrocytes that disappear with MTZ treatment. White asterisks indicate oligodendrocytes that survive the treatment. One cell, which was still seen at T3, had disappeared in R3. In R3, red arrows point to new GFP$^+$ cells that have appeared, during the first 3 d of recovery. Yellow arrows in R6 indicate additional GFP$^+$ cells that have been generated between 3 and 6 d of recovery. Scale bar, 15 μm.

Discussion

We have generated a transgenic *Xenopus* line reliably and specifically expressing the fluorescent reporter GFP fused to a suicide gene in myelinating oligodendrocytes. This transgenic animal should prove useful to investigate myelination and remyelination. To date, the mouse provides the most powerful mammalian model for *in vitro* and *in vivo* modeling CNS myelination and remyelination (Jarjour et al., 2012). However, despite impressive improvements, live imaging remains complex and limited, both during early development, since embryogenesis is intrauterine, and during the postnatal period and adulthood due to the opacity of the skull and vertebrae (Fenrich et al., 2012). To circumvent this difficulty, some laboratories have developed transgenic zebrafish to take advantage of the transparency of the embryos, and interesting results have already been reported in this species (Kirby et al., 2006; Czopka and Lyons, 2011; Perlin et al., 2011). However, as far as myelination is concerned, the large difference in myelin protein composition of zebrafish compared with mammals may limit the transposition of data obtained in the zebrafish to higher vertebrates and human, in particular. For instance, in teleosts the major CNS myelin protein is a 36 kDa protein exhibiting no structural homology with any of the known mammalian myelin proteins (Moll et al., 2003). Similarly, bony fish oligodendrocytes (and CNS myelin) express protein zero (P0), a strictly PNS myelin constituent in mammals (Lanwert and Jeserich, 2001).

This situation contrasts with the numerous similarities between mammals and amphibian CNS myelin proteins. For instance, PLP, the most abundant CNS myelin protein that accounts for 50% of total myelin protein, has been shown to bear a high degree of conservation between amphibian and mammalian within the hydrophobic domains (Schliess and Stoffel, 1991; Yoshida and Colman, 1996), and PLP emerged at the root of tetrapods by the acquisition of an enlarged cytoplasmic loop in the evolutionary older DM20 isoform (Möbius et al., 2008). Similarly, in *Xenopus* as in mammals, alternative transcripts encoding Nogo protein are generated giving rise to *Xenopus* Nogo-A, -B, and -C (Diekmann et al., 2005). Since Nogo-A is one of the myelin-associated CNS axon growth inhibitor, this observation led the authors to conclude that Nogo-A in *Xenopus* myelin might contribute to the failure of spinal cord regeneration in frogs, a feature that may have evolved during the transition from fish to land vertebrates. Along the same line, we have been able to use antibodies raised against the mouse pan-neurofascin (NF186 and NF155) to successfully label the nodal and paranodal domains of *Xenopus* myelinated axons in the optic nerve as described in the mouse (Zonta et al., 2011). Furthermore, not only the coding sequences of myelin protein between mouse and *Xenopus* are highly conserved, but regulatory sequences are also similar. In the mouse, it has been shown that the −1.9 kb proximal upstream sequence of mouse *MBP* gene drives specific expression of the transgene in mature oligodendrocytes, but not in Schwann cells (Gow et al., 1992; Stankoff et al., 1996). Here, we show that this 1.9 kb regulatory sequence drives specifically trans-

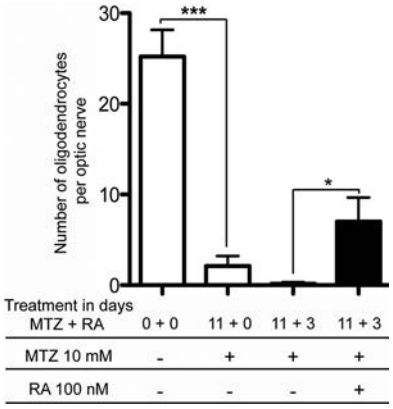

Figure 7. Retinoic acid improves spontaneous oligodendrocyte recovery. *pMBP-eGFP-NTR* tadpoles at stage 50 were treated for 11 d with MTZ (10 mM), then put either in fresh water or in water containing 13-*cis*-retinoic acid (100 nM) for 3 additional days. GFP $^+$ cells were counted *in vivo* on the optic nerve. Note that in the control animal the number of GFP $^+$ cells continued to decrease even 3 d after cessation of MTZ treatment, in contrast to tadpoles exposed to retinoic acid ($n = 6$, $p < 0.03$). *$p < 0.05$ and ***$p < 0.001$, significant differences.

gene expression in mature oligodendrocytes and not Schwann cells of *Xenopus laevis* tadpoles. Together, these results consolidate the demonstration that the mouse *MBP* gene used in the present study contains the regulatory information required for oligodendrocyte-specific expression in tadpole and illustrates a functional conservation between the two species.

The *E. coli* suicide gene *NTR* activates the aziridine compound CB1954 (5-aziridin-1-yl-2,4-dinitrobenzamide) into its cytotoxic DNA interstrand cross-linking derivative. Among NTR substrates, MTZ is preferred since its toxic form remains confined to the NTR-expressing cell, allowing the exclusive ablation of NTR $^+$ cells without bystander effects (Bridgewater et al., 1995). This property initially used to eliminate cancer cells (Bridgewater et al., 1995; Bailey et al., 1996) has also been used to conditionally ablate different cell types in transgenic animals. In the mouse, expression of NTR driven by the control elements of the human CD2 locus has allowed to induce an extensive and specific T cell depletion in thymus and spleen (Drabek et al., 1997). More recently, transgenic expression of NTR has been successfully used in zebrafish and *Xenopus* to induce temporally controlled cell-specific ablation of cardiomyocytes, pancreatic β-cells, hepatocytes and rod photoreceptors (Curado et al., 2007, 2008; Pisharath et al., 2007; Choi et al., 2011). Here, we demonstrate that the same experimental strategy can be exploited to eliminate oligodendrocytes in a temporal- and spatial-specific manner in a transgenic *Xenopus* tadpole. We also show that the hydroxyamino derivative produced following NTR-catalyzed reduction of MTZ kills cells predominantly by caspase-dependent apoptosis, similar to the mechanism activated by CB 1954, an alternative substrate of NTR (Palmer et al., 2003).

Understanding the molecular mechanisms controlling remyelination of axons in demyelinating diseases, like multiple sclerosis, is of significant clinical interest to define new therapeutic targets aimed at inducing or increasing endogenous repair. The different *in vitro* strategies to explore myelination and remyelination in rodents have recently been reviewed (Jarjour et al., 2012).

For *in vivo* studies of demyelination and remyelination, there is a relatively large panel of experimental models in rodents and primates. Experimental autoimmune encephalitis (EAE) is probably the most widely used model for MS, since it associates inflammation and demyelination and mimics immunopathological characteristics found in MS (for recent reviews, see Steinman and Zamvil, 2005; Baker et al., 2011; Batoulis et al., 2011; Constantinescu et al., 2011). Although EAE is far from being a perfect model for MS, most of currently used treatments for MS have been investigated in EAE. To be convincing, studies based on EAE require a large number of animals and are therefore costly and lengthy. This is due to the fact that the localization and size of lesions are not predictable and highly variable between animals and that the lack of reliable *in vivo* markers limits longitudinal studies of the same animal to evaluate biology of the disease and remyelination. Moreover, the introduction of targeted EAE (Kerschensteiner et al., 2004) has advanced the field being readily applicable in the rat, but more delicate to apply in the mouse (Tepavčević et al., 2011).

In toxin-mediated models, the inflammatory component is less important but the demyelination is localized, therefore facilitating analyses of demyelination and remyelination (Miller and Fyffe-Maricich, 2010). The demyelinating property of lysolecithin was first demonstrated in rat cerebellum myelinating cultures (Perier, 1965), before being used *in vivo* as demyelinating agent following injection in the white matter of the mouse spinal cord (Hall, 1972). Focal demyelination and remyelination is also observed following ethidium bromide injection. The first reports using ethidium bromide as a demyelinating toxin involved intracisternal injection in the rat (Yajima and Suzuki, 1979) or local injection in the cat spinal cord (Blakemore, 1982). Another widely used model consists in the introduction of cuprizone into the diet of adult mice for several weeks. This treatment results in focal demyelination of the superior cerebellar peduncle and the corpus callosum. When allowed to recover on a normal diet, mice rapidly remyelinate until a complete repair of all axons (Blakemore, 1973; Ludwin, 1978). Despite their considerable advantages compared with EAE models, toxin-mediated models are still quite demanding and not ideally suited for large screening of compounds potentially favoring remyelination.

More recently a novel screening for potential promyelination compounds was developed using laser ablation of GFP-expressing oligodendrocytes in zebrafish larvae (Buckley et al., 2010). However, as stated above, the large differences of myelin constituents usage between teleost and higher vertebrate may be misleading to translate from the zebrafish to human. In this respect, *Xenopus* tadpole provides a signficant advantage over zebrafish. In addition, and in comparison with other *in vivo* animal models of demyelination, the *NTR* suicide gene allows a simple conditional and reversible demyelination. Introduction of the demyelinating agent in the water avoids stereotactic intracerebral or spinal cord injections. In comparison with cuprizone, which is also introduced in the nutrient, MTZ-induced demyelination is much faster (3 d vs 6 weeks) and the extent of demyelination can be monitored from 50% to ~100% simply by varying the duration of MTZ treatment, between 3 and 11 d, respectively (compare Figs. 3 and 7). Another advantage of our *Xenopus* model is the rapidity of remyelination, an important criterion for large-scale screening of molecules. Finally, and of particular interest also for screening, amphibian tadpoles can be produced in very large numbers (thousands of transparent embryos, which develop in water).

In conclusion, the *pMBP-eGFP-NTR Xenopus* described here should prove useful, not only to identify either new therapeutics targeted at promoting myelin repair or reprofiling currently available drugs, but also to exploit the transparent feature of the tadpoles to visualize and record the process and mechanisms of myelination, demyelination and remyelination *in vivo*.

References

Ainger K, Avossa D, Diana AS, Barry C, Barbarese E, Carson JH (1997) Transport and localization elements in myelin basic protein mRNA. J Cell Biol 138:1077–1087.

Bailey SM, Knox RJ, Hobbs SM, Jenkins TC, Mauger AB, Melton RG, Burke PJ, Connors TA, Hart IR (1996) Investigation of alternative prodrugs for use with E. coli nitroreductase in 'suicide gene' approaches to cancer therapy. Gene Ther 3:1143–1150.

Baker D, Gerritsen W, Rundle J, Amor S (2011) Critical appraisal of animal models of multiple sclerosis. Mult Scler 17:647–657.

Batoulis H, Recks MS, Addicks K, Kuerten S (2011) Experimental autoimmune encephalomyelitis—achievements and prospective advances. APMIS 119:819–830.

Bhat RV, Axt KJ, Fosnaugh JS, Smith KJ, Johnson KA, Hill DE, Kinzler KW, Baraban JM (1996) Expression of the APC tumor suppressor protein in oligodendroglia. Glia 17:169–174.

Blakemore WF (1973) Remyelination of the superior cerebellar peduncle in the mouse following demyelination induced by feeding cuprizone. J Neurol Sci 20:73–83.

Blakemore WF (1982) Ethidium bromide induced demyelination in the spinal cord of the cat. Neuropathol Appl Neurobiol 8:365–375.

Bridgewater JA, Springer CJ, Knox RJ, Minton NP, Michael NP, Collins MK (1995) Expression of the bacterial nitroreductase enzyme in mammalian cells renders them selectively sensitive to killing by the prodrug CB1954. Eur J Cancer 31A:2362–2370.

Buckley CE, Marguerie A, Roach AG, Goldsmith P, Fleming A, Alderton WK, Franklin RJ (2010) Drug reprofiling using zebrafish identifies novel compounds with potential pro-myelination effects. Neuropharmacology 59:149–159.

Chesneau A, Sachs LM, Chai N, Chen Y, Du Pasquier L, Loeber J, Pollet N, Reilly M, Weeks DL, Bronchain OJ (2008) Transgenesis procedures in *Xenopus*. Biol Cell 100:503–521.

Choi RY, Engbretson GA, Solessio EC, Jones GA, Coughlin A, Aleksic I, Zuber ME (2011) Cone degeneration following rod ablation in a reversible model of retinal degeneration. Invest Ophthalmol Vis Sci 52:364–373.

Cima C, Grant P (1982) Development of the optic nerve in *Xenopus laevis*. II. Gliogenesis, myelination and metamorphic remodelling. J Embryol Exp Morphol 72:251–267.

Constantinescu CS, Farooqi N, O'Brien K, Gran B (2011) Experimental autoimmune encephalomyelitis (EAE) as a model for multiple sclerosis (MS). Br J Pharmacol 164:1079–1106.

Curado S, Anderson RM, Jungblut B, Mumm J, Schroeter E, Stainier DY (2007) Conditional targeted cell ablation in zebrafish: a new tool for regeneration studies. Dev Dyn 236:1025–1035.

Curado S, Stainier DY, Anderson RM (2008) Nitroreductase-mediated cell/tissue ablation in zebrafish: a spatially and temporally controlled ablation method with applications in developmental and regeneration studies. Nat Protoc 3:948–954.

Czopka T, Lyons DA (2011) Dissecting mechanisms of myelinated axon formation using zebrafish. Methods Cell Biol 105:25–62.

de Luze A, Sachs L, Demeneix B (1993) Thyroid hormone-dependent transcriptional regulation of exogenous genes transferred into *Xenopus* tadpole muscle in vivo. Proc Natl Acad Sci U S A 90:7322–7326.

Denarier E, Forghani R, Farhadi HF, Dib S, Dionne N, Friedman HC, Lepage P, Hudson TJ, Drouin R, Peterson A (2005) Functional organization of a Schwann cell enhancer. J Neurosci 25:11210–11217.

De Smet F, Carmeliet P, Autiero M (2006) Fishing and frogging for anti-angiogenic drugs. Nat Chem Biol 2:228–229.

Diekmann H, Klinger M, Oertle T, Heinz D, Pogoda HM, Schwab ME, Stuermer CA (2005) Analysis of the reticulon gene family demonstrates the absence of the neurite growth inhibitor Nogo-A in fish. Mol Biol Evol 22:1635–1648.

Drabek D, Guy J, Craig R, Grosveld F (1997) The expression of bacterial nitroreductase in transgenic mice results in specific cell killing by the prodrug CB1954. Gene Ther 4:93–100.

Eng LF, Vanderhaeghen JJ, Bignami A, Gerstl B (1971) An acidic protein isolated from fibrous astrocytes. Brain Res 28:351–354.

Fenrich KK, Weber P, Hocine M, Zalc M, Rougon G, Debarbieux F (2012) Long-term in vivo imaging of normal and pathological mouse spinal cord with subcellular resolution using implanted glass windows. J Physiol 590:3665–3675.

Geisler S, Heilmann H, Veh RW (2002) An optimized method for simultaneous demonstration of neurons and myelinated fiber tracts for delineation of individual trunco- and palliothalamic nuclei in the mammalian brain. Histochem Cell Biol 117:69–79.

Giacomotto J, Ségalat L (2010) High-throughput screening and small animal models, where are we? Br J Pharmacol 160:204–216.

Gow A, Friedrich VL Jr, Lazzarini RA (1992) Myelin basic protein gene contains separate enhancers for oligodendrocyte and Schwann cell expression. J Cell Biol 119:605–616.

Graus F, Ferrer I (1990) Analysis of a neuronal antigen (Hu) expression in the developing rat brain detected by autoantibodies from patients with paraneoplastic encephalomyelitis. Neurosci Lett 112:14–18.

Hall SM (1972) The effect of injections of lysophosphatidyl choline into white matter of the adult mouse spinal cord. J Cell Sci 10:535–546.

Howell OW, Palser A, Polito A, Melrose S, Zonta B, Scheiermann C, Vora AJ, Brophy PJ, Reynolds R (2006) Disruption of neurofascin localization reveals early changes preceding demyelination and remyelination in multiple sclerosis. Brain 129:3173–3185.

Huang JK, Jarjour AA, Nait Oumesmar B, Kerninon C, Williams A, Krezel W, Kagechika H, Bauer J, Zhao C, Evercooren AB, Chambon P, Ffrench-Constant C, Franklin RJ (2011) Retinoid X receptor gamma signaling accelerates CNS remyelination. Nat Neurosci 14:45–53.

Jarjour AA, Zhang H, Bauer N, Ffrench-Constant C, Williams A (2012) In vitro modeling of central nervous system myelination and remyelination. Glia 60:1–12.

Joubert L, Foucault I, Sagot Y, Bernasconi L, Duval F, Alliod C, Frossard MJ, Pescini Gobert R, Curchod ML, Salvat C, Nichols A, Pouly S, Rommel C, Roach A, Hooft van Huijsduijnen R (2010) Chemical inducers and transcriptional markers of oligodendrocyte differentiation. J Neurosci Res 88:2546–2557.

Kanfer J, Parenty M, Goujet-Zalc C, Monge M, Bernier L, Campagnoni AT, Dautigny A, Zalc B (1989) Developmental expression of myelin proteolipid, basic protein, and 2′,3′-cyclic nucleotide 3′-phosphodiesterase transcripts in different rat brain regions. J Mol Neurosci 1:39–46.

Kerschensteiner M, Stadelmann C, Buddeberg BS, Merkler D, Bareyre FM, Anthony DC, Linington C, Brück W, Schwab ME (2004) Targeting experimental autoimmune encephalomyelitis lesions to a predetermined axonal tract system allows for refined behavioral testing in an animal model of multiple sclerosis. Am J Pathol 164:1455–1469.

Kirby BB, Takada N, Latimer AJ, Shin J, Carney TJ, Kelsh RN, Appel B (2006) In vivo time-lapse imaging shows dynamic oligodendrocyte progenitor behavior during zebrafish development. Nat Neurosci 9:1506–1511.

Kroll KL, Amaya E (1996) Transgenic *Xenopus* embryos from sperm nuclear transplantations reveal FGF signaling requirements during gastrulation. Development 122:3173–3183.

Lanwert C, Jeserich G (2001) Structure, heterologous expression, and adhesive properties of the P(0)-like myelin glycoprotein IP1 of trout CNS. Microsc Res Tech 52:637–644.

Latasa MJ, Ituero M, Moran-Gonzalez A, Aranda A, Cosgaya JM (2010) Retinoic acid regulates myelin formation in the peripheral nervous system. Glia 58:1451–1464.

Ludwin SK (1978) Central nervous system demyelination and remyelination in the mouse: an ultrastructural study of cuprizone toxicity. Lab Invest 39:597–612.

Miller RH, Fyffe-Maricich SL (2010) Restoring the balance between disease and repair in multiple sclerosis: insights from mouse models. Dis Model Mech 3:535–539.

Möbius W, Patzig J, Nave KA, Werner HB (2008) Phylogeny of proteolipid proteins: divergence, constraints, and the evolution of novel functions in myelination and neuroprotection. Neuron Glia Biol 4:111–127.

Moll W, Lanwert C, Stratmann A, Strelau J, Jeserich G (2003) Molecular cloning, tissue expression, and partial characterization of the major fish CNS myelin protein 36k. Glia 44:57–66.

Nieuwkoop PD, Faber J (1994) Normal Table of *Xenopus laevis* (Daudin). New York: Garland Publishing.

Palmer DH, Milner AE, Kerr DJ, Young LS (2003) Mechanism of cell death induced by the novel enzyme-prodrug combination, nitroreductase/CB1954, and identification of synergism with 5-fluorouracil. Br J Cancer 89:944–950.

Perier O (1965) [Demyelinization of central nervous tissue cultures by lysolecithin]. Acta Neurol Belg 65:78–95.

Perlin JR, Lush ME, Stephens WZ, Piotrowski T, Talbot WS (2011) Neuro-

nal Neuregulin 1 type III directs Schwann cell migration. Development 138:4639–4648.

Pernet V, Joly S, Christ F, Dimou L, Schwab ME (2008) Nogo-A and myelin-associated glycoprotein differently regulate oligodendrocyte maturation and myelin formation. J Neurosci 28:7435–7444.

Pisharath H, Rhee JM, Swanson MA, Leach SD, Parsons MJ (2007) Targeted ablation of beta cells in the embryonic zebrafish pancreas using *E. coli* nitroreductase. Mech Dev 124:218–229.

Saito RM, van den Heuvel S (2002) Malignant worms: what cancer research can learn from *C. elegans*. Cancer Invest 20:264–275.

Schliess F, Stoffel W (1991) Evolution of the myelin integral membrane proteins of the central nervous system. Biol Chem Hoppe Seyler 372:865–874.

Soula C, Danesin C, Kan P, Grob M, Poncet C, Cochard P (2001) Distinct sites of origin of oligodendrocytes and somatic motoneurons in the chick spinal cord: oligodendrocytes arise from Nkx2.2-expressing progenitors by a Shh-dependent mechanism. Development 128:1369–1379.

Sparrow DB, Latinkic B, Mohun TJ (2000) A simplified method of generating transgenic *Xenopus*. Nucleic Acids Res 28:E12.

Stankoff B, Demerens C, Goujet-Zalc C, Monge M, Peyron F, Mikoshiba K, Zalc B, Lubetzki C (1996) Transcription of myelin basic protein promoted by regulatory elements in the proximal 5′ sequence requires myelinogenesis. Mult Scler 2:125–132.

Steinman L, Zamvil SS (2005) Virtues and pitfalls of EAE for the development of therapies for multiple sclerosis. Trends Immunol 26:565–571.

Tepavčević V, Lazarini F, Alfaro-Cervello C, Kerninon C, Yoshikawa K, Garcia-Verdugo JM, Lledo PM, Nait-Oumesmar B, Baron-Van Evercooren A (2011) Inflammation-induced subventricular zone dysfunction leads to olfactory deficits in a targeted mouse model of multiple sclerosis. J Clin Invest 121:4722–4734.

Yajima K, Suzuki K (1979) Demyelination and remyelination in the rat central nervous system following ethidium bromide injection. Lab Invest 41:385–392.

Yoshida M (1997) Oligodendrocyte maturation in *Xenopus laevis*. J Neurosci Res 50:169–176.

Yoshida M, Colman DR (1996) Parallel evolution and coexpression of the proteolipid proteins and protein zero in vertebrate myelin. Neuron 16:1115–1126.

Yoshida M, Macklin WB (2005) Oligodendrocyte development and myelination in GFP-transgenic zebrafish. J Neurosci Res 81:1–8.

Zalc B, Colman DR (2000) Origins of vertebrate success. Science 288:271–272.

Zalc B, Goujet D, Colman D (2008) The origin of the myelination program in vertebrates. Curr Biol 18:R511–R512.

Zonta B, Tait S, Melrose S, Anderson H, Harroch S, Higginson J, Sherman DL, Brophy PJ (2008) Glial and neuronal isoforms of Neurofascin have distinct roles in the assembly of nodes of Ranvier in the central nervous system. J Cell Biol 181:1169–1177.

Zonta B, Desmazieres A, Rinaldi A, Tait S, Sherman DL, Nolan MF, Brophy PJ (2011) A critical role for Neurofascin in regulating action potential initiation through maintenance of the axon initial segment. Neuron 69:945–956.

REFERENCES

Abney ER, Williams BP, Raff MC. Tracing the development of oligodendrocytes from precursor cells using monoclonal antibodies, fluorescence-activated cell sorting, and cell culture. Dev Biol. 1983 Nov;100(1):166-71.

Aaron W. McGee, Yupeng Yang, Quentin S. Fischer, Nigel W. Daw and Stephen M. Strittmatter. Experience-Driven Plasticity of Visual Cortex Limited by Myelin and Nogo Receptor.Science. Sep 30, 2005; 309(5744): 2222–2226.

Antonellis A, Huynh JL, Lee-Lin SQ, Vinton RM, Renaud G, Loftus SK, Elliot G, Wolfsberg TG, Green ED, McCallion AS, Pavan WJ. Identification of neural crest and glial enhancers at the mouse Sox10 locus through transgenesis in zebrafish. PLoS Genet. 2008 Sep 5;4(9)

Ascherio A, Munger KL, Lünemann JD. The initiation and prevention of multiple sclerosis.Nat Rev Neurol. 2012 Nov 5;8(11):602-12.

Bansal R, Pfeiffer SE. Reversible inhibition of oligodendrocyte progenitor differentiation by a monoclonal antibody against surface galactolipids. Proc Natl Acad Sci U S A. 1989 Aug;86(16):6181-5

Barbazuk W. B., Korf I., Kadavi C., Heyen J., Tate S., Wun E., Bedell J. A., McPherson J. D., Johnson S. L. The syntenic relationship of the zebrafish and human genomes. (2000). Genome Res. 10, 1351–1358

Barres BA, Raff MC. Axonal control of oligodendrocyte development. J Cell Biol. 1999 Dec 13;147(6):1123-8.

Barnett MH, Henderson AP, Prineas JW.The macrophage in MS: just a scavenger after all? Pathology and pathogenesis of the acute MS lesion. Mult Scler. 2006 Apr;12(2):121-32

Baumann N, Pham-Dinh D. Biology of oligodendrocyte and myelin in the mammalian central nervous system. Physiol Rev. 2001 Apr;81(2):871-927.

Berghs S, Aggujaro D, Dirkx R Jr, Maksimova E, Stabach P, Hermel JM, Zhang JP, Philbrick W, Slepnev V, Ort T, Solimena M. BetaIV spectrin, a new spectrin localized at axon initial segments and nodes of ranvier in the central and peripheral nervous system. J Cell Biol. 2000 Nov 27;151(5):985-1002

Bhat, M.A., J.C. Rios, Y. Lu, G.P. Garcia-Fresco, W. Ching, M. St Martin, J. Li, S. Einheber, M. Chesler, J. Rosenbluth, et al. 2001. Axon-glia interactions and the domain organization of myelinated axons requires neurexin IV/Caspr/Paranodin. Neuron. 30:369–383.

Bö L, Dawson TM, Wesselingh S, Mörk S, Choi S, Kong PA, Hanley D, Trapp BD. Induction of nitric oxide synthase in demyelinating regions of multiple sclerosis brains.Ann Neurol. 1994 Nov;36(5):778-86.

Bostock H, Sears TA.The internodal axon membrane: electrical excitability and continuous conduction in segmental demyelination. J Physiol. 1978; Jul;280:273-301.

Boyle, M.E., E.O. Berglund, K.K. Murai, L. Weber, E. Peles, and B. Ranscht. 2001. Contactin orchestrates assembly of the septate-like junctions at the paranode in myelinated peripheral nerve. Neuron. 30:385–397

Bisbee CA, Baker MA, Wilson AC, Haji-Azimi I, Fischberg M. Albumin phylogeny for clawed frogs (Xenopus). Science 1977;195:785–787.

Brok HP, Bauer J, Jonker M, Blezer E, Amor S, Bontrop RE, Laman JD, 't Hart BA. Non-human primate models of multiple sclerosis.Immunol Rev. 2001 Oct;183:173-85

Brosamle C., Halpern M. E. Characterization of myelination in the developing zebrafish. (2002). Glia39, 47–57

Buckley C., Chappell C., Munday P., Wardle W., Peacock M., Goldsmith P., Marguerie A., Franklin R.. Zebrafish myelination: a transparent model for remyelination? (2007) Neuron Glia Biol. 3, S117

Bunge MB, Bunge RP, RIS H. Ultrastructural study of remyelination in an experimental lesion in adult cat spinal cord. J Biophys Biochem Cytol. 1961 May;10:67-94.

Bittner S, Afzali AM, Wiendl H, Meuth SG. Myelin oligodendrocyte glycoprotein (MOG35-55) induced experimental autoimmune encephalomyelitis (EAE) in C57BL/6 mice. J Vis Exp. 2014 Apr 15;(86).

Buckley CE, Marguerie A, Alderton WK, Franklin RJ. Temporal dynamics of myelination in the zebrafish spinal cord. Glia. 2010 May;58(7):802-12.

Charles, P., S. Tait, C. Faivre-Sarrailh, G. Barbin, F. Gunn-Moore, N. Denisenko-Nehrbass, A.M. Guennoc, J.A. Girault, P.J. Brophy, and C. Lubetzki. 2002. Neurofascin is a glial receptor for the paranodin/Caspr-contactin axonal complex at the axoglial junction. Curr. Biol. 12:217–220

Cima C, Grant P. Development of the optic nerve in Xenopus laevis. II. Gliogenesis, myelination and metamorphic remodelling. J Embryol Exp Morphol. 1982 Dec;72:251-67.

Chalmers AD, Goldstone K, Smith JC, Gilchrist M, Amaya E, Papalopulu N. A Xenopus tropicalis oligonucleotide microarray works across species using RNA from Xenopus laevis. Mech Dev 2005;122:355–363

Chari DM, Blakemore WF. Efficient recolonisation of progenitor-depleted areas of the CNS by adult oligodendrocyte progenitor cells. Glia 2002; 37(4):307-13

Chen MS, Huber AB, van der Haar ME, Frank M, Schnell L, Spillmann AA, Christ F, Schwab ME.Nogo-A is a myelin-associated neurite outgrowth inhibitor and an antigen for monoclonal antibody IN-1. Nature. 2000;403:434–439.

Chen SX, Tari PK, She K, Haas K. Neurexin-neuroligin cell adhesion complexes contribute to synaptotropic dendritogenesis via growth stabilization mechanisms in vivo.Neuron. 2010 Sep 23;67(6):967-83.

Chung AY, Kim PS, Kim S, Kim E, Kim D, Jeong I, Kim HK, Ryu JH, Kim CH, ChoiJ, SeoJH, ParkHC.Generation of demyelination models by targeted ablation of oligo dendrocytes in the zebrafish CNS. Mol Cells. 2013 Jul;36(1):82-7

Chesneau. A, Laurent M. Sachs, Norin Chai, Yonglong Chen, Louis Du Pasquier,Jana Loeber,Nicolas Pollet, Michael Reilly, Daniel L. Weeks, and Odile J. Bronchain Transgenesis procedures in Xenopus.Biol Cell. Sep 2008; 100(9): 503–521.

Coen L, du Pasquier D, Le Mevel S, Brown S, Tata J, Mazabraud A Demeneix BA Xenopus Bcl-X(L) selectively protects Rohon-Beard neurons from metamorphic degeneration.,.Proc Natl Acad Sci U S A. 2001 Jul 3; 98(14):7869-74.

Craner MJ, Newcombe J, Black JA, Hartle C, Cuzner ML, Waxman SG.Molecular changes in neurons in multiple sclerosis: altered axonal expression of Nav1.2 and Nav1.6 sodium channels and Na+/Ca2+ exchanger. PNAS 2004;May 17 25;101(21):8168-73

Curado S., Anderson R. M., Jungblut B., Mumm J., Schroeter E., Stainier D. Y. (2007). Conditional targeted cell ablation in zebrafish: a new tool for regeneration studies. Dev. Dyn. 236, 1025–1035

Davis, J.Q., S. Lambert, and V. Bennett. 1996. Molecular composition of the node of Ranvier: identification of ankyrin-binding cell adhesion molecules neurofascin (mucin+/third FNIII domain−) and NrCAM at nodal axon segments. J. Cell Biol. 135:1355–1367.

Demerens C, Stankoff B, Logak M, Anglade P, Allinquant B, Couraud F, Zalc B, Lubetzki C. Induction of myelination in the central nervous system by electrical activity. Proc Natl Acad Sci U S A. 1996 Sep 3;93(18):9887-92.

Dubois-Dalcq M[1], Williams A, Stadelmann C, Stankoff B, Zalc B, Lubetzki C. From fish to man: understanding endogenous remyelination in central nervous system demyelinating diseases.Brain. 2008 Jul;131(Pt 7):1686-700.

Dupouey P,Jacque C, Bourre JM, Cesselin F, Privat A, Baumann N. Immunochemical studies of myelin basic protein in shiverer mouse devoid of major dense line of myelin. Neurosci Lett. 1979 Apr;12(1):113-8.

Dupree JL, Mason JL, Marcus JR, Stull M, Levinson R, Matsushima GK, Popko BOligodendrocytes assist in the maintenance of sodium channel clusters independent of the myelin sheath. Neuron Glia Biol. 2004;1:1–14

Dousset V, Brochet B, Vital A, Gross C, Benazzouz A, Boullerne A, Bidabe AM, Gin AM, Caille JM. Lysolecithin-induced demyelination in primates: preliminary in vivo study with MR and magnetization transfer.AJNR Am J Neuroradiol. 1995 Feb;16(2):225-31.

Eva Jolanda Münzel.Zebrafish regenerate full thickness optic nerve myelin after demyelination, but this fails with increasing age.Acta Neuropathologica 2014.Communications

Evans BJ, Kelley DB, Tinsley RC, Melnick DJ, Cannatella DC. A mitochondrial DNA phylogeny of African clawed frogs: phylogeography and implications for polyploid evolution. Mol Phylogenet Evol 2004;33:197–213.

Evans BJ, Kelley DB, Melnick DJ, Cannatella DC. Evolution of RAG-1 in polyploid clawed frogs. Mol Biol Evol 2005;22:1193–1207.

Falk J, Drinjakovic J, Leung KM, Dwivedy A, Regan AG, Piper M, Holt CE. Electroporation of cDNA/Morpholinos to targeted areas of embryonic CNS in Xenopus.BMC Dev Biol. 2007 Sep 27;7:107.

Fünfschilling U, Supplie LM, Mahad D, Boretius S, Saab AS, Edgar J, Brinkmann BG, Kassmann CM, Tzvetanova ID, Möbius W, Diaz F, Meijer D, Suter U, Hamprecht B, Sereda MW, Moraes CT, Frahm J, Goebbels S, Nave KA. Glycolytic oligodendrocytes maintain myelin and long-term axonal integrity.
Nature. 2012 Apr 29;485(7399):517-21.

Fuiisawa. H.. N. Tani. K. Watanabe, and Y. lbata Branchinq of regenerating retinal axons and preferential selection ‘of appropriate branches for specific neuronal connections in the newt. (1982) Dev. BIoI. 90: 43- 57.

Franco-Pons N, Torrente M, Colomina MT, Vilella E. Behavioral deficits in the cuprizone-induced murine model of demyelination/remyelination.Toxicol Lett. 2007 Mar 30;169(3):205-13. Epub 2007 Feb 2.

Francis DA, Bain P, Swan AV, Hughes RA. An assessment of disability rating scales used in multiple sclerosis. Arch Neurol. 1991 Mar;48(3):299-301.

Friede RL, Bischhausen R. How are sheath dimensions affected by axon caliber and internode length? Brain Res. 1982 Mar 11;235(2):335-50.

Franklin RJ, Ffrench-Constant C. Remyelination in the CNS: from biology to therapyNat Rev Neurosci. 2008 Nov;9(11):839-55

Frohman EM, Racke MK, Raine CS. Multiple sclerosis--the plaque and its pathogenesis. N Engl J Med. 2006 Mar 2;354(9):942-55.

Girard C, Bemelmans A-P, Dufour N, Mallet J, Bachelin C, Nait-Oumesmar Bet al (2005). Grafts of brain-derived neurotrophic factor and neurotrophin 3-transduced primate Schwann

cells lead to functional recovery of the demyelinated mouse spinal cord. J Neurosci 25: 7924–7933

Gregg C, Shikar V, Larsen P, Mak G, Chojnacki A, Yong VW et al (2007). White matter plasticity and enhanced remyelination in the maternal CNS. J Neurosci 27: 1812–1823.

Hohlfeld R, Wiendl H. The ups and downs of multiple sclerosis therapeutics. Ann Neurol. 2001 Mar;49(3):281-4

Gao F.B., Apperly,J. and Raff,M. (1998) Cell-intrinsic timers and thyroid hormone regulate the probability of cell-cycle withdrawal and differentiation of oligodendrocyte precursor cells. Dev. Biol., 197, 54–66

Gay CT, Hardies LJ, Rauch RA, Lancaster JL, Plaetke R, DuPont BR, Cody JD, Cornell JE, Herndon RC, Ghidoni PD, Schiff JM, Kaye CI, Leach RJ, Fox PT. Magnetic resonance imaging demonstrates incomplete myelination in 18q- syndrome: evidence for myelin basic protein haploinsufficiency. Am J Med Genet. 1997 Jul 25;74(4):422-31.

Genain CP, Hauser SL. Experimental allergic encephalomyelitis in the New World monkey Callithrix jacchus.Immunol Rev. 2001 Oct;183:159-72. Review.

Genain CP, Hauser SL. Creation of a model for multiple sclerosis in Callithrix jacchus marmosets. J Mol Med (Berl). 1997 Mar;75(3):187-97. Review.

Giacomotto J, Ségalat L. High-throughput screening and small animal models, where are we? Br J Pharmacol. 2010 May;160(2):204-16.

Gibson EM, Purger D, Mount CW, Goldstein AK, Lin GL, Wood LS, Inema I, Miller SE, Bieri G, Zuchero JB, Barres BA, Woo PJ, Vogel H, Monje M. Neuronal activity promotes oligodendrogenesis and adaptive myelination in the mammalian brain. Science. 2014 May 2;344(6183)

Gow A, Lazzarini RA. A cellular mechanism governing the severity of Pelizaeus-Merzbacher disease. Nat Genet. 1996 Aug;13(4):422-8.

Guo X, Zhang T, Hu Z, Zhang Y, Shi Z, Wang Q, Cui Y, Wang F, Zhao H, Chen Y. Efficient RNA/Cas9-mediated genome editing in Xenopus tropicalis. Development. 2014 Feb;141(3):707-14.

Hamlet MR, Yergeau DA, Kuliyev E, Takeda M, Taira M, Kawakami K, Mead PE. Tol2 transposon- mediated transgenesis in Xenopus tropicalis. Genesis 2006;44:438–445.

Hartline DK, Colman DR. Rapid conduction and the evolution of giant axons and myelinated fibers. Curr Biol. 2007 Jan 9;17(1):R29-35.

Huxley AF, Stämpfli R. Evidence for saltatory conduction in peripheral myelinated nerve fibres..J Physiol. 1949 May 15;108(3):315-39.

Hohlfeld R, Wiendl H. The ups and downs of multiple sclerosis therapeutics. Ann Neurol. 2001 Mar;49(3):281-4.

Ibanez C., Shields S. A., El-Etr M., Baulieu E. E., Schumacher M., Franklin R. J. M. (2004). Systemic progesterone administration results in a partial reversal of the age-associated decline in CNS remyelination following toxin-induced demyelination in male rats. Neuropathol. Appl. Neurobiol.30, 80–89

Ishibashi T, Dakin KA, Stevens B, Lee PR, Kozlov SV, Stewart CL, Fields RD. Astrocytes promote myelination in response to electrical impulses.Neuron. 2006 Mar 16;49(6):823-32.

Jenkins SM, Bennett V. Developing nodes of Ranvier are defined by ankyrin-G clustering and are independent of paranodal axoglial adhesion. Proc Natl Acad Sci U S A. 2002 Feb 19;99(4):2303-8.

Johnson KP, Brooks BR, Cohen JA, Ford CC, Goldstein J, Lisak RP, Myers LW, Panitch HS, Rose JW, Schiffer RB. Copolymer 1 reduces relapse rate and improves disability in relapsing-remitting multiple sclerosis: results of a phase III multicenter, double-blind placebo-controlled trial. The Copolymer 1 Multiple Sclerosis Study Group.Neurology. 1995 Jul;45(7):1268-76

Kaplan MR, Meyer-Franke A, Lambert S, Bennett V, Duncan ID, Levinson SR, Barres BA. Induction of sodium channel clustering by oligodendrocytes. Nature. 1997 Apr 17;386(6626):724-8.

Kaya F, Mannioui A, Chesneau A, Sekizar S, Maillard E, Ballagny C, Houel-Renault L, Dupasquier D, Bronchain O, Holtzmann I, Desmazieres A, Thomas JL,Demeneix BA, Brophy PJ, Zalc B, Mazabraud A. Live imaging of targeted cell ablation in Xenopus: a new model to study demyelination and repair. J Neurosci. 2012 Sep 12;32(37):12885-95.

Káradóttir R, Hamilton NB, Bakiri Y, Attwell D. Spiking and nonspiking classes of oligodendrocyte precursor glia in CNS white matter.Nat Neurosci. 2008 Apr;11(4):450-6.

Kara G. Pratt, Arseny S. Khakhalin. Modeling human neurodevelopmental disorders in the Xenopus tadpole: from mechanisms to therapeutic targets. Dis Model Mech. Sep 2013; 6(5): 1057–1065.

Kazarinova-Noyes, K., J.D. Malhotra, D.P. McEwen, L.N. Mattei, E.O. Berglund, B. Ranscht, S.R. Levinson, M. Schachner, P. Shrager, L.L. Isom, and Z.C. Xiao. 2001. Contactin associates with Na+ channels and increases their functional expression. J. Neurosci. 21:7517–7525.

Koeppen AH, Ronca NA, Greenfield EA, Hans MB. Defective biosynthesis of proteolipid protein in Pelizaeus-Merzbacher disease.Ann Neurol. 1987 Feb;21(2):159-70.

Komoly S, Jeyasingham MD, Pratt OE, Lantos PL Decrease in oligodendrocyte carbonic anhydrase activity preceding myelin degeneration in cuprizone induced demyelination. 1987.J Neurol Sci 79:141–148

Kerschensteiner M, Bareyre FM, Buddeberg BS, Merkler D, Stadelmann C, Brück W, Misgeld T, Schwab ME. Remodeling of axonal connections contributes to recovery in an animal model of multiple sclerosis. J Exp Med. 2004 Oct 18;200(8):1027-38.

Kroll KL, Amaya E. Transgenic Xenopus embryos from sperm nuclear transplantations reveal FGF signaling requirements during gastrulation. Development 1996;122:3173–3183

Lachapelle F[1], Bachelin C, Moissonnier P, Nait-Oumesmar B, Hidalgo A, Fontaine D, Baron-Van Evercooren A.Failure of remyelination in the nonhuman primate optic nerve. Brain Pathol. 2005 Jul;15(3):198-207.

Lassmann H. The pathology of multiple sclerosis and its evolution. Philos Trans R Soc Lond B Biol Sci. 1999 Oct 29;354(1390):1635-40.

Lee Y, Morrison BM, Li Y, Lengacher S, Farah MH, Hoffman PN, Liu Y, Tsingalia A, Jin L, Zhang PW, Pellerin L, Magistretti PJ, Rothstein JD Oligodendroglia metabolically support axons and contribute to neurodegeneration. Nature. 2012 Jul 26;487 (7408):443-8.

Lubetzki C, Demerens C, Zalc B.Signaux axonaux et myélinogenèse dans le système nerveux centra (1997) l. Médecine/Sciences 13:1097–1105

Lucchinetti C, Brück W, Parisi J, Scheithauer B, Rodriguez M, Lassmann H.
Heterogeneity of multiple sclerosis lesions: implications for the pathogenesis of demyelination..Ann Neurol. 2000 Jun;47(6):707-17.

Luo X, Cerullo J, Dawli T, Priest C, Haddadin Z, Kim A, Inouye H, Suffoletto BP, Avila RL, Lees JP, Sharma D, Xie B, Costello CE, Kirschner DA. Peripheral myelin of Xenopus laevis: role of electrostatic and hydrophobic interactions in membrane compaction. J Struct Biol. 2008 Apr;162(1):170-83. Epub 2007 Nov 1.

Ludwin SK Central nervous system demyelination and remyelination in the mouse: an ultrastructural study of cuprizone toxicity. Lab Invest. 1978 Dec;39(6):597-612.

Mathey EK, Derfuss T, Storch MK, Williams KR, Hales K, Woolley DR, Al-Hayani A, Davies SN, Rasband MN, Olsson T, Moldenhauer A, Velhin S, Hohlfeld R,Meinl E, Linington C. Neurofascin as a novel target for autoantibody-mediated axonal injury. J Exp Med. 2007 Oct 1;204(10):2363-72. Epub 2007 Sep 10

Massacesi L, Genain CP, Lee-Parritz D, Letvin NL, Canfield D, Hauser SL. Active and passively induced experimental autoimmune encephalomyelitis in common marmosets: a new model for multiple sclerosis. Ann Neurol. 1995 Apr;37(4):519-30.

McCallum C. M., Comai L., Greene E. A., Henikoff S. Targeted screening for induced mutations. (2000). Nat. Biotechnol. 18, 455–457

McDonald, W. I. Pathophysiology in multiple sclerosis. Brain (1974a) 97: 179-196.

McDonald, W. I. Remyelination in relation to clinical lesions of the central nervous system. Br. Med. Bull (1974b) 30: 186-l 89.

MacFaul R, Cavanagh N, Lake BD, Stephens R, Whitfield AE. Metachromatic leucodystrophy: review of 38 cases. Arch Dis Child. 1982 Mar;57(3):168-75

Malone MJ, Conole J. Sulfatides and demyelination. Subcellular localization in metachromatic leukodystrophy. Arch Neurol. 1969 Jul;21(1):32-43

Matthieu JM, Ginalski-Winkelmann H, Jacque C. Similarities and dissimilarities between two myelin deficient mutant mice, Shiverer and mld. Brain Res. 1981 Jun 9;214(1):219-22.

Matalon R, Kaul R, Michals K.Canavan disease: biochemical and molecular studies.
J Inherit Metab Dis. 1993;16(4):744-52. Review.

McDonald WI, Sears TA. The effects of experimental demyelination on conduction in the central nervous system Brain. 1970,93(3):583-98.

McKerracher L, David S, Jackson DL, Kottis V, Dunn RJ, Braun PE. Identification of myelin-associated glycoprotein as a major myelin-derived inhibitor of neurite growth. Neuron. 1994;13:805–811
McGee et al, 2005

Menegoz M, Gaspar P, Le Bert M, Galvez T, Burgaya F, Palfrey C, Ezan P, Arnos F, Girault JA. Paranodin, a glycoprotein of neuronal paranodal membranes.
Neuron. 1997 Aug;19(2):319-31.

Miller, R. H. Dorsally derived oligodendrocytes come of age. 2005. Neuron 45, 1-3.

Merkler D, Boretius S, Stadelmann C, Ernsting T, Michaelis T, Frahm J, Brück W. Multicontrast MRI of remyelination in the central nervous system. NMR Biomed. 2005 Oct;18(6):395-403.

Miller RH. Regulation of oligodendrocyte development in the vertebrate CNS.
Prog Neurobiol. 2002 Aug;67(6):451-67. Review.

Morin RD, Chang E, Petrescu A, Liao N, Griffith M, Chow W, Kirkpatrick R, Butterfield YS, Young AC, Stott J, et al. Sequencing and analysis of 10,967 full-length cDNA clones from Xenopus laevis and Xenopus tropicalis reveals post-tetraploidization transcriptome remodeling. Genome Res 2006;16:796–803.

Moser HW. Clinical and therapeutic aspects of adrenoleukodystrophy and adrenomyeloneuropathy. J Neuropathol Exp Neurol. 1995 Sep;54(5):740-5.

Münzel EJ, Becker CG, Becker T, Williams A.Zebrafish regenerate full thickness optic nerve myelin after demyelination, but this fails with increasing age. Acta Neuropathol Commun. 2014 Jul 15;2(1):77.

Nave KA. Myelination and support of axonal integrity by glia. Nature. 2010; Nov 11;468 (7321):244-52. doi: 10.1038/nature09614.

Nieuwkoop and Faber (1994) Normal Table of Xenopus laevis (Daudin). Garland Publishing Inc, New York

Neuronal activity promotes oligodendrogenesis and adaptive myelination in the mammalian brain .Science. 2014 May 2;344(6183):1252304.

Ogino H, McConnell WB, Grainger RM. High-throughput transgenesis in Xenopus using I-SceI meganuclease. Nat Protoc 2006a;1:1703–1710.

Prineas JW, Parratt JD. Oligodendrocytes and the early multiple sclerosis lesion Ann Neurol. 2012 Jul;72(1):18-31

Pan FC, Chen Y, Loeber J, Henningfeld K, Pieler T. I-SceI meganuclease-mediated transgenesis in Xenopus. Dev Dyn 2006;235:247–252.

P.del.Hortega , Tecera aportacion al conocimento morphogico e interpretacion Functional de la oligodendroglia memorias de la real sociedad espanola de historia Natural 14:5-122,1928

Peles E, Nativ M, Lustig M, Grumet M, Schilling J, Martinez R, Plowman GD, Schlessinger J. Identification of a novel contactin-associated transmembrane receptor with multiple domains implicated in protein-protein interactions.EMBO J. 1997 Mar 3;16(5):978-88.

Penfield W.Neuroglia: normal and pathological. Cytology and cellular pathology of the nervous system, (1932) Vol 2, pp 437–443.

Penderis J., Woodruff R. H., Lakatos A., Li W. W., Dunning M. D., Zhao C., Marchionni M., Franklin R. J. M. (2003). Increasing local levels of neuregulin (glial growth factor-2) by direct infusion into areas of demyelination does not alter remyelination in the rat CNS. Eur. J. Neurosci. 18, 2253–2264

Poliak S, Salomon D, Elhanany H, Sabanay H, Kiernan B, Pevny L, Stewart CL, Xu X, Chiu SY, Shrager P, Furley AJ, Peles E. Juxtaparanodal clustering of Shaker-like K+ channels in myelinated axons depends on Caspr2 and TAG-1. J Cell Biol. 2003 Sep 15;162(6):1149-60.

Postlethwait J. H., Woods I. G., Ngo-Hazelett P., Yan Y. L., Kelly P. D., Chu F., Huang H., Hill-Force A., Talbot W. S.. Zebrafish comparative genomics and the origins of vertebrate chromosomes. (2000)Genome Res. 10, 1890–1902

Quarles RH, Sakuragawa N, Everly JL, Pasnak CF, Webster HD, Trapp BD. A biochemical comparison of Xenopus laevis and mammalian myelin from the central and peripheral nervous systemsJ Neurobiol. 1978 May;9(3):217-28.

Raff MC, Fields KL, Hakomori SI, Mirsky R, Pruss RM, Winter J. Cell-type-specific markers for distinguishing and studying neurons and the major classes of glial cells in culture.Brain Res. 1979 Oct 5;174(2):283-308.

Ravkina L, Rogova V, Lazarenko L.Chronic experimental allergic encephalomyelitis in rhesus monkeys and its modification by treatment. J Neurol Sci. 1978 Oct;38(3):281-93.

Readhead C, Hood L. The dysmyelinating mouse mutations shiverer (shi) and myelin deficient (shimld). Behav Genet. 1990 Mar;20(2):213-34.

Rhodes KJ, Strassle BW, Monaghan MM, Bekele-Arcuri Z, Matos MF, Trimmer JS. Association and colocalization of K^+ channel α and β-subunit polypeptides in rat brain. J Neurosci. 1997;15:5360–5371

Robinson S, Miller RH (1999) Contact with central nervous system myelin inhibits oligodendrocyte progenitor maturation. Dev Biol 216: 359–368

Rodrigues DH, Vilela Mde C, Lacerda-Queiroz N, Miranda AS, Sousa LF, Reis HJ, Teixeira AL. Behavioral investigation of mice with experimental autoimmune encephalomyelitis. Arq Neuropsiquiatr. 2011 Dec;69(6):938-42.

Ritchie JM, Waxman SG, Waksman BH. Basic and clinical electrophysiology of demyelinating disease. Neurology 1981; Oct;31(10):1308-10.

Ricard D, Rogemond V, Charrier E, Aguera M, Bagnard D, Belin MF, Thomasset N, Honnorat J..Isolation and expression pattern of human Unc-33-like phosphoprotein 6/collapsin response mediator protein 5 (Ulip6/CRMP5): coexistence with Ulip2/CRMP2 in Sema3a- sensitive oligodendrocytes.J Neurosci. 2001 Sep 15;21(18):7203-14.

Ruthazer ES, Li J, Cline HT. Stabilization of axon branch dynamics by synaptic maturation. J Neurosci. 2006 Mar 29;26(13):3594-603

Sakaguchi DS, Murphey RK. Map formation in the developing Xenopus retinotectal system: an examination of ganglion cell terminal arborizations J Neurosci. 1985 Dec;5(12):3228-45.

Saito RM, van den Heuvel S. Malignant worms: what cancer research can learn from C. elegans. Cancer Invest. 2002;20(2):264-75.

Saab AS, Tzvetanova ID, Nave KA.The role of myelin and oligodendrocytes in axonal energy metabolism. Curr Opin Neurobiol. 2013 Dec;23(6):1065-72

Suzuki K. Formation and turnover of myelin gangliosideJ Neurochem. 1970 Feb;17(2):209-13.

Sim F. J., Zhao C., Penderis J., Franklin R. J. M. The age-related decrease in CNS remyelination efficiency is attributable to an impairment of both oligodendrocyte progenitor recruitment and differentiation. J. Neurosci. (2002). 22, 2451–2459.

Sherman, D.L., S. Tait, S. Melrose, R. Johnson, B. Zonta, F.A. Court, W.B. Macklin, S. Meek, A.J. Smith, D.F. Cottrell, and P.J. Brophy. . Neurofascins are required to establish axonal domains for saltatory conduction. Neuron2005. 48:737–742.

Sherman, D.L., and P.J. Brophy. Mechanisms of axon ensheathment and myelin growth. Nat. Rev. Neurosci. 2005.6:683–690.

Shields SA, Gilson JM, Blakemore WF, Franklin RJ. Remyelination occurs as extensively but more slowly in old rats compared to young rats following gliotoxin-induced CNS demyelination. Glia. 1999 Oct;28(1):77-83.

Smith, K. G. and Waxman, S. G. The Conduction Properties of Demyelinated and Remyelinated Axons 85-101. Waxman, S. G. (ed.). Multiple Sclerosis as a Neuronal Disease, , 2005.

Smith, K. J., and S. M. Hall Nerve conduction during peripheral demyelination and remyelination. J. Neurol. Sci. (1980) .48: 20 1-2 l

Smith KJ, Bostock H, Hall SM. Saltatory conduction precedes remyelination in axons demyelinated with lysophosphatidyl choline. J Neurol Sci. 1982 Apr; 54(1):13-31.

Smith SJ, Mohun TJ. Frog transgenesis made simple. Nat Methods 2005;2:897–898.

Spassky N, Olivier C, Cobos I, LeBras B, Goujet-Zalc C, Martínez S, Zalc B, Thomas JL. The early steps of oligodendrogenesis: insights from the study of the plp lineage in the brain of chicks and rodents. Dev Neurosci. 2001;23(4-5):318-26.

Sparrow DB, Latinkic B, Mohun TJ. A simplified method of generating transgenic Xenopus. Nucleic Acids Res 2000;28:E12.

Stankoff B, Aigrot MS, Noël F, Wattilliaux A, Zalc B, Lubetzki C.Ciliary neurotrophic factor (CNTF) enhances myelin formation: a novel role for CNTF and CNTF-related molecules.J Cell Biol. 1999 Dec 13;147(6):1123-8.

Stevens B, Porta S, Haak LL, Gallo V, Fields RD (2002) Adenosine: aneuron-glial transmitter promoting myelination in the CNS in response to action potentials. Neuron 36:855–868.

Stangel M, Compston A, Scolding NJ. Polyclonal immunoglobulins for intravenous use do not influence the behaviour of cultured oligodendrocytes.J Neuroimmunol. 1999 May 3;96(2):228-33.

Stankoff B, Demerens C, Goujet-Zalc C, Monge M, Peyron F, Mikoshiba K, Zalc B, Lubetzki C. Transcription of myelin basic protein promoted by regulatory elements in the proximal 5' sequence requires myelinogenesis.Mult Scler. 1996 Oct;2(3):125-32.

Stewart WA[1], Alvord EC Jr, Hruby S, Hall LD, Paty DW. Magnetic resonance imaging of experimental allergic encephalomyelitis in primates. Brain. 1991 Apr;114 (Pt 2):1069-96.

Sawcer S. The major cause of multiple sclerosis is environmental: genetics has a minor role.Mult Scler. 2011 Oct;17(10):1174-5.

Suzuki K, Grover WD. Krabbe's leukocystrophy (globoid cell leukodystrophy). An ultrastructural study.Am J Obstet Gynecol. 1970 Apr 1;106(7):385-96.

Tait S, Gunn-Moore F, Collinson JM, Huang J, Lubetzki C, Pedraza L, Sherman DL, Colman DR,Brophy PJ. An oligodendrocyte cell adhesion molecule at the site of assembly of the paranodal axo-glial junction.J Cell Biol. 2000 Aug 7;150(3):657-66.

Tauber H, et al. Myelination in rabbit optic nerves is accelerated by artificial eye opening. Neurosci Lett. 1980;16:235–238

Tepavčević V, Lazarini F, Alfaro-Cervello C, Kerninon C, Yoshikawa K, Garcia-Verdugo JM, Lledo PM, Nait-Oumesmar B, Baron-Van Evercooren A. Inflammation-induced subventricular zone dysfunction leads to olfactory deficits in a targeted mouse model of multiple sclerosis. J Clin Invest. 2011 Dec;121(12):4722-34

Temple S, Raff MC. Clonal analysis of oligodendrocyte development in culture: evidence for a developmental clock that counts cell divisions.Cell. 1986 Mar 14;44(5):773-9.

Tress O, Maglione M, May D, Pivneva T, Richter N, Seyfarth J, Binder S, Zlomuzica A, Seifert G, Theis M, Dere E, Kettenmann H, Willecke K. Panglial gap junctional communication is essential for maintenance of myelin in the CNS.J Neurosci. 2012; May 30; 32 (22):7499-518.

Tiwari-Woodruff S, Morales LB, Lee R, Voskuhl RR. Differential neuroprotective and antiinflammatory effects of estrogen receptor (ER)alpha and ERbeta ligand treatment.Proc Natl Acad Sci U S A. 2007 Sep 11;104(37):14813-8.

Timonthy DJ, Hoshijima K, Jurynec MJ, Gunther D, Starker CG, et al. Simple Methods for Generating and Detecting Locus-Specific Mutations Induced with TALENs in the Zebrafish Genome. (2012) PLoS Genet 8(8):

Traka, M., K. Arasi, R.L. Avila, J.R. Podojil, A. Christakos, S.D. Miller, B. Soliven, B. Popko. A genetic mouse model of adult-onset, pervasive central nervous system demyelination with robust remyelination. Brain. 2010 133:3017–3029

Traka M, Dupree JL, Popko B, Karagogeos D.The neuronal adhesion protein TAG-1 is expressed by Schwann cells and oligodendrocytes and is localized to the juxtaparanodal region of myelinated fibers. J Neurosci. 2002 Apr 15;22(8):3016-24

't Hart BA, van Meurs M, Brok HP, Massacesi L, Bauer J, Boon L, Bontrop RE, Laman JD. A new primate model for multiple sclerosis in the common marmoset.
Immunol Today. 2000 Jun;21(6):290-7.

Wang H, Kunkel DD, Martin TM, Schwartzkroin PA, Tempel BL. Heteromultimeric K^+ channels in terminal and juxtaparanodal regions of neurons. Nature. 1993;365:75–79.

Wake H, Lee PR, Fields RD (2011) Control of local protein synthesis and initial events in myelination by action potentials. Science 333:1647–1651.

Waxman, S. G., and J. M. Ritchie Demyelinating disease: Basic and clinical electrophysiology. (1981) In Advances in Neurology, Raven, New York

Waxman S G, J A Black, J D Kocsis, J M Ritchie. Low density of sodium channels supports action potential conduction in axons of neonatal rat optic nerve. PNAS 1989 February; 86(4): 1406–1410.

Warrington AE, Asakura K, Bieber AJ, Ciric B, Van Keulen V, Kaveri SV, Kyle RA, Pease LR, Rodriguez M. Human monoclonal antibodies reactive to oligodendrocytes promote remyelination in a model of multiple sclerosis. Proc Natl Acad Sci U S A. 2000 Jun 6;97(12):6820-5.

woodruff R. H., Fruttiger M., Richardson W. D., Franklin R. J. M. (2004). Platelet-derived growth factor regulates oligodendrocyte progenitor numbers in adult CNS and their response following CNS demyelination. Mol. Cell Neurosci. 25, 252–262

Werner H., Jung M., Klugmann M., Sereda M., Griffiths I.R., and Nave K. A. Mouse models of myelin disease Brain Pathol. 1998 8:771-93.

Wucherpfennig KW, Weiner HL, Hafler DA. T-cell recognition of myelin basic protein.Immunol Today. 1991 Aug;12(8):277-82.

Willard HF, Riordan JR. Assignment of the gene for myelin proteolipid protein to the X chromosome: implications for X-linked myelindisorders. Science. 1985 Nov 22;230(4728):940-2

Yamada M, Ivanova A, Yamaguchi Y, Lees MB, Ikenaka K.Proteolipid protein gene product can be secreted and exhibit biological activity during early development. J Neurosci. 1999 Mar 15;19(6):2143-51.

Yamazaki Y, Hozumi Y, Kaneko K, Sugihara T, Fujii S, Goto K, Kato H. Modulatory effects of oligodendrocytes on the conduction velocity of action potentials along axons in the alveus of the rat hippocampal CA1 region. Neuron Glia Biol. 2007 Nov;3(4):325-34.

Yang Y, Lacas-Gervais S, Morest DK, Solimena M, Rasband MN.BetaIV spectrins are essential for membrane stability and the molecular organization of nodes of Ranvier.J Neurosci. 2004 Aug 18;24(33):7230-40.

Yoshida M. Oligodendrocyte maturation in Xenopus laevis..J Neurosci Res. 1997 Oct 15;50(2):169-76.

Zalc B, Monge M, Dupouey P, Hauw JJ, Baumann NA. Immunohistochemical localization of galactosyl and sulfogalactosyl ceramide in the brain of the 30-day-old mouse.Brain Res. 1981 May 4;211(2):341-54

Zalc B, Colman DR..Origins of vertebrate success. Science. 2000 Apr 14;288(5464):271-2.

Résumé en Francais

La lignée transgénique *pMBP-eGFP-NTR,* que nous avons générée chez *Xenopus laevis,* permet une ablation conditionnelle des oligodendrocytes myélinisants, dont la conséquence est une démyélinisation. Dans cette lignée transgénique, le transgène est formé par une protéine de fusion entre le rapporteur GFP (Green Fluorescent Protein= protéine fluoresçant en vert) et une enzyme de sélection, la nitroréductase d'*E. Coli.* Cette enzyme, a la propriété de réduire le radical nitrite (NO2) de certains substrats (comme le métronidazole) en dérivé hydroxylamine extrêmement toxique pour la cellule qui l'exprime. L'expression de ce transgène est contrôlée par la portion proximale du gène *MBP* (myelin basic protein), séquence régulatrice, dont l'équipe avait démontré, chez la souris, qu'elle ne s'exprime que dans les oligodendrocytes myélinisants, ce qui c'est vérifié chez le xénope. Mon projet se proposait d'étudier les conséquences de la démyélinisation et de la remyélinisation dans cette lignée transgénique de *Xenopus laevis*. Mon objectif avait pour but de répondre à deux questions; Tout d'abord, qu'elle est la nature des cellules qui remplacent les oligodendrocytes éliminés : Nous montrons que les cellules responsables de la remyélinisation sont les précurseurs des oligodendrocytes (OPCs), cellules GFP négatives caractérisées par l'expression du facteur de transcription Sox10. Ces cellules OPCs sont déjà présentent dans le nerf optique avant l'événement de démyélinisation. La seconde question visait à examiner les conséquences d'une démyélinisation sur l'arborisation des axones des cellules ganglionnaires de la rétine. A cette fin nous avons mis au point un outil expérimental permettant de visualiser l'arborisation des projections tectales des axones des cellules ganglionnaires de la rétine par microscopie *in vivo* réalisée sur le têtard au stade 55. Nous montrons que bien que cette arborisation soit plus sensible à l'imagerie après démyélinisation, chez le transgénique que chez le contrôle, cela n'entraine pas de changement de la motilité de l'arborisation.